Title
Non-redundant functions of IgM and IgD B cell receptors in B cell biology

Author
Noviski, Mark Andrew

Publication Date
2018

Peer reviewed|Thesis/dissertation

Non-redundant functions of IgM and IgD B cell receptors in B cell biology

by

Mark Andrew Noviski

DISSERTATION

Submitted in partial satisfaction of the requirements for the degree of

DOCTOR OF PHILOSOPHY

in

Biomedical Sciences

in the

GRADUATE DIVISION

To my parents,
Victor and Cheryl Noviski
who have always encouraged me to follow my passions.

ACKNOWLEDGEMENTS

Every time I've hit a rough spot in my academic and professional life, somebody has always risen to the occasion to help me through it. At the end of my first year of graduate school, I found myself panicked without a lab to join. As I went around and met with colleagues, administrators, and faculty, the same question repeatedly came up: "Have you heard of Julie Zikherman?" I read a couple of her papers and sent some e-mails to set up a meeting with her. When I arrived on the 10th floor of the Medical Sciences Building, I asked someone to help me find Julie and was promptly escorted to a lab bench inside Art Weiss' lab. I hadn't realized Julie was *that* new. After meeting with her, I took a leap of faith and set up a rotation with Julie. It was a leap of faith for both of us; after all, I was a student who came to UCSF straight out of undergrad and couldn't even find a suitable lab after three rotations. Suffice it to say, the risk paid off and Julie has helped me grow tremendously as a scientist over the past five years. She has challenged me intellectually in ways I never thought possible, but she's always promoted my physical and emotional well-being along the way. When I didn't have a place to go for Thanksgiving, she invited me into her home. When we had to meet tight deadlines, she fostered my productivity without burdening me with unnecessary pressure. Graduate school can be a very trying time, but working with Julie made it not just bearable, but even enjoyable.

Of course, I didn't come to UCSF unprepared. I am ever grateful for Jeannine and Gaelle Muller-Greven, who mentored me during my high school research experience at USB/Affymetrix. Joe Carlin and Jason Hayes helped me further hone my laboratory skills while researching *Chlamydia* at Miami University, and Paul Muchowski and Angela Sia Mah introduced me to life at a major research institution during my summer internship at Gladstone. Tricia Cregger taught me the ins-and-outs of industry research during my summer at STERIS

Corporation. And finally, my teachers, professors, and rotation PIs imparted me with the knowledge to take on a demanding immunology research project. I'll never forget the time I was sitting in MBI 415 at Miami and we were going through the antibody isotypes. That's when I first asked the question that would follow me throughout my entire thesis project: "But what does IgD do?" Dr. Stevenson didn't have an answer back then, but my last few years of research have certainly made a lot of progress. I'm extremely appreciative of my thesis committee members, Art Weiss and Jason Cyster, who have provided their extensive expertise and helped push my project through difficult patches. Tony DeFranco also suggested performing a few very critical experiments that uncovered some striking phenotypes.

Then there are the countless friends who have kept my spirits high through the years. I'll always be thankful for Marvin Schulz and Bill Janesh for introducing me to Science Olympiad, and for Mr. Ramsey who miraculously convinced me that taking science tests on the weekend would be fun. Then there's Paddy O'Leary, who introduced me to November Project and helped me discover a new passion for distance running. There's nothing like a long run through the Marin Headlands to calm my nerves and help me think through the tough questions that come up in my work. I'm also happy to live with three fellow UCSF scientists, Aude Bouagnon, Pallavi Penumetcha, and Ed Roberts, who can commiserate with me over the less glamorous aspects of scientific research. I'm endlessly grateful for a wonderful group of coworkers and collaborators who have been so easy to work with. Al Roque's animal husbandry and James Mueller's mouse genotyping were instrumental in keeping the project moving forward efficiently. John Huizar, Corey Tan, Sarah Coughlin, Ammarina Chuwonpad, Cheryl Heyn, Carlos Castellanos, Rebecca Garrett Jaszczak, Karen Yang, and members of the Weiss Lab have all provided excellent feedback and help with experimental protocols.

Last, but certainly not least, I would have never made it this far without the unending support of my family. I'll never forget the story about the time when I was kicked out of story time at the library for playing with the tape player. My parents recognized my curiosity and creativity and always stood up for me even when those things got me in trouble. They constantly helped me strengthen my self-motivation, which has served me well in the open-ended universe of scientific research. My siblings, Daniel, Sarah, and David, have been a source of endless encouragement, and I'm so fortunate that we've been able to stay close even though we live thousands of miles apart. I hope I've made them all proud.

Contributions to the presented work

Chapter 2 is adapted from a manuscript with the following citation:

> Noviski, M., Mueller, J.L., Satterthwaite, A., Garrett-Sinha, L.A., Brombacher, F., and Zikherman, J. (2018). IgM and IgD B cell receptors differentially respond to endogenous antigens and control B cell fate. eLife *7*, e35074.

James Mueller performed selected experiments in Figure 2.2 (panels B, E, and G). Lee Ann Garrett-Sinha proposed examining Ets1 expression (Figure 2.17, panel A) and provided reagents to do so. Frank Brombacher and Anne Satterthwaite provided reagents and suggested text edits. Julie Zikherman supervised the study, generated data in Figure 2.1, panel A and Figure 2.2, panel A, and assisted with manuscript preparation. Mark Noviski designed, performed, and analyzed all other experiments, wrote and edited the majority of the manuscript, and generated all of the schematic diagrams in Chapter 2. Mark Noviski's contributions to the work in Chapter 2 were equivalent in scope to the corresponding section of a standard doctoral thesis.

Non-redundant functions of IgM and IgD B cell receptors in B cell biology

by

Mark Andrew Noviski

Abstract

Naïve B cells co-express two different BCR isotypes, IgM and IgD, which have identical antigen binding domains but distinct membrane proximal regions. Despite decades of investigation, it is still unclear why B cells co-express both isotypes. Initial studies of IgD- and IgM-deficient mice concluded that IgM and IgD can largely substitute for each other. However, the isotypes differ in structure and expression pattern. IgD is highly expressed on the surface of all naïve B cells, but surface IgM expression is downregulated on autoreactive B cells. Here we demonstrate that IgD is less sensitive than IgM to self-antigen, and the isotypes differ in their ability to drive rapid antibody responses. We generated competitive chimeras in which B cells expressed either IgD or IgM alone. IgD-expressing cells adopted a developmental pattern consistent with reduced self-antigen recognition; they did not enter the B1a compartment but efficiently generated marginal zone cells. We crossed a reporter of endogenous antigen signaling, Nur77-eGFP, onto IgM- and IgD-deficient backgrounds. Differences in reporter expression suggest that IgD senses endogenous antigens more weakly than IgM *in vivo*. *Lyn*$^{-/-}$ mice lack a kinase essential for inhibition of BCR signaling, resulting in inappropriate B cell responses to self-antigen and aberrant short-lived plasma cell (SLPC) generation. *Lyn*$^{-/-}$ B cells expressing exclusively IgD did not differentiate into SLPCs, but were competent to generate germinal center (GC) responses. Similarly, B cells expressing exclusively IgD exhibit normal GC but impaired IgG1^{+} SLPC generation in response to T-dependent immunization. We propose a model in which autoreactive cells are excluded from rapid antibody responses due to predominant IgD and low

IgM expression, but these cells can still participate in immune responses by entering a GC response and undergoing somatic mutation.

TABLE OF CONTENTS

LIST OF TABLES

Chapter 2

LIST OF FIGURES

Chapter 1

Chapter 2

Chapter 3

Appendix

CHAPTER 1: INTRODUCTION

Development and function of the B cell lineage

B cells are the immune cell lineage responsible for generating antibody responses against foreign antigens. Their importance is illustrated by the range of infections observed in patients who lack B cells or have defects in B cell function. For example, patients with a total lack of B cells and circulating antibodies experience recurrent pyogenic infections (Gaspar and Conley, 2000). Furthermore, patients with hematological malignancies treated with B cell-depleting therapies are at an increased risk of infection (Kelesidis et al., 2011). To provide optimal protection against pathogens, B cells must be capable of responding to an astronomically diverse array of antigens, and the B cell repertoire must adapt to viruses that are constantly mutating. Vaccination strategies can be designed to optimize this protection; sequential vaccination can induce broadly neutralizing antibodies that protect against many influenza strains (Wei et al., 2010). Broadly neutralizing antibodies can also provide protection during HIV rebound from latent viral reservoirs (Halper-Stromberg et al., 2014). However, B cells must avoid mounting antibody responses against self antigens, and a failure to do so can lead to autoimmunity. For example, the autoimmune disease systemic lupus erythematosus (SLE) is characterized by "a volcanic explosion of autoantibodies" (Yaniv et al., 2015). While autoreactive B cell specificities are heavily pruned throughout development (Wardemann et al., 2003), this can come at a cost. Certain classes of anti-HIV broadly neutralizing antibodies recognize autoantigens (Liu et al., 2015; Yang et al., 2013), and potential precursors for broadly neutralizing antibodies are recognized as autoreactive and pruned from the repertoire (Chen et al., 2013; Doyle-Cooper et al., 2013; Verkoczy et al., 2010). How B cells maintain a balance between immune responsiveness and the potential for autoimmunity represents a central question of B cell biology.

The earliest stages of B cell development serve to generate diversity within the B cell repertoire, and subsequent tolerance mechanisms remove and restrain excessive autoreactivity within the repertoire (Figure 1.1). Every B cell expresses a B cell receptor (BCR), which is a membrane-bound version of the antibody it is capable of producing. Because of this, a B cell can "sense" how its antibody would interact with its surroundings upon secretion. At the start of B cell development, the B cell rearranges its heavy chain immunoglobulin (Ig) locus through V(D)J recombination (Jung et al., 2006). The B cell first joins together germline-encoded D and J segments, and then it joins an upstream V segment with the fused DJ segment. RAG1 and RAG2 cooperate to recognize recombination signal sequences (RSS) flanking the V, D, and J segments and generate DNA breaks. Because the pairing of these segments is random and the human heavy chain locus contains 46, 23, and 6 V, D, and J segments, respectively, this process can generate 6348 distinct heavy chain rearrangements (Nemazee, 2017). Furthermore, the enzyme terminal deoxynucleotidyl transferase (TdT) adds additional nucleotides to the ends of the broken DNA segments before they are repaired, incorporating an additional level of diversity generation into the process (Bertocci et al., 2006).

Due to the randomness of V(D)J recombination and nucleotide insertion, the rearranged DNA sequence may contain frameshift mutations that produce a truncated or otherwise non-functional immunoglobulin protein. Following heavy chain rearrangement, the B cell begins expressing surrogate light chain proteins (λ5 and VpreB), which can pair with functionally rearranged heavy chains and facilitate their transport to the cell surface as the pre-BCR (Melchers et al., 1993). Combined signals from the pre-BCR and IL-7R promote the proliferation and survival of these large Pre-B cells (Rickert, 2013). If heavy chain rearrangement generated a frameshift mutation, this pairing cannot occur, and the B cell dies by apoptosis (Nemazee and

Burki, 1989). It is not fully understood how a B cell knows that a functional pre-BCR has been transported to its surface, but one model proposes that the surrogate light chains allow the pre-BCR to auto-dimerize, and this auto-dimerization initiates a survival signal. In this way, the pre-BCR behaves like an autoreactive BCR and promotes light chain rearrangement (Ubelhart and Jumaa, 2015). Next, B cells with functionally rearranged heavy chains undergo a round of proliferation before moving on to light chain rearrangement during the immature B cell stage. Similar to heavy chain rearrangement, light chain rearrangement involves joining V and J segments, although light chain loci lack D segments (Tonegawa, 1983). The light chain then pairs with the heavy chain to form the BCR. If the resulting BCR is autoreactive, the immature B cell will rearrange additional light chains until autoreactivity is ameliorated, and it will die by apoptosis if this is unsuccessful (Nemazee, 2006).

Immature B cells then exit the bone marrow and travel to the spleen where they become T1, or early transitional, B cells. If the T1 B cell encounters self antigen, it will undergo deletion, otherwise it matures into a T2 B cell that is less susceptible to BCR-mediated apoptosis (Su and Rawlings, 2002). Depending on additional signals, T2 B cells can then differentiate into fully mature follicular (Fo) or marginal zone (MZ) B cells (Allman and Pillai, 2008). B1a cells are an additional mature B cell subset with unique properties. They develop during fetal development, have restricted diversity, have few N nucleotide insertions, reside primarily in the peritoneal cavity, and produce so-called “natural” antibodies to provide constitutive protection against some classes of pathogens (Hardy, 2006; Kantor et al., 1997). A final B cell lineage that also resides primarily in the peritoneal cavity (B1b) participates in adaptive responses towards pathogens (Haas et al., 2005).

Upon encounter with foreign antigen, B cells can adopt several fates depending on the nature of the antigen. These responses have been traditionally categorized into three classes: T-dependent (TD) and T-independent 1 and 2 (TI-1 and TI-2). TD antigens contain proteins or peptides that can be presented to T cells via MHC-2, TI-1 antigens contain mitogenic stimuli such as TLR ligands, and TI-2 antigens contain highly repetitive epitopes that are recognized by the BCR (Mond et al., 1995). In the classical TD response, follicular B cells encounter antigen, present it to T cells, and form germinal centers where they undergo somatic hypermutation (SHM) and affinity maturation (MacLennan et al., 1992). High affinity, antibody-secreting long-lived plasma cells (LLPCs) and memory B cells then arise from the GC to provide long-term protection and enable rapid recall responses (Kurosaki et al., 2015; McHeyzer-Williams and Ahmed, 1999). In the classical TI response, B1 and marginal zone B cells unite in a rapid antibody response characterized by short-lived plasma cell production without significant GC formation (Martin et al., 2001). Indeed, B1 and MZ B cells are primed to differentiate into plasma cells upon TLR stimulation (Genestier et al., 2007). However, the lines between TI and TD responses can be blurred, and the participating cell types can differ depending on the circumstances. Classical T-dependent antigens can promote T-independent responses via immune complex deposition on follicular dendritic cells (FDCs) (El Shikh et al., 2009), and marginal zone B cells can participate in T-dependent responses (Martin and Kearney, 2002). Furthermore, TI-2 immunizations can induce memory B cells, albeit ones that are phenotypically distinct from those induced by TD immunization (Obukhanych and Nussenzweig, 2006). The TI-2 antigen NP-FICOLL also induces germinal center formation, but these GCs quickly die off by apoptosis and don’t promote high levels of SHM (Toellner et al., 2002).

Early during TD immunization, B cells decide whether to enter the germinal center or whether to participate in an extrafollicular short-lived plasma cell (SLPC) response (MacLennan et al., 2003). Antigen affinity and BCR signal strength play a major role in regulating this decision; in cells with the same BCR specificity, high affinity antigen promotes extrafollicular SLPC generation, and lower affinity antigen promotes germinal center entry (Paus et al., 2006). This makes intuitive sense because the classical view of the germinal center is that the iterative process of somatic hypermutation and affinity-based selection increases affinity towards foreign antigens (Chan and Brink, 2012). However, recent work has demonstrated that the germinal center response can also serve to decrease affinity towards self antigens, a process termed "redemption" by the Goodnow lab (Reed et al., 2016; Sabouri et al., 2014). How exactly B cells "know" that they are autoreactive and should be shunted away from the SLPC fate and into a GC response is unclear and remains an active area of investigation.

B cell receptor and antibody isotypes

Antibodies, and B cell receptors by extension, can take the form of different isotypes that share the same antigen binding domain but differ in the rest of the heavy chain. Sequencing of the Balb/C heavy chain locus revealed that it consists of V, D, and J segments followed by C_{μ}, C_{δ}, $C_{\gamma 3}$, $C_{\gamma 1}$, $C_{\gamma 2b}$, $C_{\gamma 2a}$, C_{ε}, and C_{α} (Shimizu et al., 1982). C57BL/6 mice have a similar heavy chain locus, except they express $C_{\gamma 2c}$ instead of $C_{\gamma 2a}$ (Zhang et al., 2012). There is also a switch motif immediately 5' to all mouse constant domains except C_{δ} (Shimizu and Honjo, 1984). According to immunoglobulin naming convention, the Greek subscript corresponds to the Latin letter of the isotype; for example, C_{μ} represents the constant domain of IgM and $S_{\gamma 1}$ corresponds to the switch motif of IgG1.

A series of three studies published in 1980 sought to characterize the differences between the secreted and membrane-bound versions of antibodies. One hybridization study found that the transcripts for secreted and membrane-bound IgM are identical throughout most of their length but differ at the 3' end, and much of this difference is genomically encoded (Alt et al., 1980). Transcript sequencing revealed that they are identical through the first four domains of the IgM constant region (C_μ1-4), but they have different amino acid and untranslated sequences at the 3' end (Rogers et al., 1980). Sequence similarity at the 3' end of the other isotypes suggests that this is a feature shared by all isotype classes (Rogers et al., 1980). Indeed, all isotype classes can be expressed on the surface of B cells (Reth, 1992). A third study examined the amino acid sequences of membrane-bound and secreted IgM and found that they are identical from V_H through C_μ4, but while the secreted form only has 20 amino acids downstream of C_μ4, the membrane-bound form has 41 primarily hydrophobic amino acids downstream (Kehry et al., 1980). In this way, C-terminal addition of a hydrophobic stretch of amino acids allows the isotypes to be expressed in a membrane-bound form.

The membrane-bound forms of the antibody isotypes are capable of initiating biochemical signals that influence cell fate, a topic that will be covered in a later section. With some minor exceptions, membrane-bound Ig requires pairing with Igα/β for transport to the cell surface and initiation of signaling, and all isotypes have been co-purified with Igα/β (Reth, 1992). While the intracellular domains of mouse IgM and IgD only consist of three amino acids (lysine-valine-lysine), the other three isotype classes have 14-28 amino acid intracellular tails that can modulate BCR signaling and cell fate (Achatz et al., 2008). Indeed, while IgG can initiate signaling in response to weak mechanical forces, replacing its long intracellular tail with that of IgM substantially raises the threshold to initiate signaling (Wan et al., 2015). The

following sections consider each isotype individually and cover their structural properties and secreted functions.

Structure and function of IgM

IgM is the first isotype expressed on the surface of developing B cells, and it can be expressed in all known B cell lineages (Figure 1.2). The isotype is held together by disulfide bonds between the $C_\mu1$ and the light chain and by disulfide bonds between $C_\mu2$ of adjacent heavy chains (Heyman and Shulman, 2016). Secreted IgM often exists in a pentameric or hexameric form, and a high concentration of J chain during assembly favors pentamer generation (Randall et al., 1992). These secreted IgM multimers are held together by disulfide bonds between the $C_\mu3$ and $C_\mu4$ domains of individual antibodies (Heyman and Shulman, 2016). Multimeric structure increases the avidity of interactions between secreted IgM and antigen, and this enhances IgM's ability to neutralize pathogens and promote debris clearance. Secreted IgM is the first antibody produced during an immune response, and it mediates rapid protection on the basis of its polyreactivity, neutralization, clearance of debris, and activation of the complement cascade (Ehrenstein and Notley, 2010). Given its role as an abundant and rapidly secreted antibody, elimination of secreted IgM can affect everything from B cell development to immune responses. Mice that cannot secrete IgM (but can express membrane-bound IgM) have impaired IgG antibody responses, and their B1 compartments are expanded, likely in an attempt to restore serum IgM levels (Boes et al., 1998). Furthermore, when secreted IgM-deficient mice are crossed onto a lupus-prone background, IgG autoantibody generation is accelerated and disease progression is worsened (Boes et al., 2000). Because of this, it is critical to confirm that any phenotypes observed in IgM-deficient B cells are cell intrinsic.

Structure and function of IgD

An evolutionary study of IgD revealed that while IgD is an ancient isotype, its structure is not very well conserved apart from a long hinge region found in many placental mammals (Sun et al., 2011). The long hinge comprises a 64 amino acid segment between $C_\delta1$ and $C_\delta2$ in human IgD, but the hinge lies between $C_\delta1$ and $C_\delta3$ in mice, which lack $C_\delta2$ (Preud'homme et al., 2000). X-ray scattering reveals that this long hinge, along with heavy O-glycosylation, gives IgD a T-shaped structure, in contrast to the Y-shaped structure of IgM (Sun et al., 2005) (Figure 1.3). The potential role of this structural difference in BCR signaling will be covered in a later section. While IgD secretion is not a feature of most model immune responses, one study found that B cells can class switch to IgD in the upper respiratory mucosa, secreting IgD that can both bind to common respiratory tract bacteria and activate basophils (Chen et al., 2009). Unlike other isotypes, serum IgD levels do not follow a log-Gaussian distribution in human patients, and while some patients have almost no detectable serum IgD, other patients produce up to 400 μg/mL (Chen and Cerutti, 2010). Therefore, it appears that secreted IgD may perform protective functions under limited circumstances.

Structure and function of IgG

Both mice and humans can produce four subclasses of IgG. The four mouse classes are (in order) IgG3, IgG1, IgG2b, and IgG2a (or IgG2c), and each IgG isotype contains V_H, C_H1, hinge, C_H2, and C_H3 domains (Akahori and Kurosawa, 1997). Similarly, the human classes are (in order) IgG3, IgG1, IgG2, and IgG4, and all of them are structurally similar, except for IgG3, which has a much longer hinge (Rispens and Vidarsson, 2014). All four mouse IgG isotypes have long intracellular tails, and IgG1's tail was shown to be necessary for generating rapid and robust IgG1 responses (Kaisho et al., 1997). Indeed, the long intracellular tails of IgG and IgE amplify BCR signaling via recruitment of the adapter protein Grb2 (Engels et al., 2009). A long

half life (about 21 days), high concentration in serum, and complement activation contribute to secreted IgG's protective function, and IgG is uniquely transferred across the placenta to offspring with under-developed immune systems (Vidarsson et al., 2014). Furthermore, secreted IgG loaded on FcγRs of natural killer (NK) cells and monocytes can mediate antibody-dependent cell-mediated cytotoxcity (ADCC) (Smalls-Mantey et al., 2013). IgG1 is often used as a therapeutic in human studies due to its ability to perform the full spectrum of IgG functions (in contrast to the other IgG isotypes): binding activating and inhibitory FcγRs, mediating ADCC, promoting phagocytosis, and activating the complement cascade (Brezski and Georgiou, 2016). The presence of four different IgG subtypes enables fine-tuning of antibody responses to optimize the particular suite of effector functions needed to fight a given infection. These diverse and powerful capabilities illustrate why class switching to IgG is tightly controlled.

Structure and function of IgE

IgE molecules contain a V_H domain followed by four constant domains (C_ε1-4) (Wu and Scheerens, 2014). As with IgG, IgE has a long cytoplasmic tail that plays a role in promoting robust antibody responses (Achatz et al., 1997). Cells expressing IgE BCRs display enhanced signaling because IgE's cytoplasmic tail dampens CD22-mediated inhibitory signaling and amplifies positive signaling via recruitment of Grb2 (Sato et al., 2007; Engels et al., 2009). This enables chronic signaling through the BCR in the absence of antigen, and these signals can synergize with T cell help to promote rapid plasma cell differentiation (Yang et al., 2016). Secreted IgE is thought to play a role in protection against parasitic helminths, but because it readily binds to the high affinity IgE receptor FcεRI and promotes degranulation of mast cells and basophils, IgE is a major player in asthma, allergy, and atopic dermatitis (Wu and Zarrin, 2014). IgE promotes a conformational change in FcεR1 to strengthen their interaction, and this

contributes to IgE's extremely long half-life and abundance on the surface of mast cells (Wan et al., 2002). Because of this, IgE can promote allergic responses long after sensitization takes place.

Structure and function of IgA

Human B cells are capable of expressing two IgA isotypes, IgA1 and IgA2, but there is only a single IgA isotype in mice (Mestas and Hughes, 2004). In addition to the V_H domain, mouse IgA has three additional constant domains (C_α1-3), with the hinge encoded at the 5' end of C_α2 (Tucker et al., 1981). Both human IgA isotypes have a V_H domain followed by C_α1-3, but IgA1 has a much longer hinge than IgA2 (Woof and Russell, 2011). IgA BCRs have longer intracellular tails than IgM and IgD, but in contrast to IgE, IgA does not display enhanced signaling relative to IgM (Sato et al., 2007). Secreted IgA plays an extremely important role providing protection from pathogens and toxins at mucosal surfaces. On the basolateral side of epithelial cells in the gut, dimeric IgA (linked by J chain) binds to the poly Ig receptor, and then it is shuttled across the cell to the apical membrane and then cleaved off (Pabst, 2012). This unique transport pathway is why IgA dimers in the gut lumen contain a secretory component.

Historical studies of IgM- and IgD-deficient mice

The mystery of dual expression of IgM and IgD on mature B cells has existed ever since it was observed that the two isotypes are co-expressed and move independently, indicating that they exist in separate complexes (Knapp et al., 1973; Rowe et al., 1973). With advances in mouse genetic models in the late 1980s and early 1990s enabling *in vivo* functional characterization of immunoreceptors and signaling molecules (Kulkarni and Karlsson, 1993), deleting the IgM and IgD BCR isotypes represented a promising approach for studying B cell

biology. While in the short term, deletion of these BCR isotypes led to the underwhelming conclusion of isotype redundancy, these studies illustrated the resiliency and flexibility of the BCR repertoire. This section covers the generation and characterization of two independent lines of IgD-deficient mice with similar phenotypes and then discusses two IgM-deficient mouse lines with more divergent phenotypes.

The Rajewsky lab performed the first characterization of IgD-deficient B cells *in vivo* (Roes and Rajewsky, 1991). They transfected C57BL/6 x CBA F1 ES cells with a targeting vector to introduce a neomycin cassette that disrupts the $C_\delta1$ and $C_\delta3$ exons of the CBA (allotype [a]) heavy chain locus. Because of this approach, one Ig locus was IgD-deficient and the other locus was unaffected (C57BL/6; allotype [b]). The authors screened the ES cells for the desired insertion and then injected them into SCID blasocysts, which ensured that any developing B cells would originate from the injected ES cells. In these chimeric mice, they found that the IgD-deficient B cells were able to progress to the $CD23^+$ mature-naïve stage and appeared grossly normal. They immunized chimeric mice with the T-dependent antigen NP-CG and found that while the anti-NP hapten response was dominated by the WT IgH^b cells, the anti-CG carrier response was intact. The dominance of allotype b cells over allotype a cells in anti-NP responses was previously known and was therefore not surprising (Loh et al., 1983). Roes and Rajewsky only analyzed two C57BL/6 x CFA F1 mice (with no ES cell injections) and three WT/IgD-deficient ES-into-SCID mice, so their immunization comparisons were only qualitative and were heavily influenced by the degree of chimerism in the latter mice. They also did not assay T-independent responses in these mice.

More detailed examination of IgD-deficient B cells was possible once the Rajewsky lab attained germline transmission of their IgD knockout (Roes and Rajewsky, 1993). These fully

IgD-deficient mice were able to generate normal numbers of mature $CD23^+$ splenic B cells and $CD5^+$ peritoneal B1a cells. Steady-state BrdU labeling of splenic B cells was also identical in IgD-deficient and WT mice, indicating that B cell turnover was normal. However, in heterozygous $IgD^{+/-}$ mice, where half of B cells should be WT and half should be IgD-deficient, the IgD-deficient B cells were outnumbered 2:1 by WT B cells. In these mice, NP-specific IgG1 from the IgD-deficient locus was underrepresented when mice were immunized with the T-dependent antigen NP-CG, even after adjusting for the poor anti-hapten response of the allotype [a] locus. Both primary and secondary T-dependent responses in $IgD^{-/-}$ mice were largely normal, although affinity maturation was slightly delayed. T-independent responses to both NP-FICOLL and α-(1,3)-dextran were also normal, as were steady state serum levels of all antibody isotypes, except for IgE, which was lower in the $IgD^{-/-}$ mice (though even in WT mice, IgE levels were near the limit of detection). This suggests that $IgD^{-/-}$ mice generate largely normal LLPC responses. Because of these results, the authors concluded that IgD largely functions as an "auxiliary" receptor that helps recruit B cells into rapid antibody responses. However, it remains unclear how the expression of IgD could influence affinity maturation when it is not normally expressed on germinal center B cells (Butcher et al., 1982; Kraal et al., 1982).

An independent IgD knockout mouse was also characterized and published in 1993 (Nitschke et al., 1993). To generate this mouse, the authors inserted a stop codon and neomycin cassette into the $C_\delta 3$ exon of the IgD constant region of the 129/Sv (allotype [a]) heavy chain locus. Similar to the line generated by the Rajewsky lab, IgD-deficient B cells were reduced by 50% when competing against WT B cells in $IgD^{+/-}$ mice. However, unlike in the Rajewsky line, the total number of splenocytes was reduced in this $IgD^{-/-}$ mouse line. The other notable difference was that IgD-deficient locus did not display a reduced anti-hapten IgG1 (allotype [a])

response when comparing *IgD*$^{+/-}$ and *IgH*$^{a/b}$ mice immunized with the T-dependent antigen DNP-ova. As the haptens and carriers differed in these two papers, the difference in T-dependent anti-hapten responses could arise from either the way the knockouts were generated or the exact haptens and carriers used. Regardless, any defect in T-dependent responses is too minor and inconsistent for generalization. Nitschke et al. also examined anti-dextran responses and found a slight defect when they immunized intraperitoneally but no defect when they immunized intravenously. Such a result would suggest that IgD-deficient mice have a slight defect in B1a responses but intact MZ responses, although it is unclear how loss of IgD could influence the function of B1a cells, as they normally express very little IgD. Steady state immunoglobulin levels were also largely normal in *IgD*$^{-/-}$ mice, though they did observe slightly reduced IgG2b and slightly increased IgA in these mice. As with the anti-hapten responses, this finding differed from the Roes and Rajewsky paper, so it is not a particularly robust phenotype. Finally, the Nitschke paper examined lymphoid organ and GC structure by microscopy and found that both were normal. This led the authors to conclude that IgD is largely or entirely dispensable for adaptive responses but might play a role in maintaining B cell homeostasis. Indeed, the only defect reproducibly and robustly demonstrated in both mouse lines was reduced competition of IgD-deficient B cells against WT B cells at steady state. The fact that subjecting IgD-deficient mice to the full battery of B cell assays (available at the time) produced such subtle phenotypes generated a consensus that IgD is a largely redundant and dispensable isotype. However, the persistence of IgD throughout evolution hinted that it might play an important yet-to-be-defined role in B cell biology (Rogers et al., 2006).

By the early 1990s, the role of IgM as the first BCR isotype expressed by developing B cells had been long appreciated (Raff et al., 1976). However, it was unclear if or how loss of

membrane-bound IgM would affect B cell development or function. The generation of *μMT* mice was the first attempt to answer this question (Kitamura et al., 1991). The *μMT* mouse was generated by targeted insertion of a neomycin cassette into one the membrane exons for the IgM constant region, thus disrupting generation of membrane-bound IgM. Notably, mice homozygous for this insertion did not develop any mature B cells and lacked detectable levels of serum IgM. Examination of the bone marrow in these mice identified only large $CD45R^{dull}$ surface IgM^- B cells, indicating that these cells were arrested at the large Pre-B stage of development and had not progressed to the proliferative small Pre-B stage. By contrast, heterozygous mutant mice, with a WT BCR locus from the C57BL/6 background and a *μMT* BCR locus from the 129/sv background, had a normal number of circulating peripheral blood B cells. In this case, all of the IgM^+ circulating B cells expressed IgM from the C57BL/6 locus (allotype [b]), indicating that the *μMT* disruption precluded expression of surface IgM from allotype [a] locus. Interestingly, the authors detected a small population of IgD^a-expressing B cells in the peripheral blood and a small amount of IgM^a in the serum. It remains unclear how these allotype [a] cells were able to develop in the heterozygous mice but not the homozygous *μMT/μMT* mice. Regardless, the authors of this study concluded that membrane expression of IgM is required for progression beyond the Pre-B stage of development.

This view persisted until a new IgM-deficient mouse was generated several years later (Lutz et al., 1998). This mouse differed from *μMT* mice in two important ways. First, the targeting construct was designed to eliminate the entire C_μ constant region and the μ-δ intron. Second, the neomycin cassette was flanked by loxP sites, and a Cre-expressing construct was transduced into the ES cells to induce removal of the cassette. As a result, the entire IgM locus was removed, and the IgD constant region was brought into closer proximity to the V(D)J region

of the Ig locus. In marked contrast to *μMT* mice, these *IgM*$^{-/-}$ mice had largely normal splenic and bone marrow B cell compartments and expressed IgD in place of IgM throughout development. The peritoneal CD5^{+} B1a compartment still developed in these mice, but it was reduced to 26% of peritoneal B cells, in comparison to 41% in WT mice.

Further phenotypic characterization of *IgM*$^{-/-}$ mice also suggested that their B cell responses were largely intact. The authors immunized mice with the T-dependent antigen DNP-ovalbumin, rechallenged them at day 14, and found that *IgM*$^{-/-}$ and WT mice produced identical titers of anti-DNP IgG1 at weekly timepoints in the following month. *IgM*$^{-/-}$ mice also produced robust anti-DNP IgD responses in this immunization, analogous to production of anti-DNP IgM in WT mice. This indicates that plasma cell generation by germinal center and/or memory B cells is intact in *IgM*$^{-/-}$ mice. Primary responses to type-II T-independent immunization (TNP-FICOLL) were also intact; *IgM*$^{-/-}$ mice produced anti-TNP IgG3 and IgD and WT mice produced anti-TNP IgG3 and IgM seven days after immunization. Microscopy revealed that marginal zone and germinal center structure was grossly normal in immunized *IgM*$^{-/-}$ mice, although the follicular dendritic cell (FDC) network did not display captured IgD and only displayed captured IgG (the FDC network captures and displays both IgM and IgG in WT mice). The most notable phenotype in these mice was a delayed antibody response to vesicular stomatitis virus (VSV), which induces both T-independent and T-dependent responses and requires neutralizing antibody production to clear (Bachmann et al., 1997). In contrast to WT mice, which produce a rapid IgM response that peaks at day 4 post-infection, the IgD response in *IgM*$^{-/-}$ mice did not peak until day 12. Perhaps due to this delayed response, the lethal viral dose for *IgM*$^{-/-}$ mice was 10-fold lower than that for WT mice, although this lethal dose was still 10x higher than the lethal dose for B cell-deficient mice. At the very least, this indicates that SLPC responses might be delayed

in *IgM*$^{-/-}$ mice. However, the authors did not explicitly examine SLPC generation in response to primary immunization, so the role of IgM in SLPC responses is not fully understood.

To summarize, characterization of IgM- and IgD-deficient mice revealed that IgM and IgD can largely substitute for each other. Indeed, the mice described by Roes and Rajewsky, Nitschke et al., and Lutz et al. did not display *any* absolute defects in B cell function; all phenotypes were either quantitative or only present during competition or early in an immune response. Because of this, further investigation into non-redundant functions of IgM and IgD was largely avoided in the following 15 years. It would take new insights into how polyclonal B cell repertoires are maintained and managed to prompt further study of IgM and IgD, as these new insights provided guidance as to where fruitful investigation might take place.

Regulation of BCR signaling

Initiation of BCR signaling

How exactly BCR signaling is initiated is the topic of ongoing debate. As described in a later section, there is controversy over whether BCR signaling is initiated by antigens binding to BCRs and bringing them together (the crosslinking model; (Packard and Cambier, 2013)), or whether the BCR exists in constitutively inhibited clusters and antigen binding disrupts these clusters to initiate productive signaling (the dissociation activation model, (Yang and Reth, 2010a)). What is generally agreed upon, however, is that signal initiation begins with phosphorylation of ITAMs in Igα/β by the Src family kinases (SFKs) Lyn, Blk, and Fyn (Gold et al., 1991; Saouaf et al., 1994; Weiss and Littman, 1994). The Src family kinases are normally restrained by Csk-mediated phosphorylation of their inhibitory tyrosine residues (Nada et al., 1991). When these sites are phosphorylated, they interact with an SH2 domain within the SFK to

clamp the kinase into an inactive conformation (Young et al., 2001). This inhibitory phosphorylation is counteracted by the partially redundant phosphatases CD45 and CD148 (Hermiston et al., 2009). B cells deficient for both CD45 and CD148 display greatly dampened signaling in response to BCR crosslinking because of basal hyper-phosphorylation of the C-terminal inhibitory tyrosine (Y505) of Lyn (Zhu et al., 2008). Following SFK-mediated ITAM phosphorylation, Syk kinase docks onto the intracellular tails of Igα/β via its tandem SH2 domains (Rowley and Burkhardt, 1995). After docking on Igα/β, Syk trans-autophosphorylates, which in turn enhances its kinase activity (Kurosaki et al., 1995). Once Syk is brought to the BCR complex and fully activated, the BCR signaling pathway begins to branch out (Figure 1.4).

Propagation of BCR signaling

Syk phosphorylates the linker protein BLNK (also known as SLP-65) (Goitsuka et al., 1998), which then recruits Btk and PLCγ2 via their SH2 domains (Ishiai et al., 1999). Concerted phosphorylation by Syk and Btk activates PLCγ2, which then converts phosphatidylinosito-4,5-bisphosphate (PIP_2) into diacylglycerol (DAG) and inositol-1,4,5-triphosphate (IP_3) (Rhee and Bae, 1997). These two second messengers enable further bifurcation of the signaling cascade; DAG activates protein kinase C (PKC), and IP_3 binds to IP_3R on the endoplasmic reticulum to activate calcium channels and promote calcium influx into the cytosol (Berridge, 1993; Newton, 2001). As the ER calcium stores are depleted, STIM1 accumulates at the ER-adjacent region of the plasma membrane and activates CRAC channels, which enable calcium influx from outside of the cell (Zhang et al., 2005). PKC activation and elevated intracellular calcium indirectly promote the nuclear translocation of the transcription factors NFκB and NFAT, respectively (Packard and Cambier, 2013). As these two transcription factors can be activated by different stimuli (e.g. BCR and cytokines) with different efficiencies, NFκB and NFAT nuclear

translocation allows B cells to integrate signals from divergent stimuli and adjust cell fate accordingly.

A second major pathway induced by Syk and Btk activation is the PI3 Kinase (PI3K) pathway. Btk and Syk phosphorylate tyrosines on BCR-associated protein (BCAP), which then enhances recruitment of the p85 subunit of PI3K to the plasma membrane (Okada et al., 2000). SFK-mediated phosphorylation of tyrosines 484 and 515 of the co-receptor CD19 plays a critical role in activation of the PI3K pathway, and *CD19*$^{-/-}$ B cells do not display any detectable BCR-induced PI3K activation (Buhl et al., 1997; Ishiura et al., 2010). In this way, BCAP and CD19 cooperate to promote optimal activation of the PI3K pathway. Once PI3K is recruited to the plasma membrane, it phosphorylates $PI(4,5)P_2$ to $PI(3,4,5)P_3$, and the local increase in PIP_3 allows Akt to be recruited to the membrane and activated (Scheid et al., 2002). Several biochemical events follow Akt activation, including Akt-mediated phosphorylation and degradation of the transcription factor FOXO1 (Engelman et al., 2006). Akt also indirectly activates the Raptor-mTOR complex (mTORC1), which in turn activates S6 kinase and promotes phosphorylation of the ribosomal subunit S6 (Engelman et al., 2006). The importance of the PI3K pathway in B cell survival is clearly illustrated by its ability to rescue B cell survival after deletion of the BCR (Kraus et al., 2004; Lam et al., 1997; Srinivasan et al., 2009). The role of BCR signaling in B cell survival will be discussed in greater detail in a later section.

A third pathway induced during BCR signaling is the mitogen-activated protein kinase (MAPK) pathway. Once BLNK is phosphorylated, it recruits the adapter protein Grb2, which in turn recruits SOS, a guanine nucleotide exchange factor (GEF) that converts inactive Ras-GDP to active Ras-GTP (Fu et al., 1998). GTP-bound Ras then recruits the serine/threonine kinase Raf, which phosphorylates Mek, which phosphorylates ERK1 and ERK2 (Genot and Cantrell,

2000). However, significant redundancy in this pathway exists because ERK1/2 phosphorylation is normal in cells where Grb2/Sos recruitment to BLNK is abolished via mutation of critical tyrosines on BLNK (Fu et al., 1998). Regulation of the MAPK pathway in lymphocytes is complex, depends on the balance and interplay between GEFs and GTPase activating proteins (GAPs), and has been reviewed in detail (Jun et al., 2013). As with PKC and calcium signaling, the MAPK pathway also activates a variety of transcription factors to link signaling to changes in B cell fate.

Negative regulation of BCR signaling

In addition to the positive signaling pathways described above, BCR stimulation activates negative signaling pathways that dampen and terminate BCR signaling. Negative signaling is initiated by phosphorylation of ITIMs in inhibitory receptors such as CD22 and FCγRIIB, but in contrast to ITAM phosphorylation by redundant SFKs, ITIM phosphorylation has an absolute requirement for Lyn (Ohashi and Defranco, 2002). Indeed, a study using compound heterozygous mutants found that Lyn, CD22, and the protein tyrosine phosphatase SHP-1 cooperate to suppress BCR signaling (Cornall et al., 1998). In addition, monophosphorylation of the ITAMs of Igα/β was found to recruit the negative regulator SHIP-1, thus causing the ITAM domains to behave like ITIM domains (O'Neill et al., 2011). SHIP-1 is an inositol phospholipid phosphatase that converts $PI(3,4,5)P_3$ to $PI(3,4)P_2$ (Leslie and Downes, 2002), and this inhibits BCR signaling by reducing recruitment of pleckstrin-homology (PH) domain-containing proteins such as PLCγ2 and Btk to the plasma membrane (Nitschke, 2005).

CD22 is a sialic acid-binding surface receptor that requires Lyn for its ITIM phosphorylation and suppressive function (Smith et al., 1998). Downstream suppressive function proceeds by three mechanisms. First, SHP-1 is recruited to the ITIM domain in CD22 and

dephosphorylates CD19 and BLNK (Nitschke, 2009). Second, phosphorylated CD22 interacts with the calcium efflux pump PCMA4 and promotes the efflux of calcium from the cytosol to the extracellular milieu (Chen et al., 2004). Finally, SHIP-1 is recruited indirectly to CD22 via the adapter proteins Grb2 and Shc (Poe et al., 2000).

FCγRIIB is the only IgG Fc receptor expressed constitutively on B cells, and its main function is to inhibit BCR signaling in response to IgG-containing immune complexes (Smith and Clatworthy, 2010). As with CD22, FCγRIIB's ITIM domain is phosphorylated by Lyn (Malbec et al., 1998), but unlike CD22, it's inhibitory function is mediated primarily by SHIP-1 (Ono et al., 1996). However, FCγRIIB's ITIM was also shown to bind SHP-1 *in vitro*, so SHP-1-mediated signaling suppression also remains a possibility (Malbec et al., 1998).

Siglec-G belongs to the same family of sialic-acid binding proteins as CD22, but its primary function appears to be to inhibit BCR signaling specifically in B1 cells (Nitschke, 2009). While Siglec-G over-expression in the DT40 chicken B cell line inhibits BCR signaling, *Siglec-G*$^{-/-}$ mice exhibit enhanced calcium mobilization in only the B1a compartment and not the B2 compartment (Hoffmann et al., 2007). The exact nature of Siglec-G-mediated signaling suppression is not entirely clear. One study found that Siglec-G-deficient peritoneal B cells have enhanced NFκB signaling (Ding et al., 2007), but this was not replicated in an independent study by a different group (Jellusova et al., 2010). Because the human homologue of Siglec-G (Siglec-10) binds SHP-1, it was initially suspected that Siglec-G operates through SHP-1, but SHP-1 phosphorylation is unaltered in *Siglec-G*$^{-/-}$ B cells (Nitschke, 2009). However, a later study found that Siglec-G-mediated inhibition of BCR signaling requires SHP-1 (Pfrengle et al., 2013). It may be that redundant mechanisms for SHP-1 activation explain the lack of a pSHP-1 phenotype in *Siglec-G*$^{-/-}$ B cells.

The role of BCR signaling in B cell development

Investigations of positive and negative regulation of BCR signaling has improved our understanding of the role of BCR signaling in B cell development, fate decision, and survival. Elimination or severe restriction of proximal BCR signaling leads to a complete arrest of B cell development or a severe reduction in B cell numbers. Notably, *RAG-1*$^{-/-}$ and *RAG-2*$^{-/-}$ mice, which cannot undergo V(D)J recombination and thus cannot express rearranged BCRs, arrest at the Pro-B cell stage of development and lack peripheral B cells (Mombaerts et al., 1992; Shinkai et al., 1992). Disruption of Igα/β has a similar effect; a human patient with a CD79a (Igα) splicing defect was identified due to a lack of peripheral B cells (Minegishi et al., 1999), and CD79b (Igβ)-deficient mice also lack peripheral B cells (Gong and Nussenzweig, 1996). Syk-deficient mice die perinatally, and B cell development is largely arrested at the Pro-B to Pre-B transition (Cheng et al., 1995; Turner et al., 1995). However, while a small number of transitional B cells develop in radiation chimeras reconstituted with *Syk*$^{-/-}$ fetal liver, none of these transitional B cells progress to the mature follicular stage (Turner et al., 1997). This is consistent with the idea of positive selection, which posits that the mere absence of negatively-selecting signals is insufficient to promote progression of transitional B cells to the follicular stage of development, and positive BCR signals are required. Btk deficiency or mutation can lead to X-linked agammaglobulinemia (XLA) and total B cell deficiency in humans, but while Btk-deficient mice lack B1a cells, they still have some peripheral B cells (Satterthwaite et al., 1998a). Specifically, both *Btk*$^{-/-}$ radiation chimeras and Btk kinase-dead mice display a much more severe reduction in mature follicular/recirculating B cells than transitional B cells (Kerner et al., 1995; Khan et al., 1995). *PLCγ2*$^{-/-}$ mice, which have a major defect in calcium and PKC signaling, display a similar phenotype (Wang et al., 2000). However, a mouse line that expresses

25% of normal Btk levels (Btk^{lo}) has normal numbers of mature follicular/recirculating B cells (Contreras et al., 2007). Thus, Btk and PLCγ2 provide signals required for efficient positive selection into the mature follicular/recirculating compartment, but positive selection can still occur in the face of reduced BCR signaling. This may be due to compensatory changes in the selected B cell repertoire in favor of more self-reactive specificities.

The role of SFKs in B cell development is more nuanced due to their redundancy. Deficiency in one or two of the SFKs B cells express (Lyn, Blk, and Fyn) leads to little or no reduction in mature B cell numbers, but mice that lack all three of these SFKs have almost no peripheral B cells due to defective NFκB activation by the pre-BCR (Saijo et al., 2003). Due to the role of CD45 and CD148 in positively regulating SFK signaling, the B cell compartment of CD45/CD148 doubly-deficient mice largely phenocopies $Lyn^{-/-}$ $Blk^{-/-}$ $Fyn^{-/-}$ mice, with an early block in B cell development in the bone marrow (Zhu et al., 2008). These studies illustrate that progression beyond the Pre-B stage requires signaling through the BCR-Igα/β complex, and substantially impairing BCR signaling leads to developmental arrest. In general, other signaling mutants develop mature B cells, but phenotypes are partially masked by shifts in the B cell repertoire. Indeed, while $CD45^{-/-}$ mice have a large peripheral B cell compartment (Zhu et al., 2008), $CD45^{-/-}$ B cells forced to express a hen egg lysozyme (HEL)-specific BCR largely fail to accumulate in the mature follicular compartment, and this is rescued by co-expression of high affinity soluble cognate antigen (Cyster et al., 1996). This suggests that the combined effect of CD45 deficiency and loss of antigen recognition substantially impairs positive selection into the mature follicular compartment, and BCR self-reactivity can partially compensate for defects in BCR signal transduction. By contrast, many perturbations in BCR signaling produce substantial changes in the B1a and MZ compartments in the absence of BCR transgenes.

The signal strength model of MZ and B1a B cell development posits that strong BCR signals favor the B1a fate, and weaker signals favor the MZ fate (Cariappa and Pillai, 2002). Indeed, the relative sizes of these populations are often dramatically shifted when positive regulators of BCR signaling are eliminated or overexpressed. The Rajewsky lab generated mice that express high and low levels of the Epstein-Barr virus protein LMP2A, which acts as a constitutively active BCR surrogate, and they found that high LMP2A expression leads to B1a development, and low expression promotes MZ development (Casola et al., 2004). *CD148*$^{-/-}$ mice, which have suppressed SFK signaling due to overactive Csk, have reduced B1a and expanded MZ compartments (Zhu et al., 2008). Titration of a related molecule, CD45, from subphysiological to superphysiological levels reveals a similar trend; low CD45 expression drives less B1a and more MZ development, and high CD45 expression drives more B1a and less MZ development (Zikherman et al., 2012a). Titration of Btk also reveals the exquisite sensitivity the B1a compartment to changes in signal strength. As described earlier, *Btk*$^{-/-}$ mice have a severe reduction in most B cell subsets, but while *Btk*^{lo} mice have an almost complete rescue of mature follicular B cell numbers, they still have a severe reduction in B1a numbers (Contreras et al., 2007). Finally, deletion of CD19 leads to a severe reduction in B1a development despite normal numbers of mature follicular/recirculating B cells (Rickert et al., 1995).

Mice deficient for key negative regulators display fate skewing consistent with enhanced BCR signaling: more B1a development and less MZ development. B1a development is markedly enhanced in *FCγRIIB*$^{-/-}$, *Siglec-G*$^{-/-}$, and *SHP-1*$^{-/-}$ mice (Amezcua Vesely et al., 2012; Hoffmann et al., 2007; Pao et al., 2007). Marginal zone development is decreased in *CD22*$^{-/-}$, *SHP-1*$^{-/-}$, and *SHIP-1*$^{-/-}$ mice (Maxwell et al., 2011; Pao et al., 2007; Samardzic et al., 2002). The role of Lyn is more complicated due to the fact that Lyn has a primarily negative signaling role in B2 (MZ and

Fo) B cells but a primarily positive signaling role in B1a cells (Skrzypczynska et al., 2016). Conditional deletion of Lyn in B cells led to the elimination of MZ B cells, a profound reduction in mature follicular B cells, and a relatively preserved B1a compartment (Lamagna et al., 2014). As B2 cell numbers are dramatically reduced, B1a cells predominate in the peritoneal compartment of *Lyn*$^{-/-}$ mice (Lamagna et al., 2014).

Role of BCR signaling in B cell survival

In addition to shaping development, the BCR signaling cascade plays a role in B cell survival. This is most dramatically illustrated by the rapid B cell death that follows inducible deletion of the BCR (Lam et al., 1997). Deletion of Igα also leads to rapid B cell death, with B cell half-life dropping dramatically to 3-6 days (Kraus et al., 2004). Subsequent investigation found that PI3K signaling plays a key role in mediating survival of inducibly BCR-deficient B cells; constitutively active PI3K (*P110**) and PTEN deficiency rescued survival of BCR-deficient B cells, but constitutively active NFκB and constitutively active MEK did not (Srinivasan et al., 2009). In this case, PTEN deficiency mimicked constitutively active PI3K because PTEN's normal function is to convert $PI(3,4,5)P_3$ to $PI(4,5)P_2$ (Leslie and Downes, 2002). B cell survival was rescued upon simultaneous deletion of FOXO1 and the BCR, indicating that the PI3K pathway mediates at least some of its pro-survival role through repression of FOXO1 (Srinivasan et al., 2009). However, in contrast to the *P110** and *PTEN*$^{-/-}$ BCR-deleted cells, FOXO1/BCR doubly-deficient B cells were phenotypically abnormal and failed to differentiate into MZ B cells or home to the lymph nodes.

A complementary study of inducible Syk deletion in B cells came to a similar, but subtly different, conclusion. It has been long known that mutation or loss of the B cell survival factor BAFF or BAFF receptor severely reduces the number of peripheral mature B cells (Schiemann et

al., 2001; Thompson et al., 2001). The Tybulewicz lab observed that BAFF treatment induces phosphorylation of Syk and Igα in a BCR-dependent manner; thus BAFF "co-opts" the BCR to signal (Schweighoffer et al., 2013). Interestingly, constitutively active PI3K failed to rescue survival of Syk-deficient B cells, but both PTEN deficiency and constitutively active MEK could rescue these cells (Schweighoffer et al., 2013). It could be that Syk-deficient B cells have just enough PI3K signaling to synergize with MAPK activation and promote survival. The discrepancy between constitutively active PI3K and PTEN deficiency with regards to rescue of Syk-deficient B cells also suggests that these cells are especially sensitive to the quantity of PI3K signaling. Furthermore, the different phenotypes observed in BCR- and Syk-deficient B cells indicate that B cell survival requires signals outside of the PI3K pathway. While the exact nature of these signals is unclear, they are likely Btk-independent because survival of mature follicular B cells is unaffected by inducible Btk deletion (Nyhoff et al., 2018).

The role of the BCR in B cell survival goes beyond its mere presence or absence; the amount of BCR expressed on the surface of mature B cells modulates B cell survival. A recent study identified a mutation in IgD, *dmit*, which prevents pairing of light chains with the IgD BCR and abolishes IgD surface expression without compensatory surface IgM upregulation (Sabouri et al., 2016). *Dmit* B cells have 65% less surface receptor than WT B cells and compete poorly for survival in the mature B cell compartment. Thus, tonic signals from the BCR can quantitatively promote B cell survival.

B cell survival is also influenced by the autoreactivity of a given B cell. For example, two studies of autoreactive BCR transgenic models found that autoreactive B cells depend upon elevated BAFF levels for survival (Lesley et al., 2004; Thien et al., 2004). However, when these autoreactive B cells are forced to compete with non-autoreactive competitor cells for a common

and limited supply of BAFF, their survival is greatly impaired. BAFFR signaling activates non-canonical NFκB, while the canonical NFκB pathway is activated downstream of the BCR (Gardam and Brink, 2014). Lesley et al. found that autoreactive B cells forced to compete with non-autoreactive B cells display less activation of the non-canonical NFκB pathway than they do in the absence of competition, implying reduced BAFFR signaling in this context. They went on to show that loss of autoreactive cells in competition could be rescued by increasing the supply of BAFF.

Cross talk between BCR and BAFF signaling also goes the other way. Tonic BCR signals indirectly enable BAFF/BAFFR signaling because canonical NFκB upregulates a key substrate of the non-canonical pathway, p100 (Stadanlick et al., 2008). BCR signaling mutants also indirectly influence the ability of B cells to receive BAFF signals; B cells with increased CD45 (and thus increased BCR signaling) display reduced levels of BAFF receptor and reduced survival in competition (Zikherman et al., 2012a).

Given the inextricable role of BCR signaling in normal B cell development and survival, BCR signaling mutants represent a key class of mice used to model B cell-mediated autoimmune disease. However, an understanding of the range of tolerance mechanisms that eliminate and restrain autoreactive B cells is necessary in order to fully interpret autoimmune phenotypes in BCR signaling mutants. The next section describes tolerance mechanisms identified in transgenic mice engineered to express autoreactive BCRs.

Transgenic BCR models reveal mechanisms of B cell tolerance

The random nature of heavy and light chain recombination comes with a risk of generating autoreactive BCRs. Two seminal studies published in 1993 discovered a phenomenon

called receptor editing, a process in which autoreactive B cells undergo a new round of light chain rearrangement in order to reduce or abolish their autoreactivity. The 3H9 model system expresses transgenic dsDNA-reactive heavy and light chains originally cloned from MRL/*lpr* lupus-prone mice (Gay et al., 1993). Very few peripheral B cells generated in young 3H9 mice express both the transgenic heavy and light chain, but older mice have a B cell population that expresses the 3H9 heavy chain with endogenous (non-3H9) light chains. This led the authors of this study to conclude that autoreactive B cells can rearrange additional light chains to escape deletion. In the same journal issue, an independent group published a different transgenic model with very similar conclusions (Tiegs et al., 1993). The 3-83 μ/δ model expresses transgenic heavy and light chains that recognize the H-2K^{k,b} alleles of MHC-I. When crossed onto a background that expresses either H-2K^{k} or H-2K^{b} ubiquitously, there is a severe reduction in idiotype-positive (expressing both the transgenic heavy and light chains) cells in the spleen and lymph nodes. The B cells that develop in these "centrally deleting mice" express non-transgenic (endogenous) light chains, many of them from the Igλ locus. These mice also have elevated RAG-1/2 but not TdT expression in the bone marrow. By contrast, 3-83 mice that express H-2K^{b} in only the liver, kidney, and pancreas (MT-K^{b}; "peripherally deleting") display a reduced percentage of idiotype-positive B cells but no increase in the frequency of Igλ^{+} cells. This suggests that receptor editing can occur in the bone marrow but not in peripheral B cells. A follow up study found that immature 3-83 B cells in the bone marrow are primed to undergo receptor editing; treatment of these cells with anti-idiotype antibody did not cause death or proliferation but instead induced upregulation of RAG-2 and promoted endogenous light chain rearrangement (Hertz and Nemazee, 1997). Hertz and Nemazee observed similar RAG-2 upregulation and receptor editing following BCR ligation in non-transgenic immature bone

marrow B cells. A mouse with the 3-83 transgenes knocked into the endogenous BCR locus was later generated and confirmed that this phenomenology is not an artifact of the transgene's integration site and also ruled out heavy chain rearrangement as a tolerance mechanism in this model (Pelanda et al., 1997).

A different set of transgenic mouse models helped characterize a complementary set of tolerance mechanisms employed by B cells that constitutively encounter cognate antigen *in vivo*: anergy and deletion. In a seminal study, Goodnow et al. generated transgenic mouse lines that express BCRs specific for hen egg lysozyme (HEL) and lines that constitutively express the cognate antigen (Goodnow et al., 1988). When the BCR transgene (MD-4) is crossed onto a HEL-expressing background (ML-5), B cells make it to the periphery but do not secrete high levels of anti-HEL IgM at steady state or in response to HEL-SRBC immunization. This stands in contrast to MD-4 mice, which secrete high levels of anti-HEL IgM under both conditions. The functional silencing of MD-4/ML-5 B cells is termed clonal anergy, and these cells have additional characteristics, including impaired BCR signal transduction (discussed in a subsequent section) and selective IgM downregulation. Specifically, MD-4/ML-5 anergic B cells maintain a high level of surface IgD expression but strongly downregulate surface IgM (Goodnow et al., 1988). In a follow-up study, HEL-specific BCRs were crossed onto a different background (ML-3) that constitutively expresses lower levels of HEL but can be induced to express additional HEL with zinc treatment (Goodnow et al., 1989). In this system, increases in serum HEL led to downregulation of surface IgM on HEL-specific B cells. Furthermore, the authors describe a different transgenic line (MD-5) that does not downregulate surface IgM in the presence of chronic cognate antigen stimulation, and these mice break tolerance and secrete high levels of serum anti-HEL IgM. While the mechanism is unclear, the authors speculate that IgM

downregulation might be an important feature of B cell tolerance, and they observe that non-transgenic mice have a population of IgD^{hi} IgM^{lo} B cells that might represent a naturally-occurring anergic population (Goodnow et al., 1989).

Another set of studies demonstrated that the nature of cognate antigen and developmental stage of antigen encounter shape the fate of autoreactive B cells. For example, if HEL is constitutively expressed in a membrane-bound form throughout the mouse, HEL-specific B cells undergo deletion and fail to progress beyond the immature stage of development in the bone marrow (Hartley et al., 1991). Indeed, treatment of non-transgenic bone marrow immature or splenic immature B cells with anti-IgM leads to rapid induction of apoptosis (Norvell et al., 1995). While this finding differs from what happens when immature 3-83 B cells are treated with anti-idiotype antibody (Hertz and Nemazee, 1997), it is possible that the dose and affinity of the stimulatory antibody explain the discrepancy. Furthermore, the MD-4 transgene is not incorporated into the endogenous BCR locus, which may disfavor receptor editing in MD-4/ML-5 B cells. Rapid death of autoreactive B cells can also be induced if these cells are subjected to competitive pressures. When MD-4 or MD-4/ML-5 B cells are introduced into an ML-5 mouse (with endogenous polyclonal B cells), the transferred cells are excluded from the B cell follicles and rapidly die off (Cyster and Goodnow, 1995). As alluded to earlier, it was subsequently shown that this is due to heightened dependence on BAFF for survival of autoreactive B cells, a feature that is unmasked in a competitive setting (Lesley et al., 2004; Thien et al., 2004). Thus, autoreactive B cells can be pruned from the repertoire by negative selection during development or by poor competitive fitness and greater BAFF dependence once mature, or they can be maintained in an anergic or functionally unresponsive state.

MD-4/ML-5 B cells display a marked impairment in BCR signaling that is separable from surface IgM downregulation. When stimulated with soluble HEL, MD-4/ML-5 B cells display reduced calcium entry and global protein phosphorylation compared to MD-4 B cells (Cooke et al., 1994). Because MD-4/ML-5 B cells strongly downregulate IgM, some of this impaired signaling could be explained by reduced surface receptor expression. Cooke et al. addressed this in two ways. First, they transferred MD-4/ML-5 B cells into non-HEL-expressing mice for 36 hours. In this setting, the cells regained normal levels of surface BCR but still displayed impaired calcium mobilization. Second, they stimulated MD-4/ML-5 B cells through IgD, which is maintained at a high level on these cells, and found that global protein phosphorylation is still impaired. MD-4/ML-5 B cells still mobilized calcium in response to anti-IgD, although the calcium increase was not sustained as long as it was in MD-4 B cells. Pathway-specific impairment of BCR signaling was examined in more detail in a follow-up study (Healy et al., 1997). MD-4/ML-5 B cells display elevated basal calcium, but this elevation is lost when the cells are transferred into mice without HEL for 50 hours. Healy et al. also found that MD-4/ML-5 B cells efficiently phosphorylate ERK in response to anti-IgD, but they do not phosphorylate JNK1 or activate the NFκB pathway. These perturbations in BCR signaling may contribute to the impaired antibody responses of immunized MD-4/ML-5 mice.

It is important to confirm that the anergic phenotypes observed in the MD-4/ML-5 model are also present in model systems with different BCR specificities and cognate antigens. A complementary model, Ars/A1, utilizes a heavy and light chain transgene that recognizes the p-azophenylarsonate (Ars) hapten (Benschop et al., 2001). In this model, there does not appear to be appreciable receptor editing, and the transgene mediates strong enough allelic exclusion that very few B cells express endogenous heavy chains. Somewhat surprisingly, these mice fail to

respond to Ars-KLH immunization, and their B cells display impaired BCR signaling and surface phenotypes characteristic of anergic B cells, including selective IgM downregulation. The constitutive upregulation of activation markers on Ars/A1 B cells suggests that they recognize an endogenous antigen. The affinity of the BCR for this endogenous antigen is low because treatment with 10^{-4} M monovalent Ars-conjugated tyrosine abolishes both responsiveness to Ars_8-BSA and basal activation; the affinity of the BCR for Ars hapten is 2.36 x 10^{-5} M (Sharon, 1990). These affinities are several orders of magnitude weaker than the IgHEL BCR's affinity for HEL (2 x 10^{-9} M) (Goodnow et al., 1988), making commonalities shared by both models more generalizible. The authors performed a competitive binding assay and found that the Ars/A1 antibody weakly recognizes single-stranded DNA, but it is unclear whether this is the only relevant autoantigen recognized by Ars/A1 B cells *in vivo* (Benschop et al., 2001).

While MD-4/ML-5 B cells and Ars/A1 B cells are similar with regards to surface IgM downregulation and reduced antibody production upon immunization, they differ with regards to the reversibility of their anergic phenotypes. When MD-4/ML-5 B cells are transferred to a HEL-deficient host, they take between 1-4 days to upregulate IgM expression, and they still display reduced antibody responses even 10 days after transfer (Goodnow et al., 1991). This would suggest that at least some anergic characteristics are "hardwired" into MD-4/ML-5 B cells. Indeed, MD-4/ML-5 B cells upregulate PTEN expression and display reduced calcium and PI3K signaling upon BCR stimulation (Browne et al., 2009). Illustrating the importance of PTEN upregulation in this model, Browne et al. found that deletion of PTEN completely restored calcium signaling, partially restored PI3K activity, and restored steady state antibody secretion by MD-4/ML-5 B cells. By contrast, the anergic phenotypes of Ars/A1 B cells are more rapidly reversible; the elevated basal calcium in Ars/A1 B cells falls within seconds of treatment with

monovalent Ars/Tyr, and 20 minutes of treatment with Ars/Tyr restores some responsiveness towards anti-IgM (Gauld et al., 2005). Furthermore, while Ars/A1 B cells display poor survival *in vitro*, treatment with Ars/Tyr improves their survival at 48 hours (Gauld et al., 2005). Despite the rapid reversibility of anergy in Ars/A1 mice, their anergic phenotype still requires a certain degree of inhibitory tone. Deletion of either SHIP-1 or SHP-1 breaks tolerance in Ars/A1 mice, leading to robust plasma cell differentiation and antibody secretion (Getahun et al., 2016). It does not appear that SHIP-1 in Ars/A1 B cells is elevated above the level seen in WT B cells (Getahun et al., 2016), and Ars/A1 B cells also express WT levels of PTEN (O'Neill et al., 2011). This suggests that a "normal" level of inhibitory tone is sufficient to restrain Ars/A1 B cells, while additional inhibitory tone is required to restrain MD-4/ML-5 B cells.

To summarize, transgenic BCR models have revealed a series of tolerance checkpoints and strategies that are employed to restrain autoreactive B cells: receptor editing, deletion, poor survival, IgM downregulation, and upregulation of negative regulators of BCR signaling. The next section will examine whether and where these processes occur in the polyclonal B cell repertoires of humans and non-BCR-transgenic mice.

Naturally-occurring autoreactive and anergic B cells

A seminal study in the Nussenzweig lab cloned BCRs from human B cells at sequential stages of development and analyzed their autoreactivity (Wardemann et al., 2003). Polyreactive BCR specificities (defined as binding to more than one of ssDNA, dsDNA, insulin, and LPS) make up 55% of early immature B cells, but they only make up 7% of T1 and 4% of mature B cells, suggesting that a major tolerance checkpoint prunes this autoreactivity in immature bone marrow B cells. By contrast, broader anti-nuclear (ANA) reactivity starts at 75% in early

immature B cells, decreases to 40% in T1 B cells, and falls to 20% in mature-naïve B cells. The authors noted that ANA-reactive BCRs tend to have long CDR3 sequences, and these long CDR3 sequences are counter-selected as cells progress through development. The drop in ANA reactivity between the T1 and the mature stage of development illustrates two key points: a second set of tolerance mechanisms is employed at this transition, and pruning of autoreactivity is incomplete. Furthermore, ANA assays only capture a limited range of specificities, and the assays employ arbitrary cutoffs to delineate ANA reactivity. As a result, the proportion of human B cells that are "autoreactive" may be well over 20% and may exist along a continuum.

A subsequent study identified a human B cell population (B_{ND}) that makes up 2.5% of human recirculating B cells and expresses high surface IgD but no detectable surface IgM (Duty et al., 2009). Cloning of these BCRs revealed that 16% of them are reactive towards dsDNA and 75% are ANA-reactive, figures much higher than what was calculated for the bulk mature recirculating population (Duty et al., 2009; Wardemann et al., 2003). Notably, B_{ND} cells appear to be mature-naïve B cells because they don't express markers associated with immaturity, activation, or GC/PC differentiation, and they have no evidence of somatic hypermutation or clonal relation (Duty et al., 2009). While they have the same rate of Igλ usage as bulk naive B cells, they do have longer CDR3 sequences, which were previously found to be associated with increased polyreactivity (Ichiyoshi and Casali, 1994). Consistent with their autoreactivity, B_{ND} cells display elevated basal intracellular calcium. Furthermore, B_{ND} cells display reduced tyrosine phosphorylation and calcium signaling in response to both anti-IgM and anti-IgD, despite having normal IgD expression (Duty et al., 2009). This suggests that B_{ND} cells have rewired signaling, but it is unclear which negative regulators of BCR signaling are upregulated in B_{ND} cells. Another study found that $IgD^{+}IgM^{lo}$ B cells from human blood share many phenotypes

with B_{ND} cells; they express mature B cell markers, do not express activation markers, and their BCR signaling is dampened (Quach et al., 2011). However, their anergic signaling phenotype is less dramatic in response to anti-IgD stimulation than it is in response to anti-IgM. This suggests that the rewiring occurs on a spectrum and is most profound in cells with the lowest surface IgM expression, and possibly the greatest degree of self-reactivity. Potentially linking this population to human disease, Quach et al. found that $IgD^{+}IgM^{lo}$ cells in SLE patients express elevated CD22 and decreased CD95 relative to healthy patients. However, it is unclear what drives this change in surface phenotype and whether it is necessary for disease pathogenesis.

Naturally-occurring autoreactive B cells in unperturbed mice have been described in a similar fashion. The Cambier lab observed that both MD-4/ML-5 and Ars/A1 mice have an expanded number of T3 ($B220^{+}CD93^{+}CD23^{+}IgM^{lo}$) B cells, a population they characterized in non transgenic mice and named An1 B cells (Merrell et al., 2006). After stimulating An1 B cells with LPS and performing ELIspot assays, they found that this population is enriched for ssDNA and Smith antigen-reactive B cells. Furthermore, An1 cells stimulated with anti-IgM have decreased calcium responses relative to Fo B cells, even when gating on equivalent IgM expression (Merrell et al., 2006). The intrinsically dampened signaling in An1 B cells suggests that they might be rewired, much like MD-4/ML-5 B cells. However, Merrell et al. did not examine upregulation of PTEN, SHIP-1, or SHP-1 in An1 B cells, so it is unclear what mediates their decreased signaling.

Another key model system utilizes a BAC transgene that expresses GFP under the control of the regulatory region of the immediate early gene, Nur77/*Nr4a1* (Zikherman et al., 2012b). Importantly, BCR-antigen recognition is both necessary and sufficient for induction of the Nur77-eGFP reporter; GFP expression is lost in B cells forced to express IgHEL BCR, and

expression is reconstituted by constitutive expression of the cognate ligand, sHEL. Moreover, GFP^{hi} mature B cells are enriched for ANA-reactive BCRs. Illustrating the reporter's usefulness for studying B cells with different levels of autoreactivity, surface IgM is inversely correlated with reporter expression, but IgD levels are consistent across the repertoire. Similar to An1 cells, GFP^{hi} Fo B cells display reduced calcium responses after anti-IgM stimulation, but unlike An1 cells, this defect is absent when comparing GFP^{hi} and GFP^{lo} B cells with identical surface IgM expression. Thus, the Nur77-eGFP reporter marks B cells that are anergized solely through selective IgM downregulation. This suggests that the MD-4/ML-5 model generates highly autoreactive B cells that rely upon biochemical rewiring to restrain them, but such specificities may be exceedingly rare in the physiological mature B cell repertoire. Conversely, naturally-occurring autoreactive B cells exhibit a much milder degree of self-reactivity that does not trigger profound anergy, but is adequately controlled by IgM downregulation.

Thus, evidence for both central and peripheral tolerance can be observed in polyclonal repertoires in the absence of BCR transgenes. However, autoreactivity is still present in the B cell repertoires of healthy humans and mice. This indicates that mechanisms of B cell anergy are sufficient to restrain most of this remaining autoreactivity. An examination of BCR signaling mutants reveals ways in which these tolerance mechanisms can be broken and unleash autoantibody production.

B cell tolerance in BCR signaling mutants

While transgenic models represent a powerful tool for identifying potential tolerance mechanisms, humans and (wild) mice have extremely diverse BCR repertoires. Furthermore, mutations in BCR signaling are increasingly appreciated as drivers of autoantibody production in

patients with diseases such as SLE (Chen et al., 2017; Zikherman and Lowell, 2017). Numerous models of mice with perturbed BCR signaling exist, and some (but not all) develop lupus-like diseases. Given that tolerance mechanisms are dependent on BCR signaling, it should be no surprise that tolerance is perturbed in BCR signaling mutants. As the following examples illustrate, autoantibody production is highly dependent on whether a signaling mutant enhances or dampens BCR signaling and the developmental stage at which perturbation takes place. Specifically, selective loss of inhibitory signaling is highly associated with lupus-like disease in mice.

Global loss of inhibitory signaling

Three germline knockouts of Lyn were described in rapid succession. The first paper found that *Lyn*$^{-/-}$ mice have normal numbers of immature B cells, reduced numbers of mature B cells, and elevated serum IgM, and these mice develop severe glomerulonephritis with IgG immune complex (IC) deposition in the kidneys (Hibbs et al., 1995). A second group also observed a reduction in mature B cell numbers and development of glomerulonephritis in *Lyn*$^{-/-}$ mice (Nishizumi et al., 1995). A third group found that B cells in *Lyn*$^{-/-}$ mice have enhanced proximal BCR signaling *in vitro* and increased turnover (decreased survival) *in vivo* (Chan et al., 1997). Mice with conditional deletion of Lyn in B cells were subsequently generated and displayed many of the same phenotypes: enhanced BCR signaling, reduced B cell numbers, reduced surface IgM, and IC complex deposition in the kidneys (Lamagna et al., 2014). Despite having enhanced signaling in mature B cells, *Lyn*$^{-/-}$ mice only have a minimal increase in receptor editing, likely because *Lyn*$^{-/-}$ B cells do not display enhanced signaling at the immature stage of development (Gross et al., 2009). This lack of enhanced signaling in immature B cells was also demonstrated for *CD22*$^{-/-}$ and *SHP-1*$^{-/-}$ B cells, and SHP-1 conditionally-deficient B

cells do not have an increase in lambda chain usage (Gross et al., 2009; Pao et al., 2007). These observations are consistent with the finding that Lyn, CD22, and SHP-1 work in concert to quantitatively inhibit BCR signaling (Cornall et al., 1998). This also illustrates how inhibitory tone is acquired in a developmental stage-dependent manner; this negative regulatory network is not expressed early in development when receptor editing and deletion take place, but it is present at the stage at which anergic B cells need to be restrained. Teleologically, it would make sense to permit strong signaling during central tolerance and then dampen signaling when aberrant B cell activation would be harmful. Additional examples of positive and negative perturbations in BCR signaling further illustrate this distinction.

Loss of specific inhibitory receptors and mediators

CD22 deficiency drives many phenotypes similar to those observed in *Lyn*$^{-/-}$ mice. Two independently generated *CD22*$^{-/-}$ mouse lines displayed a reduction in mature recirculating B cells and enhanced calcium signaling in B cells (Nitschke et al., 1997; Sato et al., 1996). CD22 deletion promotes a gene dosage-dependent downregulation of surface IgM on mature B cells; *CD22*$^{-/-}$ B cells strongly downregulate surface IgM and only modestly downregulate surface IgD, and *CD22*$^{+/-}$ B cells express an intermediate level of surface IgM (Sato et al., 1996). Similar to *Lyn*$^{-/-}$ B cells, *CD22*$^{-/-}$ mature B cells have a reduced lifespan, as determined by steady-state BrdU incorporation (Nitschke et al., 1997). Thus, *CD22*$^{-/-}$ B cells engage the tolerance mechanisms of reduced lifespan and surface IgM downregulation, but these mechanisms are insufficient to dampen BCR signaling to WT levels. *CD22*$^{-/-}$ mice break tolerance and develop anti-dsDNA IgG autoantibodies starting at 10 months of age with variable penetrance, a phenotype that is milder than what is observed in *Lyn*$^{-/-}$ mice (O'Keefe et al., 1999). Going downstream of CD22, SHP-1-mutant (*motheaten*) mice die between 3 and 8 weeks of age and

display characteristics of severe immunodeficiency (Green and Shultz, 1975; Shultz et al., 1993). The poor viability of SHP-1 mutant mice necessitated generation of conditional knockout mice to study the phosphatase's role in B cell autoimmunity. Mice that lack SHP-1 in B cells are viable, though their B cell compartment is abnormal; almost all peripheral B cells take on a $CD5^+$ B1a phenotype, and the conventional B2 cells that develop have incomplete deletion of SHP-1 (Pao et al., 2007). Splenic SHP-1-deficient B cells have decreased surface IgM and IgD, though the low IgD expression could be a feature of the B1a lineage phenotype. Similar to *Lyn*$^{-/-}$ mice, mice with B cell conditional deletion of SHP-1 have enhanced BCR signaling and develop anti-dsDNA autoantibodies at 5-7 months of age (Pao et al., 2007). While SHP-1 and Lyn are both involved in CD22-mediated inhibitory signaling, their loss likely promotes a more robust autoimmune phenotype than CD22 loss does because they both play a role in other inhibitory pathways, such as Siglec-G and FCγRIIB.

FCγRIIB$^{-/-}$ mice develop a highly-penetrant disease at 8-10 months characterized by anti-dsDNA and anti-dsDNA-H2A/2B antibodies, IC deposition in the kidneys, and glomerulonephritis (Bolland and Ravetch, 2000). While the phenotype tracks with FCγRIIB-deficient B cells transferred into *FCγRIIB*$^{+/+}$ (but B cell deficient) mice, Balb/C and Balb/C x C57BL/6 F1 mice are completely protected from disease (Bolland and Ravetch, 2000). Crossing the 56R transgene (a high affinity version of 3H9) onto the C57BL/6 and Balb/C backgrounds revealed that Balb/C mice more efficiently edit to light chains that abolish dsDNA reactivity (Fukuyama et al., 2005). However, Fukuyama et al. found that FCγRIIB deficiency did not alter the efficiency of light chain editing in B6.56R mice. Thus, FCγRIIB acts primarily at the level of peripheral tolerance, and its loss can exacerbate defects in central tolerance.

Perturbations in positive regulators of BCR signaling

Mutations in positive regulators of BCR signaling also influence tolerance checkpoints. Repertoire sequencing in XLA patients (who have Btk deletions or hypomorphic mutations) revealed that these patients have a distinct BCR repertoire enriched for autoreactive clones (Ng et al., 2004). *Btk*$^{-/-}$ mice have a defect in receptor editing and a 50% reduction in frequency of Igλ^+ B cells, while mice that express constitutively active Btk^{E41K} have an increase in lambda chain usage (Dingjan et al., 2001; Middendorp and Hendricks, 2004). *PLCγ2*$^{-/-}$ mice largely phenocopy *Btk*$^{-/-}$ mice: they have reduced lambda chain usage, and surface IgM is increased on IgD$^+$ splenocytes (Bai et al., 2007). Despite these impairments in B cell tolerance, Btk reduction or elimination is not considered of a driver of autoimmune disease. XLA patients, who have mutations that eliminate or render Btk non-functional, are not predisposed to autoimmune disease (Smith et al., 2007). Instead, Btk deletion or reduction can ameliorate autoantibody production in autoimmune-prone mice such *Lyn*$^{-/-}$ and SHP-1 mutants (Satterthwaite et al., 1998b; Scribner et al., 1987). Several Btk inhibitors are also being studied as potential therapeutic agents in autoantibody-mediated disease (Akinleye et al., 2013). By contrast, elevated Btk activity can promote autoimmune disease. Mice with transgene-driven Btk overexpression have enhanced BCR signaling, downregulate IgM expression on IgD$^+$ splenocytes, have spontaneously expanded germinal center and plasma cell compartments, and develop a lupus-like disease with kidney pathology (Kil et al., 2012). Thus, hyperactivation of Btk signaling can still break tolerance in the face of enhanced central tolerance.

Modulation of CD45 expression also perturbs B cell tolerance. In an allelic series of CD45 expression, lambda chain usage in immature bone marrow B cells increases along with CD45 levels, and surface IgM expression on mature B cells falls with increasing CD45 (Zikherman et al., 2012a). Mice with the highest levels of CD45, H/H, have a diminished mature

B cell compartment, possibly due to decreased expression of BAFFR on these cells. However, enhanced deletion also plays a role in shrinking this compartment because H/H B cells in chimeric H/H:WT/WT mice have a sharp drop in competitive fitness at the T1-T2 transition (Zikherman et al., 2012a). A role in CD45 in regulating B cell turnover and fitness is further supported by the finding that removal of CD45 in MD-4/ML-5 B cells reduces their normally high turnover rate (Cyster et al., 1996). Conversely, adding soluble antigen improves the accumulation of mature *CD45*$^{-/-}$ MD-4 B cells, but adding membrane bound antigen (which increases the avidity of BCR recognition) still leads to deletion (Cyster et al., 1996). Thus, perturbations in CD45 and BCR-antigen recognition engage different tolerance mechanisms that push the B cell repertoire towards a "goldilocks" level of signaling.

Importantly, superphysiological CD45 expression drives enhanced BCR signaling without promoting autoantibody production (Zikherman et al., 2013). This stands in marked contrast to *Lyn*$^{-/-}$ and *CD22*$^{-/-}$ mice, which display enhanced BCR signaling and develop autoantibodies. All of these mice (and MD-4/ML-5 mice) employ common tolerance mechanisms such as surface IgM downregulation and reduced mature B cell life span. Thus, hyperactive signaling and high-affinity autoantigen recognition are sufficient to trigger these tolerance mechanisms. In the case of MD-4/ML-5 mice and mice with superphysiological CD45 expression, these tolerance mechanisms combine with inhibitory signaling to restrain autoantibody production. However, loss of inhibitory signaling in *Lyn*$^{-/-}$ and *CD22*$^{-/-}$ mice is able to overcome these tolerance mechanisms and promote autoantibody generation. Furthermore, as described above, Btk overexpression leads to autoimmune disease. The discrepancy between Btk and CD45 overexpression is likely due to the fact that CD45 activates Lyn (and subsequent inhibitory signaling), while Btk lies downstream of Lyn and therefore selectively enhances

positive signaling. In this way, the balance of activating and inhibitory signaling plays a crucial role in enforcing B cell tolerance.

Analysis of these signaling mutants highlights the resiliency of B cell tolerance mechanisms. Mice with decreased BCR signaling at early stages of development might have a more autoreactive repertoire due to reduced receptor editing, but this weak signaling carries over to the mature stage of development and disfavors B cell activation. Conversely, enhanced BCR signaling can be counteracted by increased receptor editing, decreased survival, and surface IgM downregulation. The most dramatic breaks in tolerance occur when BCR signaling is selectively enhanced at later stages of development (*Lyn*$^{-/-}$ and *SHP-1*$^{-/-}$) and earlier tolerance checkpoints are not compensatorily enhanced. This suggests that the inhibitory tone acquired at the mature stage of B cell development plays an important role in restraining autoantibody production. Notably, IgD expression is highest at precisely the stage when inhibitory tone is acquired, and IgM is downregulated on autoreactive B cells and B cells that experience enhanced signaling. This raises the central question of whether predominant IgD expression restrains autoreactive B cells and whether it plays a role in their survival. How would switching to predominant IgD expression affect the signals a B cell receives?

IgM and IgD signaling

As IgM and IgD are both B cell receptors that transmit biochemical signals, a detailed examination of how each isotype signals may provide insight into non-redundant isotype functions. This section begins with a historical analysis of mice that express HEL-specific IgM or IgD alone, highlighting the *in vivo* phenotypes each isotype can drive. Then biochemical properties of IgM and IgD signaling will be covered, followed by a detailed analysis of a series

of studies that examined BCR clustering and co-localization with co-receptors on the cell surface. The final part of this section will examine how the BCR senses different forms of antigens and how IgM and IgD might differ in this regard.

The first study to directly probe *in vivo* responsiveness of IgM and IgD BCRs to bona fide antigens utilized HEL-specific IgM (MM-7) and HEL-specific IgD (DD-6) BCR transgenic mice (Brink et al., 1992). In the absence of cognate antigen, these BCRs drove allelic exclusion of endogenous heavy chains, promoted B cell development to maturity, and generated normal follicular and marginal zone architecture. MM-7 and DD-6 B cells bound equivalent amounts of HEL across a broad dose titration, and mice expressing each receptor secreted antibodies in response to HEL immunization and LPS treatment. As with MD-4 mice (described earlier), both lines of mice had reduced steady state anti-HEL antibody titers when crossed onto the HEL-secreting ML-5 background. Consistent with an anergic phenotype, neither MM-7/ML-5 nor DD-6/ML-5 mice showed a boost in anti-HEL antibody titers upon immunization with SRBC-conjugated HEL. Furthermore, both DD-6 and MM-7 B cells failed to reach the mature stage of development in bone marrow chimeras expressing membrane-bound HEL, indicating that deletion is intact for both isotypes. The only notable difference between the lines was receptor downregulation in the presence of soluble cognate antigen. On the ML-5 background, MM-7 B cells downregulated surface IgM 34-fold, but DD-6 B cells only downregulated surface IgD 4.3-fold. For reference, MD-4 B cells downregulated surface IgM 75- fold and surface IgD 1.4-fold on the ML-5 background. These findings suggest that while IgM downregulation is more pronounced in the presence of IgD, its downregulation on anergic cells is a receptor-intrinsic property. In a follow-up study, the authors observed that IgD-only HEL-specific B cells express significantly more surface BCR than IgM-only B cells, and this occurs despite lower receptor

mRNA expression (Brink et al., 1995). This efficient surface IgD expression is especially apparent when HEL-specific IgM and IgD are co-expressed, as IgD predominates during co-expression. The authors found that IgM is more efficiently downregulated in response to HEL antigen *in vitro*, and this occurs regardless of whether IgD is co-expressed. Finally, they found that while HEL induced greater CD80/CD86 upregulation in IgD-only B cells, this was entirely accounted for by the higher surface BCR expression. These two studies demonstrate that HEL-specific BCRs of both isotype classes can mediate the same *in vivo* functions, but regulation of surface receptor expression is drastically different.

The first study to directly compare *in vitro* signaling through IgM and IgD BCRs took a reconstitution-based approach in the J558L B cell line (Kim and Reth, 1995a). This cell line expresses Igλ and Igβ but requires the addition of heavy chain and Igα for full BCR assembly and surface BCR expression. The authors transfected J558L cells with IgM and IgD heavy chains that express the B1-8 V_H domain and thus recognize 4-hydroxy-3-iodo-5-nitrophenyl (NIP) hapten. They selected clones with comparable surface receptor levels and stimulated them with NIP-BSA, anti-IgM, and anti-IgD. As demonstrated with a 4G10 blot, the anti-IgM and anti-IgD stimuli produced comparable levels of peak global tyrosine phosphorylation in their respective cell lines. However, global phosphorylation was much stronger in the IgD-expressing cells when both lines were stimulated with either NIP-BSA or anti-idiotype antibody. Regardless of stimulation mode, phosphorylation in the IgM-expressing cells peaked at 1 minute, but phosphorylation in the IgD-expressing cells peaked and remained elevated between 10 and 60 minutes. The authors went on to determine which part of the BCR confers this signaling phenotype. To do so, they made chimeric receptors containing IgG C_γ1-2 and either C_μ4 or C_δ3 (the membrane proximal and transmembrane domains of IgM and IgD). Stimulation with either

antigen or anti-IgG produced similar kinetics to what was observed in the experiments with full-length IgM and IgD; IgD's membrane proximal and transmembrane domains conferred prolonged signaling upon the IgG chimeric receptor. Despite these dramatic findings, the results could be skewed by the use of this particular cell line, which lacks CD19, CD22, and CD45 expression. The authors did not show dose titrations of the different stimuli, nor did they account for surface receptor downregulation, which was a major difference between the IgM and IgD BCRs in the HEL studies (Brink et al., 1995; Brink et al., 1992).

The intersection between BCR signaling and IgM and IgD surface expression is poignantly illustrated by a study in a fibroblast cell line that found that IgM absolutely requires Igα/β for surface expression, but IgD is readily transported to the surface in the absence of Igα/β (Venkitaraman et al., 1991). Indeed, IgD can be expressed in a glycosylphosphatidylinositol (GPI)-linked form on the surface of B cells, and this form has unique signaling properties (Chaturvedi et al., 2002). Chaturvedi et al. observed that while inhibition of calcium influx or PKC activity ablated all BCR-induced activation marker upregulation, PKA inhibition left CD86 upregulation intact while ablating MHC-2, GL-7, and CD80 upregulation. As PKA is activated by cAMP, the authors stimulated B cells and found that anti-IgD induces cAMP production independent of calcium influx or PKC activity. The authors observed that a fraction of IgD is localized in lipid rafts, and either chemical disruption of these rafts or PI-PLC mediated cleavage of GPI-linked proteins ablated BCR-induced cAMP increases without affecting calcium signaling. A similar selective defect was seen in cells treated with mannosamine, an inhibitor of GPI synthesis. Notably, PI-PLC treatment did not appreciably decrease surface IgD expression, but it eliminated most of the IgD partitioning into lipid rafts. In order to confirm that this GPI-linked form of IgD confers cAMP signaling capabilities, they transfected IgD into J558 cells

without Igα (thus forcing expression of the GPI-linked form). In these cells, anti-IgD induces a cAMP increase without inducing calcium signaling. Furthermore, anti-IgD dose titrations revealed that weak BCR simulation induces calcium signaling, but stronger BCR stimulation is required for cAMP increases. Illustrating the importance of this pathway in IgD signaling, PI-PLC treatment ablated nuclear translocation of NFκB and CREB phosphorylation in anti-IgD stimulated cells, but both events were intact in anti-IgM stimulated cells. The defect could be rescued by addition of dibutyryl cAMP, and the rescue is reversed by PKA inhibition, indicating that anti-IgD stimulation induces a cAMP increase that activates PKA, NFκB, and CREB. In many of these experimental setups, the authors also transferred stimulated cells into hosts and found that this pathway is required for anti-IgD stimulated cells to enter the GC. As such, this study provides the first evidence of qualitative differences in IgD signaling that may influence *in vivo* phenotypes.

Interpreting the next studies, which describe co-localization of IgM and IgD with various co-receptors, requires an understanding of the dissociation activation model of BCR signaling. This model was proposed following a study that used bifluorescence complementation assays (BiFC) to study organization of the BCR on resting cells (Yang and Reth, 2010b). This assay involves linking the N terminal domain of YFP (YN) and the C terminal domain of CFP (CC) onto target proteins and then observing whether the proteins are close enough to allow the YFP and CFP fragments to interact and create fluorescent reconstituted YFP (cYFP). The authors validated their system in *Drosophila* S2 cells by showing that complementation occurs when Igα-YN and Igβ-CC are co-expressed with BCR heavy and light chain. The interaction is specific because complementation does not occur when the fragments are expressed on Igα and CD8. Notably, when they co-expressed WT Igβ with Igα-YN, Igα-CC, and the BCR, they observed

complementation, indicating that Igα molecules in neighboring BCRs are in close proximity. The authors went on to define a BiFC efficiency index (with Igα-Igβ interaction set at 100%) in order to study BCR oligomerization when different components are mutated. Because the TM-C domain of IgD is responsible for interacting with Igα/β, the authors wanted to determine whether the other transmembrane portion of IgD, TM-S, is involved in oligomerization. Notably, if they introduce a cysteine-serine mutation in Igα and mutate the TM-S domain of IgD, BCR formation is intact but oligomerization is lost. These non-oligomerized BCRs have unique properties. When Syk and Lyn are expressed, non-oligomerized BCRs induce constitutive protein phosphorylation and are downregulated, but stabilizing them with irreversible BiFC complementation restores high surface expression. Because BiFC-stabilized BCRs display slightly dampened calcium signaling, the authors proposed that oligomerization inhibits BCR signaling. In a follow-up review, the authors provided additional evidence for their model (Yang and Reth, 2010a). First, they note that BCRs can respond to a very diverse array of antigens, and a simple crosslinking model would not explain how all of the antigens could bring the BCRs into the right orientation to initiate signaling. In addition, large monomeric antigens, which presumably can't crosslink the BCR, can induce BCR signaling (Kim et al., 2006). And finally, Yang and Reth argue that their BiFC study and a prior native PAGE biochemical study (Schamel and Reth, 2000) demonstrate that the BCR exists in pre-formed oligomers on resting cells.

An independent study from the Batista lab partially validated and partially contradicted the dissociation activation model (Mattila et al., 2013). This study took advantage of super-resolution microscopy (dSTORM), which uses repeated stochastic activation of small number of fluorophore molecules to construct an image with resolution beyond the diffraction limit of visible light (Rust et al., 2006). Mattila et al. found that both IgM and IgD exist in clusters on the

surface of resting B cells, and the IgD clusters are denser. To better understand the behavior of these clusters, the authors observed their migration during cytoskeletal disruption. Latrunculin A (LatA) and cytochalasin D (CytoD) disrupt the actin cytoskeleton by sequestering actin monomers and capping growing actin filaments, respectively (Braet et al., 1996). Mattila et al. observed that both of these agents can induce calcium influx in B cells, but this influx requires both the BCR and CD19. Notably, LatA treatment did not alter the architecture of the IgD and IgM nanoclusters, and coverslip-bound antigen caused the clusters to grow larger. Therefore, signaling in this model does not require nanocluster dispersal and can take place in the face of *increased* clustering. Instead, the authors found that during cytoskeletal disruption, BCR cluster mobility increases and CD19 recruits Vav, PI3K, and PLCγ2 to induce calcium signaling. They also found that CD19 normally exists in nanoclusters immobilized by the tetraspanin CD81, but cytoskeletal disruption-induced calcium signaling requires CD81 expression. Therefore, the authors proposed that CD81 holds together a network of immobilized CD19 molecules that can interact with mobile BCR nanoclusters upon cytoskeletal disruption. Because actin remodeling occurs during BCR signaling, the authors suggest that encounters between CD19 and BCR nanoclusters are a feature of normal BCR signaling.

As the work by Mattila et al. cast doubt on the dissociation activation model, the next two studies from the Reth lab provided additional evidence for their model. The first of these studies used a proximity ligation assay (PLA) to study membrane receptor organization (Klasener et al., 2014). PLA utilizes oligonucleotide-conjugated antibodies (or Fab fragments) against target proteins, and if these proteins are close enough together, the oligonucleotides can hybridize, undergo rolling circle amplification, and bind a fluorophore-conjugated probe. Since the hybridization event is very sensitive to distance, PLA can probe interactions at different

distances depending on whether Fab fragments, full antibodies, or primary and secondary antibodies are used to label target proteins. Klasener et al. titrated their reagents to generate only a few PLA events per cell, and then analyzed a large population of cells to estimate the number of interactions taking place. Using this approach, they found that BCRs exist in nanoclusters on resting B cells, and the non-oligomerizing IgD-Igα mutant described earlier (Yang and Reth, 2010b) does not generate PLA events. Upon antigen treatment, the number of PLA clusters per cell decreases, which Klasener et al. interpret as an opening of the BCR oligomers. Dose titration of anti-IgM and in the presence and absence of Syk inhibitor revealed that Syk inhibition raises the threshold for disrupting IgM clusters. Finally, they found that CD19 is closely associated with IgD in resting B cells and with IgM in BCR-stimulated B cells. The second study used dSTORM imaging and electron microscopy to examine BCR clusters at rest and during activation (Chandra Maity et al., 2015). This study used "triple knockout" (TKO; RAG/SLP65/λ5-triple deficient) Pro-B cells transduced with HEL-specific IgD and NIP-specific IgM. Both of these BCRs clustered independently on resting cells, and activation with anti-BCR or LatA caused the clusters to shrink and come closer together. They also used PLA to verify that IgM and IgD come in closer proximity during antigen or LatA treatment. Anti-IgM caused only the IgM clusters to shrink, and anti-IgD caused only the IgD clusters to shrink, suggesting that activation of one BCR cluster does not affect the other. The authors posit that these changes in cluster size during B cell stimulation are evidence in favor of a dissociation model of signaling. However, their findings differ from those presented by Mattila et al., which may be in part due to Mattila's use of primary mature B cells instead of *Drosophila* S2 and Pro-B cell lines.

Differential interaction with other co-receptors might lead to differences in IgM and IgD signaling. Similar to the BCR, CD22 exists in nanoclusters on the surface of resting B cells, and

LatA treatment enhances CD22 nanocluster diffusion without disrupting cluster architecture (Gasparrini et al., 2016). Gasparrini et al. quantified the number of CD22, CD19, IgM, and IgD molecules on the surface of resting B cells (65,000, 88,000, 40,000, and 286,000, respectively), and using models membrane area and cluster size, they determined that the inhibitory receptor CD22 is vastly outnumbered by activating receptors CD19, IgM, and IgD. However, they also found that CD22 has an extremely fast diffusion rate, allowing it to rapidly surveil the abundant BCR clusters. This surveillance is modulated by the presence of other co-receptors and sialic acid motifs, which siglecs such as CD22 bind. Notably, CD22 clusters are much bulkier and move more slowly on *CD45*$^{-/-}$ B cells, but enzymatically cleaving off sialic acids shrinks the CD22 cluster sizes. This positive regulation of BCR signaling by CD45 vis-à-vis CD22 mobility is consistent with the finding that phosphatase-dead CD45 rescues many *CD45*$^{-/-}$ B cell phenotypes via modulation of CD22 (Coughlin et al., 2015). Given the importance of CD45 and CD22 in modulating BCR signaling, it is possible that differences in IgM and IgD cluster density might affect the ability of these receptors to access each isotype. One final study examining BCR interactions with other surface receptors found that CXCR4 signaling requires IgD expression (Becker et al., 2017). Notably, CXCL12 (SDF-1; CXCR4's ligand) does not induce calcium signaling or transwell migration in IgD-deficient or Syk inhibitor-treated B cells. However, the defects in *IgD*$^{-/-}$ B cells can be rescued with CD19 crosslinking. Becker et al. also used PLA to determine that CXCR4 co-localizes with the BCR in WT and *IgM*$^{-/-}$, but not *IgD*$^{-/-}$, B cells. They proposed that CXCR4 signals in a Syk-dependent manner and cooperates with IgD and CD19 to promote B cell migration and spreading.

In addition to differential pairing with co-receptors, IgM and IgD signaling and antigen sensing could be influenced by the nature of the antigens B cells encounter. Imaging studies have

found that when B cells encounter an antigen-containing surface, they first spread out and then contract in order to bring antigen into a central aggregate (Fleire et al., 2006). Fleire et al. found that if B cells encounter a sterically-restricted space and are unable to spread, they lose the ability to discriminate between low and high affinity antigens. This spreading is also important to ensure that enough BCR molecules encounter antigen, as B cells detach and abort signaling if an insufficient number of receptors are occupied within 60 seconds. The stiffness of antigen-containing surfaces also influences BCR signaling and spreading. PKCβ activates focal adhesion kinase (FAK) to promote B cell spreading, and stiffness discrimination is lost in FAK-deficient B cells (Shaheen et al., 2017). As PKCβ activation is part of the canonical BCR signaling cascade, there appears to be a feed-forward loop where B cells encounter antigen, initiate low-level BCR signaling that promotes spreading, which can lead to stronger signaling depending on antigen affinity or substrate stiffness. Given the structural differences between IgM and IgD, examining how each isotype interacts with antigen-containing surfaces represents a potentially fruitful avenue of investigation. Indeed, the flexible structure of IgD improves its ability to bind antigen-containing surfaces at low epitope density, but IgM displays better binding at high epitope density (Løset et al., 2004).

The ability of IgM and IgD to sense different forms of soluble antigens is the topic of ongoing investigation and intense debate. A key study in the Jumaa lab found that the flexible hinge of IgD renders it unresponsive to monovalent antigens (Ubelhart et al., 2015). Here, the authors transduced TKO Pre-B cells with IgM and IgD BCRs specific for HEL and NIP. Monomeric HEL and monovalent NIP-peptide could induce calcium signaling in IgM-expressing cells but not IgD expressing cells, but both isotypes responded robustly to HEL complexes or peptides with multiple NIP haptens. In chimeric receptors, the unresponsiveness towards

monvalent antigens was conferred by the IgD hinge; IgM molecules with IgD's hinge could not respond to monomers, and IgD molecules with IgM's hinge could respond to monomers. The authors also replaced IgD's hinge with varying lengths of serine-glycine peptide linkers and found that the longer the hinge, the more weakly the receptor responds to monomeric antigen. The authors went on to explore potential *in vivo* consequences of this phenomenon. They found that B cells from MD-4/ML-5 mice were unresponsive to monomeric HEL but could signal in response to HEL complexes. In addition, spiking in monomeric HEL reduced the responsiveness of IgD to HEL complexes, presumably by blocking access to antigen binding sites. Finally, the authors found that phosphatidylcholine (PtC)-reactive IgD-only cells could not respond to ethanol-solublized PtC lipsomes, but they could respond to intact lipsomes. They speculate that this lack of responsiveness explains the reduction in PtC-reactive peritoneal B cells in $IgM^{-/-}$ mice, although the nature of the actual PtC-containing antigens encountered during B1a development remains unexplored. While this study presented very dramatic phenotypes and elegant model, it is worth emphasizing that much of the mechanistic work was done in TKO Pre-B cells, a cell type that behaved differently from mature B cells in the dSTORM studies described above.

This cell type distinction is important because mature HEL-specific IgM-only and IgD-only B cells both responded robustly to soluble HEL in a subsequent study (Sabouri et al., 2016). This study went on to examine IgM-only (MM-4), IgD-only (DD-6), and IgM/IgD (MD-4) B cells in the presence or absence of chronic cognate antigen. As measured by a gene expression array, MM-4 and DD-6 B cells induced most of the genes upregulated in MD-4 B cells upon exposure to chronic antigen on the ML-5 background. Surprisingly, IgM-only cells induced transcription of several anergy-associated genes more strongly than MD-4 cells despite

expressing less total surface BCR. Because of this, the authors concluded that IgD "attenuates" the anergy program. They went on to explore a potential survival function of IgD in this model. Comparing MM-4/ML-5 mice to MD-4/ML-5 mice, they found that the MM-4/ML-5 mice had a much smaller mature B cell compartment. The same reduction in mature anergized B cells was seen in *Zfp318*$^{-/-}$ MD-4/ML-5 B cells, which cannot express IgD due to defective BCR transcript splicing (Enders et al., 2014). In conclusion, Sabouri et al. proposed that IgD promotes survival of anergic B cells, and it can respond to soluble antigen *in vitro* and *in vivo*.

The conflict between the Ubelhart and Sabouri monomer/multimer studies and a similar conflict between the Mattila and Chandra Maity BCR oligomerization studies illustrate a key point: B cell signaling can vary wildly depending on the model antigen system and cell type used. Features and artifacts of different imaging and stimulation techniques can also produce wildly different results depending on the readout used. For the field to move forward, it is critical to take a step back and look more closely at how B cells respond to bona fide endogenous antigens *in vivo*. How does the dual expression of IgM and IgD on mature B cells affect their ability to sense and respond to these antigens? Do all of these proposed differences in IgM and IgD signaling and clustering have physiological consequences *in vivo*?

Topics to be covered

Chapter 2 will examine the ability of IgM and IgD to sense endogenous antigens in the context of a polyclonal repertoire. Special attention will be paid to the *in vivo* consequences of antigen sensing by IgM and IgD, including B cell development and autoimmune disease progression. Chapter 3 will revisit many of the questions from Chapter 1 in light of these new results and will discuss potential future directions and unanswered questions about the functions of IgM and IgD BCRs. Chapter 3 also introduces additional preliminary data that provide insight

into non-redundant functions of IgM and IgD and could inform future studies of the isotypes. The Appendix will discuss an interesting set of experiments that identified a critical role of the V(D)J locus in permitting autoantibody generation in BAFF transgenic mice.

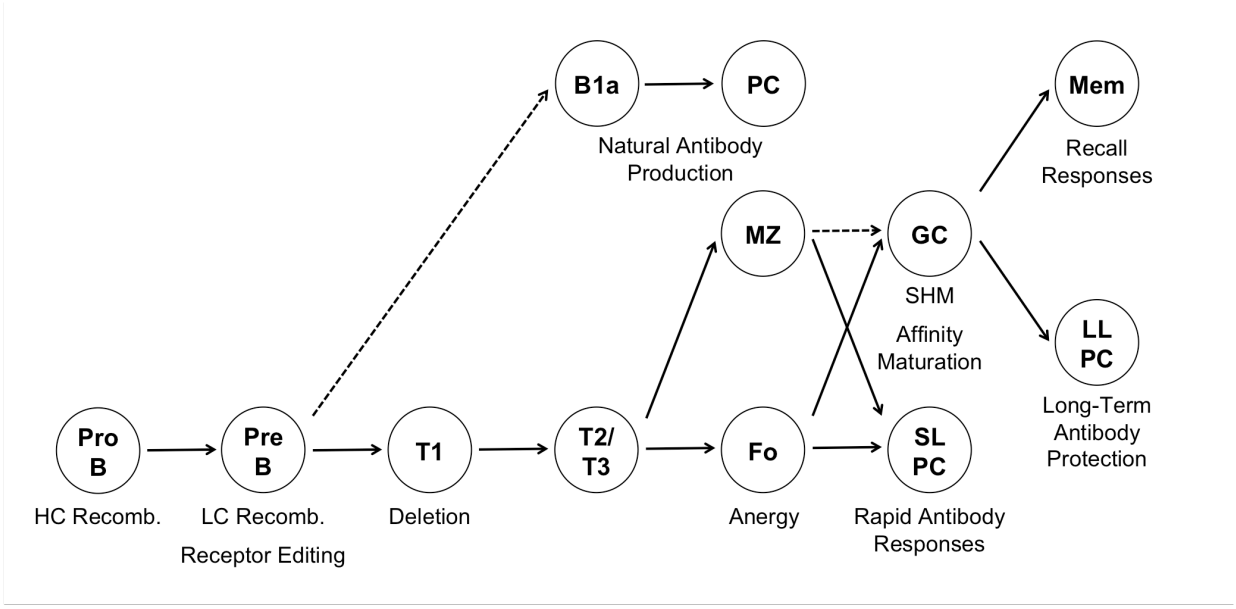
B1a
PC
Natural Antibody
Production
Mem
Recall
Responses
MZ
GC
SHM
Affinity
Maturation
LL
PC
Long-Term
Antibody
Protection
Pro
B
Pre
B
T1
T2/
T3
Fo
SL
PC
HC Recomb.
LC Recomb.
Receptor Editing
Deletion
Anergy
Rapid Antibody
Responses

Figure 1.1. Development and function of B cell subsets.

Schematic of B cell development highlighting functional properties of selected subsets and developmental processes that take place during or between stages. Dashed lines refer to the fetal origin of B1a cells and the propensity of marginal zone B cells to differentiate rapidly into plasma cells. Abbreviations: heavy chain (HC), light chain (LC), recombination (recomb.), plasma cell (PC), marginal zone (MZ), follicular (Fo), germinal center (GC), short-lived plasma cell (SLPC), memory B cell (Mem), and long-lived plasma cell (LLPC).

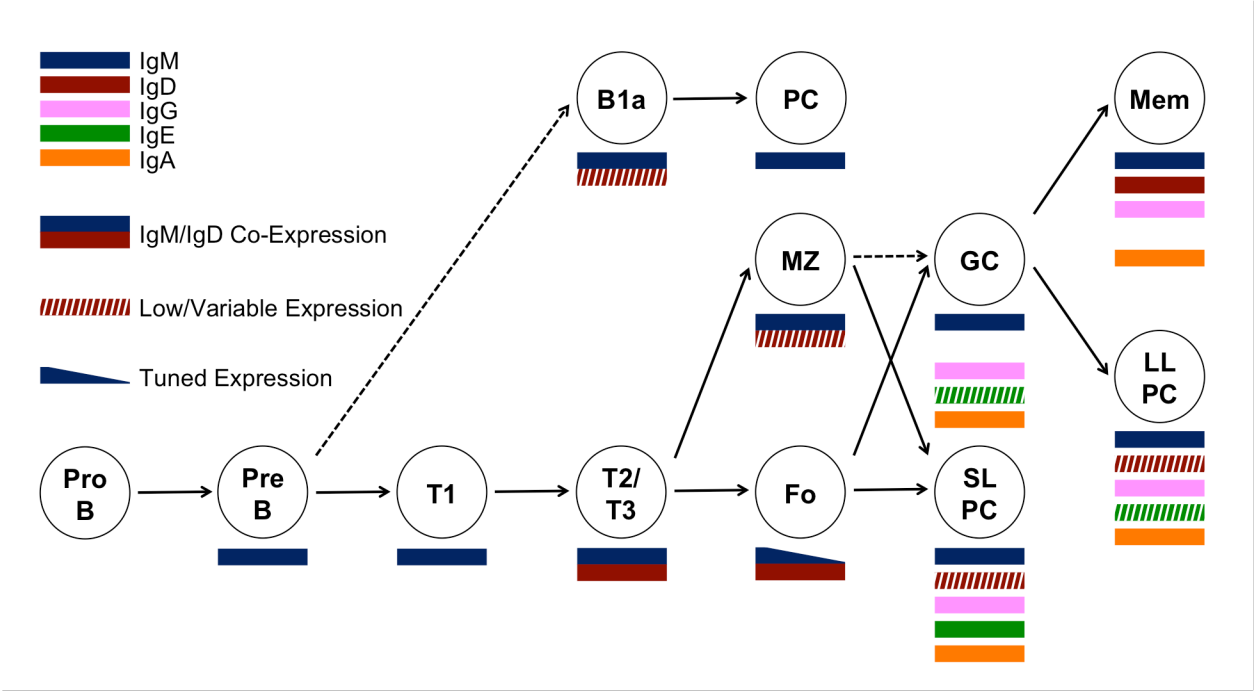
IgM
IgD
IgG
IgE
IgA
IgM/IgD Co-Expression
Low/Variable Expression
Tuned Expression
Pro B
Pre B
T1
T2/ T3
B1a
PC
MZ
Fo
GC
SL PC
Mem
LL PC

Figure 1.2. Expression pattern of BCR isotypes on B cell subsets.

Expression of different BCR isotypes on the subsets defined in Figure 1.1. Pro-B cells do not express surface BCR. Dashed boxes refer to either constitutively low expression of that isotype on a particular subset (e.g. IgD on MZ B cells) or a low frequency of cells that express that isotype within a subset (e.g. IgD^+ PCs, IgE^+ LLPCs). Tuned expression refers to selective downregulation of IgM on Fo B cells that experience high levels of BCR signaling. Note: while some plasma cell populations express detectable surface IgM, isotype expression is primarily intracellular in class-switched plasma cells.

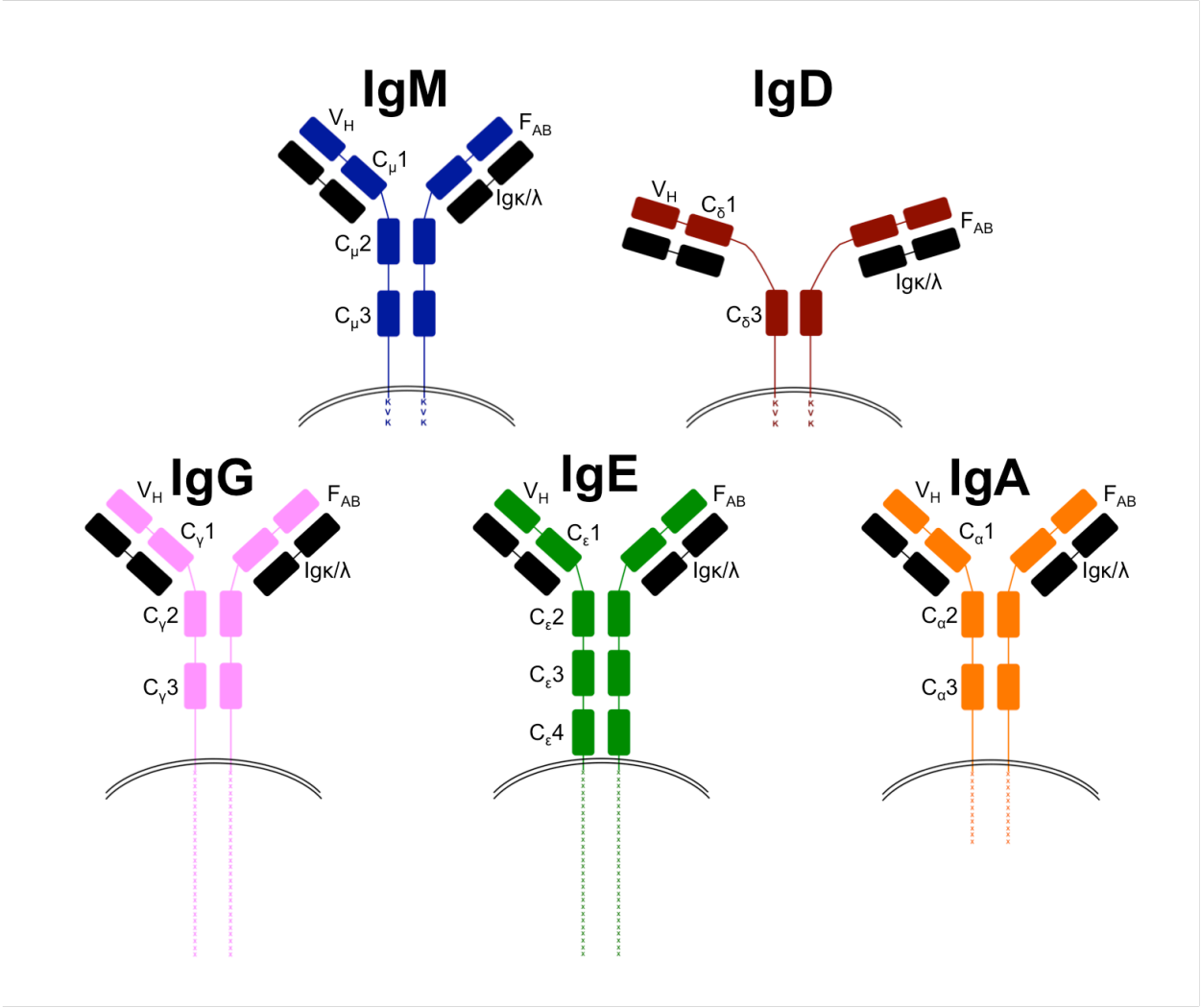
IgM
VH
FAB
Cμ1
Igκ/λ
Cμ2
Cμ3
IgD
VH
Cδ1
FAB
Igκ/λ
Cδ3
IgG
VH
FAB
Cγ1
Igκ/λ
Cγ2
Cγ3
IgE
VH
FAB
Cε1
Igκ/λ
Cε2
Cε3
Cε4
IgA
VH
FAB
Cα1
Igκ/λ
Cα2
Cα3

Figure 1.3. Domain structure of the BCR isotypes.

Structure of mouse Ig isotypes in their membrane-bound forms. The four IgG isotypes differ in their hinge length and the sequence of their intracellular tails, and a consensus structure is shown. F_{AB} refers to the entire antibody structure above the hinge, but the label is placed in close proximity to the antigen-binding domain. Igα/β and GPI-linked IgD are omitted for clarity.

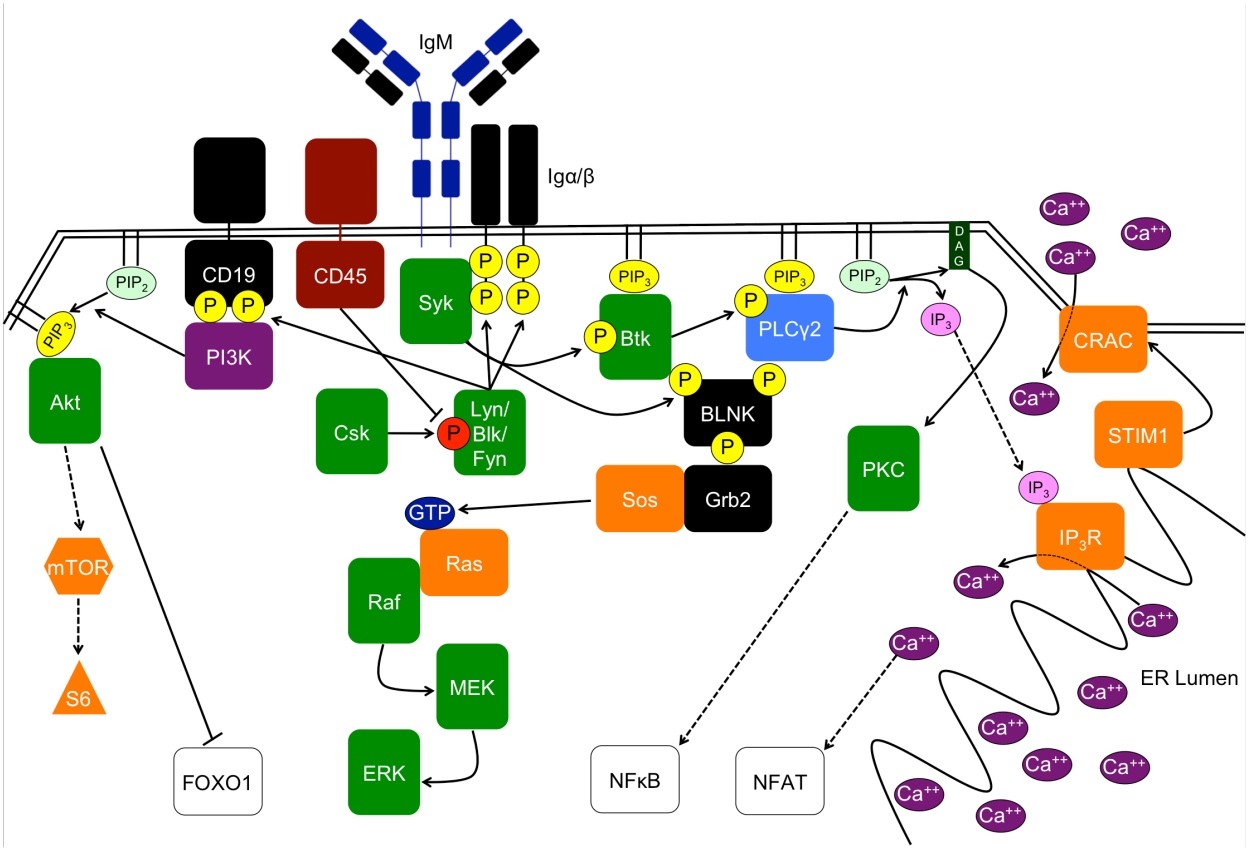
IgM
Igα/β
CD19
CD45
Syk
PI3K
Akt
Csk
Lyn/
Blk/
Fyn
Btk
PLCγ2
BLNK
Grb2
Sos
GTP
Ras
Raf
MEK
ERK
mTOR
S6
FOXO1
PKC
NFκB
NFAT
CRAC
STIM1
IP3R
ER Lumen
PIP2
PIP3
IP3
DAG
Ca++

Figure 1.4. BCR signaling cascade.

Simplified diagram of BCR signaling. Protein kinases are green, scaffolds and adapters are black, and transcription factors are white. CD45 is a protein phosphatase that removes the C-terminal inhibitory tyrosine (shown in red) on Src-family kinases (SFKs), and is counteracted by the kinase Csk. SFKs initiate the BCR signaling cascade by phosphorylating the ITAM domains of Igα/β, which promotes recruitment of Syk kinase. PI3K is a multi-subunit phosphatidylinositol kinase that converts $PI(4,5)P_2$ to $PI(3,4,5)P_3$, which promotes the recruitment of PH-domain-containing proteins to the plasma membrane. PLCγ2 converts $PI(4,5)P_2$ into IP_3 and diacylglycerol (DAG). IP_3R and CRAC are calcium channels, and STIM1 is a calcium sensor that activates CRAC channels when ER calcium stores are depleted. SOS is a guanine nucleotide exchange factor that causes Ras to release GDP and bind GTP. GTP-bound Ras recruits Raf, and this interaction enhances Raf kinase activity and initiates the MAP kinase cascade. Not shown: DAG can also promote MAP kinase signaling via recruitment of the guanine nucleotide exchange factor RasGRP (Das et al., 2009). Akt indirectly promotes activation of the Raptor-mTOR complex (mTORC1), which indirectly promotes phosphorylation of the S6 ribosomal subunit. Akt also phosphorylates the FOXO1 transcription factor, which prevents FOXO1 translocation into the nucleus and promotes its degradation.

CHAPTER 2

IgM and IgD B cell receptors differentially respond to endogenous antigens and control B cell fate

Abstract

Naive B cells co-express two BCR isotypes, IgM and IgD, with identical antigen-binding domains but distinct constant regions. IgM but not IgD is downregulated on autoreactive B cells. Because these isotypes are presumed to be redundant, it is unknown how this could impose tolerance. We introduced the Nur77-eGFP reporter of BCR signaling into mice that express each BCR isotype alone. Despite signaling strongly *in vitro*, IgD is less sensitive than IgM to endogenous antigen *in vivo* and fate decisions are skewed accordingly. IgD-only *Lyn*$^{-/-}$ B cells cannot generate autoantibodies and short-lived plasma cells (SLPCs) *in vivo*, a fate thought to be driven by intense BCR signaling induced by endogenous antigens. Similarly, IgD-only B cells generate normal germinal center, but impaired IgG1^{+} SLPC responses to T-dependent immunization. We propose a role for IgD in maintaining the quiescence of autoreactive B cells and restricting their differentiation into autoantibody secreting cells.

Introduction

The pre-immune mature naïve B cell compartment must balance the need for a diverse antibody repertoire with the risk of autoantibody-mediated disease. Early in development, B cells randomly rearrange their immunoglobulin genes through VDJ recombination and encounter a series of tolerance checkpoints that serve to remove autoreactive B cell receptors (BCRs) from the repertoire. Strongly autoreactive immature B cells rearrange additional light chains to "edit" their autoreactivity, and they ultimately undergo deletion if this is unsuccessful (Shlomchik, 2008). Yet, despite stringent counter-selection of autoreactivity, the mature follicular (Fo) B cell compartment retains cells reactive towards endogenous antigens (Wardemann et al., 2003; Zikherman et al., 2012b). How these cells are restrained from mounting autoimmune responses is not fully understood.

We previously described a BAC Tg reporter mouse (Nur77-eGFP) in which GFP expression is under the control of the regulatory region of *Nr4a1*, an immediate early gene rapidly induced by antigen receptor signaling (Mittelstadt and Defranco, 1993; Winoto and Littman, 2002). We showed that Nur77-eGFP expression in naïve B cells is proportional to strength of antigenic stimulation and consequently to autoreactivity (Zikherman et al., 2012b). The most prominent characteristic of GFP^{hi} reporter B cells is decreased surface IgM BCR relative to GFP^{lo} cells. Goodnow and colleagues first suggested that IgM downregulation may mark autoreactive B cells in the normal mature repertoire shortly after they reported selective downregulation of IgM in the IgHEL (hen egg lysozyme) BCR Tg / soluble HEL Tg model system of B cell autoreactivity (Goodnow et al., 1988; Goodnow et al., 1989). Indeed, multiple studies in mice and humans have identified naturally occurring $IgD^{+}IgM^{lo}$ cells as autoreactive and "anergic" or functionally unresponsive (Duty et al., 2009; Kirchenbaum et al., 2014; Quach

et al., 2011; Zikherman et al., 2012b). These results corroborate observations with several BCR transgenic model systems (Cambier et al., 2007). However, whether or how IgM downregulation might constrain autoreactivity remains unclear because naturally-occurring autoreactive B cells maintain high expression of the IgD BCR isotype (Zikherman et al., 2012b).

IgM and IgD are splice isoforms of a common precursor heavy chain mRNA (Moore et al., 1981). While they differ in their Fc domains, both BCR isotypes contain the same antigen-binding domain, as well as identical 3-amino acid cytoplasmic tails, and they pair with Igα/β in order to initiate the canonical BCR signaling cascade (Blum et al., 1992; Radaev et al., 2010). However, the expression pattern of the isotypes differs; IgM expression begins as soon as heavy and light chains recombine early in B cell development, and persists until class switch recombination occurs following B cell activation (Chen and Cerutti, 2010). IgD is uniquely co-expressed with IgM during a narrow developmental window on late transitional and mature naïve Fo B cells as a result of alternate splicing regulated by the zinc-finger protein ZFP318 (Enders et al., 2014; Pioli et al., 2014). This suggests that IgD may play a critical role specifically in mature naïve B cells. Initial characterization of IgM- and IgD-deficient mice revealed only mild phenotypes and substantial redundancy; each isotype could mediate B cell development, initiate antibody responses to T-dependent and -independent immunization, and induce normal levels of steady-state serum IgG (Lutz et al., 1998; Nitschke et al., 1993; Roes and Rajewsky, 1993). This is consistent with prior studies in BCR transgenic model systems demonstrating that each isotype alone can mediate B cell development, deletion, and activation (Brink et al., 1992).

IgM and IgD differ structurally; IgD has a much longer, flexible hinge region linking its Fab and Fc regions than IgM does (Chen and Cerutti, 2010). Recently, Ubelhart, Jumaa, and

colleagues demonstrated that a short and inflexible hinge confers upon IgM the unique capacity to signal in response to monovalent antigens, while both isotypes can respond to multivalent antigens (Ubelhart et al., 2015). However, the Goodnow lab subsequently showed that IgHEL Tg splenic B cells expressing either the IgD or IgM BCR exclusively could mobilize calcium in response to soluble HEL antigen *in vitro*, and each isotype can mediate a common gene expression program characteristic of anergy *in vivo* (Sabouri et al., 2016). Therefore, it remains unclear whether IgM and IgD BCRs expressed in an unrestricted B cell repertoire differentially sense bona fide endogenous antigens *in vivo*, particularly as the identity and nature of such antigens is largely unknown and not restricted to soluble monovalent antigens. For example, 5-10% of circulating naïve B cells in healthy humans express the well-characterized unmutated and autoreactive human heavy chain V-segment IGHV4-34, and these cells exhibit anergy, selective IgM downregulation, and recognize cell-surface antigens on erythrocytes and B cells *in vivo* (Quach et al., 2011; Reed et al., 2016).

We and others previously hypothesized that downregulation of IgM on Fo B cells might serve to restrain their response to endogenous antigen. Conversely, high expression of IgD on these cells might play a "tolerogenic" role (Zikherman et al., 2012b). To determine how IgM and IgD differentially regulate B cell responses to endogenous antigens, we generated Nur77-eGFP reporter mice deficient for either IgM or IgD (Lutz et al., 1998; Nitschke et al., 1993). Using this reporter of antigen-dependent signaling, we show that IgD is less sensitive than IgM to bona fide endogenous antigens *in vivo* despite higher surface expression and robust responsiveness to receptor ligation *in vitro*. Indeed, marginal zone (MZ) and B1a cells that express IgD but lack IgM induce less Nur77-eGFP than WT, and this is not attributable to repertoire differences. To further support these observations, we examine a series of cell fate decisions for which *in vivo*

BCR signaling requirements have been previously defined. We show that IgD drives a pattern of development consistent with reduced endogenous antigen recognition, favoring MZ B cell fate and disfavoring B1a cell fate. Similarly, IgD alone is less efficient than IgM at driving SLPC expansion in response to endogenous antigens, a process that requires robust BCR signaling. However, IgD is sufficient for germinal center B cell differentiation. Our data suggest that reduced endogenous antigen sensing (i.e. signal transduction in response to antigen binding) by the IgD BCR isotype shunts autoreactive IgD^{hi} IgM^{lo} follicular B cells away from differentiation into SLPCs. We propose that predominant IgD expression maintains the quiescence of autoreactive B cells in response to chronic endogenous antigen stimulation, and limits autoantibody secretion in the context of rapid immune responses.

Results

Endogenous antigen is both necessary and sufficient for expression of Nur77-eGFP reporter in B cells *in vivo*

We previously showed that antigen recognition was both necessary and sufficient for Nur77-eGFP reporter expression by B cells *in vivo* (Figure 2.1A)(Zikherman et al., 2012b). Thus, reporter expression reflects endogenous antigen recognition *in vivo*. Conversely, under steady-state conditions *in vivo*, the Nur77-eGFP reporter does not reflect signaling through other receptors expressed in B cells; indeed, loss of either CD40, or TLR3, 7, and 9 signaling has no effect on reporter expression in B cells *in vivo* (Figure 2.2A). Moreover, neither BAFF, nor IL-4, nor CXCR4-dependent signaling can regulate reporter expression *in vitro* (Figure 2.2B-C) (Zikherman et al., 2012b). To further confirm that Nur77 expression in naïve B cells under steady state conditions is not regulated by microbial stimulation of pattern recognition receptors

(e.g. TLRs 1, 2, 4, 6, and the TLR-4-like molecule RP105), we studied mice raised under either germ-free conditions or conventional specific-pathogen-free conditions. We observed no induction of endogenous Nur77 protein in splenic B cells or endogenous *Nr4a1* transcript in splenocytes in the presence of commensal flora (Figure 2.2D-E). Moreover, MyD88-deficient and MyD88-sufficient splenocytes and peritoneal B1a cells express comparable amounts of endogenous *Nr4a1* transcript and protein respectively under steady state conditions (Figure 2.2F-G). Taken together, these data demonstrate that Nur77-eGFP expression in B cells under steady-state conditions *in vivo* is a *specific* readout of antigen-dependent signaling through the BCR (Table 2.1). We therefore sought to take advantage of the Nur77-eGFP reporter in order to probe the responsiveness of a diverse BCR repertoire of mature B cells expressing either IgM or IgD alone to the vast range of endogenous antigens they may encounter *in vivo*.

Dual expression of IgM and IgD BCRs is required to establish a broad dynamic range of BCR responsiveness across the repertoire

Surface IgM, but not IgD, expression is inversely correlated with endogenous antigen recognition and GFP expression across a diverse repertoire of mature naïve follicular (Fo) B cells, such that B cells reactive to endogenous antigens express high levels of IgD and low levels of IgM on their surface (Figure 2.1B) (Zikherman et al., 2012b). The variation in surface IgM expression across the B cell repertoire is profound, spanning a 100-fold range. However, because IgD is expressed at high and invariant levels in all WT naïve follicular B cells, total surface BCR, unlike IgM, has little dynamic range across the WT repertoire (Figure 2.3A).

To explore how IgM and IgD differentially regulate B cells reactive to endogenous antigens, we generated Nur77-eGFP mice deficient for either IgM or IgD (Lutz et al., 1998;

Nitschke et al., 1993). In *IgM*$^{-/-}$ mice, all B cells express IgD alone prior to class switch recombination (CSR), and in *IgD*$^{-/-}$ mice, all B cells express IgM alone prior to CSR. We observed that IgM is still downregulated on *IgD*$^{-/-}$ GFP^{hi} Fo B cells, but the dynamic range of IgM expression is highly restricted relative to the broad range observed on WT cells (Figure 2.1B).

We previously showed that IgM down-modulation on GFP^{hi} reporter B cells largely accounts for impaired signaling through IgM (Figure 2.1C) (Zikherman et al., 2012b). However, the narrow dynamic range of IgM on IgD-deficient cells renders GFP^{hi} reporter B cells unable to fine-tune signaling through the IgM BCR across the GFP repertoire (Figure 2.1C). Furthermore, IgD-mediated signaling is not altered across the GFP repertoire in the presence or absence of IgM (Figure 2.1C). As a result, reduced responsiveness of GFP^{hi} B cells is most profound in B cells that express the IgM isotype in the presence of IgD. This suggests that IgD expression may be necessary to establish and/or maintain a broad and functionally dynamic range of surface IgM expression across the B cell repertoire. This is consistent with a previously proposed survival function for the IgD BCR (Roes and Rajewsky, 1993; Sabouri et al., 2016).

IgM$^{-/-}$ follicular B cells express more surface BCR than *IgD*$^{-/-}$ follicular B cells, but similar Nur77-eGFP

Deletion of either the IgM or the IgD BCR isotype results in compensatory upregulation of the remaining isotype. This may be due in part to a change in competition for pairing with Igα/β heterodimers, which is essential for trafficking of IgM to the cell surface (Hombach et al., 1990; Sabouri et al., 2016). *IgM*$^{-/-}$ B cells express about twice as much surface BCR as *IgD*$^{-/-}$ B

cells, as measured by surface anti-light chain staining (Figures 2.1D and 2.3B-E). Nevertheless, distribution of Nur77-eGFP expression across the naïve B cell repertoire is nearly identical in *IgM*$^{-/-}$ and *IgD*$^{-/-}$ Fo B cells (Figure 2.1E). Further, at every level of Nur77-eGFP, cells that express IgD alone require more surface BCR to drive an equivalent amount of GFP compared to cells that express IgM alone (Figure 2.1F). This suggests that on a per-receptor basis, IgD BCR may be less efficient at inducing Nur77-eGFP in response to endogenous antigens. Importantly, this is not attributable to differential dependence upon IgM or IgD expression for signaling via CXCR4 or downstream of canonical TLR ligands (Figures 2.2C and 2.4A).

IgD BCR crosslinking induces robust signaling *in vitro*

Because IgD drives less Nur77-eGFP per receptor than IgM *in vivo*, we wanted to determine whether there were defects in signal transduction downstream of IgD. To mimic antigen binding to the membrane-distal end of the BCR and allow for direct comparison between the isotypes, we stimulated IgD-only (*IgM*$^{-/-}$) and IgM-only (*IgD*$^{-/-}$) cells with anti-Igκ and compared downstream signaling. BCR ligation in IgD-only Fo B cells induced equivalent amounts of Erk phosphorylation relative to IgM-only B cells (Figure 2.5A), and there were no gross differences in pErk kinetics (Figure 2.5B). Additionally, IgD-only cells induced more robust intracellular calcium increase and S6 phosphorylation than IgM-only cells (Figures 2.5C and 2.6A). This was not due to differential effects of the Fc portion of the stimulatory antibody on IgM-only and IgD-only B cells as anti-Igκ-F(ab')$_2$ and anti-Igκ stimulation produced identical signaling (Figure 2.6B).

IgD BCRs sense endogenous antigens less efficiently than IgM BCRs

Due in part to increased surface receptor expression, IgD-only B cells induce comparable Erk phosphorylation and enhanced calcium mobilization relative to IgM-only B cells stimulated with anti-Igκ. As a result, we observe significantly more CD86 and Nur77-eGFP induction in IgD-only B cells after 18 hours of anti-Igκ stimulation *in vitro* (Figure 2.5D-F). However, IgD-only cells induced less Nur77-eGFP and MHC-II upregulation when cultured in the absence of exogenous stimulus (Figure 2.5G-H). This discrepancy suggests that despite increased receptor expression and efficient coupling to downstream signaling machinery, residual *ex vivo* antigens occupying the IgD BCR are less efficient at inducing signaling. Consistent with this hypothesis, basal calcium analyzed immediately *ex vivo* is depressed in cells that express only IgD (Figure 2.5I). These data suggest that while signal transduction downstream of the IgD BCR is robust *in vitro*, IgD responds less efficiently than IgM to the relevant antigens it encounters *in vivo*.

Reduced endogenous antigen sensing by IgD BCR in innate-like B cells

While IgD-only and IgM-only Fo B cells express comparable levels of Nur77-eGFP (Figure 2.1E), we suspected that competitive pressures for survival might constrain the acceptable range of BCR signaling among mature Fo B cells. We further speculated that compensatory mechanisms such as altered surface receptor and altered BCR repertoire might fine tune how much signaling Fo B cells experience *in vivo* in order to lie within this range. In contrast to Fo B cells, IgD-only marginal zone (MZ) and B1a cells expressed significantly less Nur77-eGFP than WT cells despite higher levels of surface BCR (Figures 2.7A and 2.3B-E). To determine whether this difference was due to isotype or altered BCR repertoire, we probed GFP expression in B1a cells specific for phosphatidylcholine (PtC), an endogenous antigen exposed

on the surface of dying cells that is thought to select developing B cells into the B1a compartment (Baumgarth, 2011). We found a large difference in GFP even among B1a cells with a common specificity, and this occurs in spite of high surface PtC binding in IgD-only B1a cells (Figure 2.7B-C).

We took an independent and complementary approach to address the same question in MZ B cells; we crossed *IgM*$^{-/-}$ and *IgD*$^{-/-}$ reporter mice to a genetic background that drives over-expression of the B cell survival factor BAFF (Gavin et al., 2005). BAFF overexpression "unrestricts" the BCR repertoire by removing competition for survival, thereby reducing both positive and negative selection pressures and permitting cells with either insufficient or excessive BCR signaling to persist in the repertoire, resulting in a massively expanded MZ compartment (Stadanlick and Cancro, 2008). Importantly, BAFF does not directly regulate reporter GFP expression, and therefore GFP reflects endogenous antigen stimulation on this genetic background (Zikherman et al., 2012b). In BAFF Tg mice, IgD-only MZ cells expressed much less GFP than those expressing IgM alone (Figure 2.7D-E). This was not explained by differences in surface receptor levels between these populations as they are comparable on this genetic background (Figure 2.8A). Indeed, IgD-only cells with low GFP and IgM-only cells with high GFP appear to be preferentially rescued in mice with excess BAFF, suggesting that distinct BCR repertoires, far from accounting for GFP differences between IgM-only and IgD-only MZ B cells, actually obscure these differences. Conversely, either "fixing" or unrestricting the BCR repertoire unmasks impaired GFP upregulation by IgD relative to IgM.

As a result of allelic exclusion of the heavy chain locus during B cell development, *IgM*$^{+/-}$ heterozygous mice develop two genetically distinct sets of B cells in which half express only IgD and the other half express both IgM and IgD. We exploited this property to confirm that

the Nur77-eGFP difference in the MZ and B1a compartments is cell intrinsic and not a consequence of the presence or absence of serum IgM (Figure 2.8B).

Since $IgM^{-/-}$ and $IgD^{-/-}$ mice were generated on the Balb/c and 129 genetic backgrounds respectively, their germline VDJ loci are different from that of C57/Bl6 mice to which they have been back-crossed. Throughout our study, we have validated our findings in either Balb/c-B6 F1 mice or $IgH^{a/b}$ heterozygous mice, which have two sets B cells with identical IgM and IgD isotype expression but distinct germline VDJ loci. We took this approach to confirm that differences in MZ GFP were due to BCR isotype and not VDJ locus (Figure 2.8C).

Cell-intrinsic skewing of B cell development by the IgM and IgD BCRs

Generation of the B1a compartment requires endogenous antigen recognition and strong BCR signaling, while the opposite is true for MZ B cells (Figure 2.9A) (Cariappa and Pillai, 2002; Casola et al., 2004). Indeed, B1a cells are modestly reduced in IgM-deficient mice, while MZ B cells are modestly increased (Figure 2.9B-C). Because serum IgM deficiency leads to increased B1a numbers, we assessed B1a and MZ B cell development in a competitive setting to isolate the cell-intrinsic effects of IgM and IgD BCRs (Boes et al., 1998). Analogous to the $IgM^{+/-}$ mice described above, $IgM^{+/-}$ $IgD^{-/+}$ heterozygous mice develop two genetically distinct sets of B cells in which half express only IgD and the other half express only IgM (Figure 2.10A). Although IgD-only B cells can partially populate the B1a compartment in the absence of competition (Lutz et al., 1998; Ubelhart et al., 2015), IgD-only cells are virtually excluded from this compartment in a competitive setting (Figure 2.10B). Indeed, this parallels the loss of PtC-binding IgD-only peritoneal B cells observed in competition with wild type cells (Ubelhart et al., 2015). In contrast, IgD-only B cells preferentially populate the MZ B cell compartment in

competition with IgM-only B cells (Figure 2.10B). These data are consistent with a signal strength model of B1a/MZ B cell development (Figure 2.9A), and this suggests that *in vivo* signaling, antigen recognition, or both are reduced in IgD-only B cells. These differences in signaling could in turn modulate the generation and/or survival of IgD-only B1a and MZ B cells.

We sought to determine whether skewed development of B cell lineages was driven primarily by properties of IgD, IgM, or both by comparing development of B cell populations in $IgM^{+/-}$ $IgD^{-/+}$, $IgM^{+/-}$, and $IgD^{+/-}$ mice (Figure 2.10C-E). We conclude that skewing of MZ and B1a fates is primarily attributable to lack of IgM expression on IgD-only cells rather than lack of IgD expression on IgM-only cells because we observe little skewing in $IgD^{+/-}$ mice (Figure 2.10E). Further, the competitive advantage of IgD-only cells in the marginal zone niche is reduced in the BAFF Tg setting, consistent with loosening of competitive selection pressures (Figure 2.10F).

IgM-only B cells exhibit a disadvantage in the mature Fo compartment relative to IgD-only B cells (Figure 2.10C). We find that absence of IgD rather than excess IgM expression accounts for some of this disadvantage as WT and IgD-only cells compete equally well in this compartment (Figure 2.10D). This may reflect impaired positive selection or survival in absence of IgD. Indeed, similar to our observations, a disadvantage for Fo B cells lacking IgD was observed in $IgD^{+/-}$ mice previously (Roes and Rajewsky, 1993). As with differences in Nur77-eGFP expression, we confirmed that the developmental fates of IgM-only and IgD-only cells were due to BCR isotype and not VDJ locus (Figure 2.9D).

Either IgD or IgM BCR is sufficient to mediate polyclonal B cell activation and germinal center differentiation in $Lyn^{-/-}$ mice

Mice deficient for either IgM or IgD can mount T-independent and T-dependent immune responses to model antigens (Lutz et al., 1998; Nitschke et al., 1993; Roes and Rajewsky, 1993). However, endogenous antigens may have unique properties that are absent in model antigen systems. To test whether each BCR isotype was competent to mediate autoimmune responses to endogenous antigens in lupus-prone mice, we generated $IgM^{+/-}$ and $IgD^{+/-}$ mice on the $Lyn^{-/-}$ background (Chan et al., 1997). The Src family kinase Lyn is essential to mediate ITIM-dependent inhibitory signals in B cells and myeloid cells (Scapini et al., 2009; Xu et al., 2005). $Lyn^{-/-}$ mice consequently develop a spontaneous lupus-like disease characterized by anti-DNA antibodies and nephritis on the C57Bl/6 genetic background (Chan et al., 1997; Hibbs et al., 1995; Nishizumi et al., 1995). It has been shown that both B-cell-specific MyD88 expression and T cells are essential for IgG2a/c anti-dsDNA autoantibody production in $Lyn^{-/-}$ mice, and conditional deletion of Lyn in B cells is sufficient for autoimmunity (Hua et al., 2014; Lamagna et al., 2014).

Secreted natural IgM is thought to play important homeostatic functions that repress autoimmunity, particularly clearance of dead cell debris (Boes et al., 2000; Manson et al., 2005). By performing our analysis in mice with wild type and IgM-only or IgD-only B cells in a common milieu ($IgM^{+/-}$ $Lyn^{-/-}$ and $IgD^{+/-}$ $Lyn^{-/-}$ mice), we could control for this and isolate the B cell-intrinsic effects of the IgM and IgD BCRs. Importantly, precursor Fo B cells are present at roughly equal ratios from WT and IgM-only or IgD-only loci in these mice, and this is unaffected by VDJ background (Figure 2.11A-C). Moreover, $Lyn^{-/-}$ B cells expressing either IgM or IgD alone exhibit enhanced BCR signaling *in vitro* relative to $Lyn^{+/+}$ B cells, suggesting that neither isotype is uniquely coupled to ITIM-containing receptors (Figure 2.12A-B).

Polyclonal B cell activation in *Lyn*$^{-/-}$ mice precedes and is genetically separable from autoantibody production; it is driven by B cell-intrinsic loss of Lyn, is thought to result from enhanced BCR signaling, and is independent of MyD88 expression (Hua et al., 2014; Lamagna et al., 2014). Indeed, *Lyn*$^{-/-}$ reporter B cells have elevated Nur77-eGFP expression consistent with enhanced BCR signal transduction *in vivo* (Figure 2.13A). We had expected that activation of IgD-only *Lyn*$^{-/-}$ B cells might be impaired due to reduced sensing of endogenous antigens, but neither CD86 nor CD69 upregulation were significantly different on WT and IgD-only B cells in the absence of Lyn (Figure 2.14A). This implies that both BCRs can provide sufficient signals to drive polyclonal activation by endogenous antigens.

Although GC fate is disfavored relative to SLPC fate in *Lyn*$^{-/-}$ mice, GCs do arise spontaneously with time (Hibbs et al., 1995; Hua et al., 2014). We found that both IgD-only and IgM-only cells in Lyn-deficient mice made comparable contributions to the GC compartment in competition with wild type B cells, independent of VDJ background (Figures 2.14B and 2.13B-C). We propose that endogenous antigen sensing by IgD, while normally dampened, is sufficient to drive both polyclonal activation and GC differentiation on the *Lyn*$^{-/-}$ background. This further implies that antigen capture by IgD and presentation on MHC-II is robust enough to recruit adequate T cell help to support these cell fates.

IgM BCR is required to drive dsDNA antibody production in *Lyn*$^{-/-}$ mice

IgM- and IgD-deficient B cells express BCR heavy chain allotype [a] (IgH^{a}), and their secreted antibodies can be differentiated from WT B6 antibodies (IgH^{b}) even after isotype switching (e.g. IgG2a[a] vs. IgG2a[b] – also referred to as IgG2c). Allotype-specific antibodies have been previously used in the context of lupus mouse models to track autoantibodies

generated by B cells of distinct genetic origin (Mills et al., 2015; Pisitkun et al., 2006). We took an analogous approach to assess IgG2a/c anti-dsDNA autoantibodies emanating from each genetic locus in $IgM^{+/-}$, $IgD^{+/-}$, and $IgH^{a/b}$ control mice deficient for Lyn. In order to compensate for reduced penetrance of autoantibody production in $IgM^{+/-}$ $Lyn^{-/-}$ mice, we collected serum from this genotype at time points beyond 24 weeks to increase the number of samples in which tolerance had been broken. While B cells expressing IgM (of either IgH locus) generated IgG2a/c anti-dsDNA, IgD-only B cells were relatively protected from generating anti-dsDNA antibodies, even at late time points (Figures 2.14C-G and 2.13D-E). Importantly, this is attributable to BCR isotype and not VDJ locus (Figure 2.13D-E).

We noted that anti-dsDNA antibody titers fluctuated substantially over time in $Lyn^{-/-}$ mice, in some cases dropping markedly over a four-week period (Figure 2.14C-D). Anti-dsDNA IgG autoantibodies in patients with systemic lupus erythematosus (SLE) similarly fluctuate over time – in contrast to other anti-nuclear specificities - and correlate with disease flares (Liu et al., 2011). Indeed, unmutated germline BCRs from naïve B cells are recruited directly into the circulating plasmablast compartment during SLE flares (Tipton et al., 2015). Taken together, this suggests that anti-dsDNA antibodies in mice and humans are secreted at least in part by SLPCs emerging from an extra-follicular immune response, rather than long-lived plasma cells (LLPCs) that originate in GCs. Our data suggests that, in the absence of Lyn, the IgD BCR is sufficient to mediate B cell activation and GC entry, but the IgM BCR is essential to produce dsDNA-specific SLPCs.

IgM BCR is required for expansion of unswitched plasma cells in $Lyn^{-/-}$ mice

In addition to stochastic generation of autoantibodies over time, *Lyn*$^{-/-}$ mice exhibit a massive expansion of the splenic IgM plasma cell compartment that corresponds to a roughly 10-fold increase in serum IgM (Hibbs et al., 1995). While natural IgM is thought to be secreted by B1a-derived plasma cells (Baumgarth, 2011), elevated serum IgM in *Lyn*$^{-/-}$ mice arises from the follicular B2 compartment since *Lyn*$^{-/-}$ mice lack MZ B cells, and bone marrow chimeras lacking the B1a compartment reconstitute the hyper-IgM secretion phenotype (Luo et al., 2014). Moreover, while BCR signaling is prominently enhanced in *Lyn*$^{-/-}$ B2 B cells, it is markedly dampened in *Lyn*$^{-/-}$ B1a cells (Figure 2.15A) (Skrzypczynska et al., 2016).

IgM plasma cell expansion is temporally and genetically separable from autoimmunity in *Lyn*$^{-/-}$ mice; this phenotype develops in mice as young as 7-10 weeks of age with 100% penetrance, is B-cell intrinsic, and is not dependent upon MyD88 expression (Hua et al., 2014; Infantino et al., 2014; Lamagna et al., 2014). A pathway involving Btk, Ets1, and Blimp-1 is thought to drive this phenotype. Ets1 inhibits differentiation into plasma cells in part by antagonizing the key transcriptional regulator of plasma cell fate, Blimp-1 (John et al., 2008). Mice deficient for Ets1 display IgM plasma cell expansion, Ets1 levels are reduced in *Lyn*$^{-/-}$ mice, and restoration of Ets1 expression normalizes IgM plasma cell numbers (Luo et al., 2014). Furthermore, reduced levels of Btk suppress IgM plasma cell expansion in *Lyn*$^{-/-}$ mice, and Ets1 levels are concomitantly restored to normal levels in *Btk*^{lo} *Lyn*$^{-/-}$ mice (Gutierrez et al., 2010; Luo et al., 2014; Mayeux et al., 2015). Therefore, exaggerated BCR stimulation of B2 B cells by endogenous antigens promotes IgM plasma cell expansion in *Lyn*$^{-/-}$ mice (Figure 2.16A). Indeed, enhanced BCR signaling has been shown to favor SLPC fate over GC differentiation in Lyn-sufficient mice as well (Chan et al., 2009; Nutt et al., 2015; Paus et al., 2006). We therefore

wondered whether impaired endogenous antigen sensing by IgD influenced Ets1 expression and unswitched PC expansion in *Lyn*$^{-/-}$ mice.

As previously shown, *Lyn*$^{-/-}$ B cells downregulate Ets1 protein expression (Figure 2.17A) (Luo et al., 2014). However, Lyn-deficient B cells expressing only IgD did not do so, consistent with a reduced ability of IgD to transmit antigen-dependent signals *in vivo*, (Figure 2.17A). As previously reported, we found that the frequency of plasma cells in the spleens of *Lyn*$^{-/-}$ mice was increased fourfold relative to *Lyn*$^{+/+}$ mice, but the bone marrow plasma cell compartment size was relatively unaffected (Figure 2.17B-C) (Infantino et al., 2014). The increase in splenic plasma cells was attributable entirely to unswitched (IgM^{+}) plasma cells (Figure 2.17C). However, unswitched plasma cell expansion was completely absent in *IgM*$^{-/-}$ *Lyn*$^{-/-}$ spleens (Figure 2.17C). This was reflected in steady-state serum antibody levels; while *Lyn*$^{-/-}$ mice have elevated serum IgM relative to WT mice, *IgM*$^{-/-}$ *Lyn*$^{-/-}$ mice did not have elevated serum IgD relative to *IgM*$^{-/-}$ mice (Figure 2.17D-E).

To confirm that resistance to unswitched plasma cell expansion was a cell-intrinsic feature of IgD-only *Lyn*$^{-/-}$ B cells, we assessed this phenotype in *IgM*$^{+/-}$ *Lyn*$^{-/-}$ mice. Similar to the non-competitive setting, IgD-only *Lyn*$^{-/-}$ cells did not contribute to an expansion in the unswitched plasma cell compartment (Figure 2.17F-G). This effect was due to isotype and not VDJ allele usage because both WT IgH^{a} and WT IgH^{b} *Lyn*$^{-/-}$ B cells generated unswitched plasma cells in a competitive setting (Figure 2.13C).

IgM BCR is required for efficient generation of short-lived IgG1^{+} plasma cells but is dispensable for GC B cell fate

IgD-only *Lyn*$^{-/-}$ Fo B cells are completely prevented from generating an expanded unswitched SLPC compartment in response to chronic endogenous antigen stimulation, but they are competent to enter the GC. To determine how this defect relates to responses towards exogenous model antigens, we sought to determine whether IgD-only *Lyn*$^{+/+}$ B cells exhibit skewing of cell fate in the context of a T-dependent response to a model antigen. To generate a robust polyclonal B cell response in which T cell help should not be limiting, we used the classic immunogen sheep RBCs. During this immune response, Fo B cells can either enter the germinal center or differentiate into IgG1^{+} extrafollicular plasma cells (Chan et al., 2009; Paus et al., 2006). We found that wild type, *IgM*$^{-/-}$, and *IgD*$^{-/-}$ mice all produced extremely robust GC responses 5 days after SRBC injection, but B cells expressing IgD alone were unable to produce IgG1^{+} SLPCs at this time point (Figure 2.18A-D).

Since serum IgM is absent in *IgM*$^{-/-}$ mice and is known to enhance PC generation (Boes et al., 1998), we wanted to assess the cell-intrinsic effect of IgD and IgM BCRs on the immune response to SRBCs. To do so, we immunized *IgM*$^{+/-}$ mice in which half of Fo B cells express IgD alone and half express both IgM and IgD. We could track the relative contribution of these two cell populations to the GC response because the bulk of GC B cells have not yet isotype-switched and express surface IgM or IgD. Both cell types made a robust contribution to the germinal center response (Figure 2.18E). Next we tracked the generation of IgG1^{+} PCs by detecting allotype [a] or allotype [b] IgG1. In contrast to the GC response, IgD-only B cells were significantly disfavored in this compartment, although the defect was less severe than that observed in *IgM*$^{-/-}$ mice, which lack serum IgM (Figure 2.18F). To control for differences in the VDJ locus, we performed this experiment using *IgH*$^{a/b}$ control mice and observed no significant

differences between allotypes, implying that BCR isotypes rather than VDJ locus accounted for our observations (Figure 2.19A-B).

In contrast to impaired IgG1 SLPC responses by IgD-only B cells, we observed that IgD-only B cells were able to generate unswitched plasma cells in response to SRBC immunization in both non-competitive and competitive settings (Figure 2.19C-D). Unswitched PC numbers correlate well with MZ B cell numbers in these mice (Figures 2.9B and 2.10D). Moreover, MZ B cells efficiently generate short-lived unswitched plasma cells even in response to TD-antigens (Phan et al., 2005; Song and Cerny, 2003). We therefore suspect that IgG1 PCs emanate from the Fo B cell compartment, while the unswitched PC response may originate in the MZ B cell compartment. Normal SLPC generation by IgM-deficient MZ B cells in response to immunization would be consistent with previously reported normal T-independent II responses in IgM-deficient mice (Lutz et al., 1998). However, we cannot exclude a contribution of follicular-derived PCs that have failed to class switch to IgG1.

We sought to confirm that the $IgG1^+$ PC defect was generalizable to other T-dependent immunogens. The B cell response to NP hapten is stereotyped and makes predominant use of the VH186-2 heavy chain (Loh et al., 1983). We therefore immunized both $IgM^{+/-}$ and $IgH^{a/b}$ mice with NP hapten conjugated to rabbit serum albumin (NP-RSA) in order to control for differences in VDJ locus. Although allotype [a] makes a less robust response to NP than allotype [b], we normalized responses of IgD-only cells to wild type allotype [a] cells and found that GC responses at early time points were intact, but $IgG1^+$ PCs and NP-specific IgG1 titers were significantly reduced 7-8 days after immunization (Figure 2.18G-I). These data suggest that IgD-only follicular B cells are competent to enter the GC, but they have defects in adopting the SLPC fate (or class-switching) in response to T-dependent immunization.

	Stimulus/perturbation	Pathway	Readout	Cell type	References
Does not modulate pathway at steady state *in vivo*	CD40L-/-	CD40	Nur77-eGFP	B cells	Figure 2.2
	TLR7-/-	TLR7	Nur77-eGFP	B cells	Figure 2.2
	Un93b1 3d/3d	TLR3/7/9	Nur77-eGFP	B cells	Figure 2.2
	MyD88 fl/fl MB1-Cre	MyD88	Endog. Nur77/*Nr4a1*	B1a cells/splenocytes	Figure 2.2
	Germ-free mice	MyD88/TRIF	Endog. Nur77/*Nr4a1*	Splenic B cells/splenocytes	Figure 2.2
	Constitutively active STAT5	Jak/Stat	Nur77-eGFP	Thymocytes	Moran et al., 2011
Does not induce pathway *in vitro*	BAFF	BAFF-R	Nur77-eGFP	B cells	Zikherman et al., 2012
	IL-4	Jak/Stat	Nur77-eGFP	B cells	Figure 2.2
	IL-2, IL-15	Jak/Stat	Nur77-eGFP	CD8 (IL-2, 15), CD4 (IL-2)	Au-Yeung et al., 2017
	CXCL12/SDF-1	CXCR4	Nur77-eGFP	B cells	Figure 2.2
Induces pathway *in vitro* but does not require IgM and IgD	LPS	TLR4, Rp150	Nur77-eGFP	B cells	Zikherman et al., 2012, Figure 2.4
	CpG	TLR9	Nur77-eGFP	B cells	Zikherman et al., 2012, Figure 2.4
	Pam3CSK4	TLR1/2	Nur77-eGFP	B cells	Figure 2.4
	Anti-Igκ	BCR	Nur77-eGFP	B cells	Figure 2.5
Modulates pathway at steady state *in vivo*	IgHEL Tg	Antigen/BCR	Nur77-eGFP	B cells	Zikherman et al., 2012, Figure 2.1
	IgHEL Tg/sHEL	Antigen/BCR	Nur77-eGFP	B cells	Zikherman et al., 2012, Figure 2.1
	Lyn-/-	BCR via ITIMs	Nur77-eGFP	B cells	Figure 2.13
	CD45 allelic series	BCR via SFKs	Nur77-eGFP	B cells	Zikherman et al., 2012

Table 2.1. Regulation of Nur77 in B Cells.

Summary of different stimuli and their ability to induce Nur77-eGFP reporter or endogenous Nur77/*Nr4a1* protein and transcript in lymphocytes. References: (Au-Yeung et al., 2017; Moran et al., 2011; Zikherman et al., 2012b).

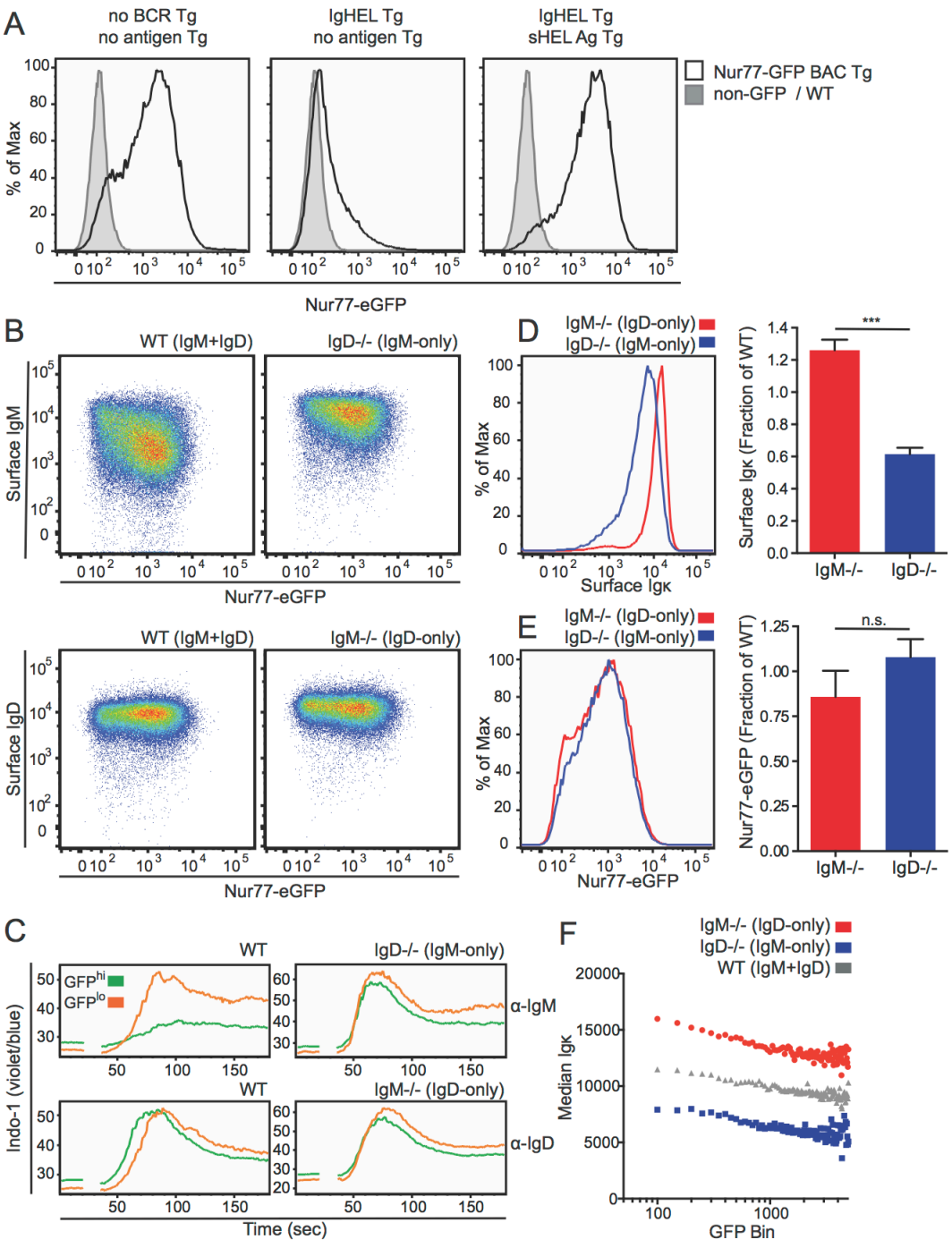
A
no BCR Tg
no antigen Tg
IgHEL Tg
no antigen Tg
IgHEL Tg
sHEL Ag Tg
Nur77-GFP BAC Tg
non-GFP / WT
% of Max
Nur77-eGFP
B
WT (IgM+IgD)
IgD-/- (IgM-only)
Surface IgM
Nur77-eGFP
WT (IgM+IgD)
IgM-/- (IgD-only)
Surface IgD
Nur77-eGFP
C
WT
IgD-/- (IgM-only)
GFPhi
GFPlo
α-IgM
WT
IgM-/- (IgD-only)
α-IgD
Indo-1 (violet/blue)
Time (sec)
D
IgM-/- (IgD-only)
IgD-/- (IgM-only)
% of Max
Surface Igκ
Surface Igκ (Fraction of WT)
***
IgM-/-
IgD-/-
E
IgM-/- (IgD-only)
IgD-/- (IgM-only)
% of Max
Nur77-eGFP
Nur77-eGFP (Fraction of WT)
n.s.
IgM-/-
IgD-/-
F
IgM-/- (IgD-only)
IgD-/- (IgM-only)
WT (IgM+IgD)
Median Igκ
GFP Bin

Figure 2.1. IgD expression enables a dynamic range of IgM responsiveness.

(A) GFP expression in mature follicular splenic B cells (CD19+CD23+CD93-) from Nur77-eGFP BAC Tg reporter mice with either a wild-type BCR repertoire (left), or harboring IgHEL Tg specific for the cognate antigen HEL (hen egg lysozyme) in the absence (middle), or presence (right) of endogenous cognate antigen driven by soluble HEL Tg. WT mature follicular B cells lacking GFP reporter are included for reference (gray shaded histograms).

(B) Surface IgM and IgD expression in splenic Fo B cells from WT, *IgM*$^{-/-}$, and *IgD*$^{-/-}$ mice expressing the Nur77-eGFP reporter.

(C) Splenocytes from WT, *IgM*$^{-/-}$, and *IgD*$^{-/-}$ mice were loaded with Indo-1 and stimulated with 2.5 μg/mL of F(ab')2 anti-IgM or 1:400 anti-IgD. Fo B cells with the highest 20% and lowest 20% Nur77-eGFP expression are compared.

(D) Representative histograms and quantification of surface Igκ expression in *IgM*$^{-/-}$ and *IgD*$^{-/-}$ Fo B cells normalized to WT.

(E) Representative histograms and quantification of Nur77-eGFP expression in *IgM*$^{-/-}$ and *IgD*$^{-/-}$ Fo B cells normalized to WT.

(F) Median surface Igκ expression of WT, *IgM*$^{-/-}$, and *IgD*$^{-/-}$ Fo B cells was calculated for 200 bins of equal width across the Nur77-eGFP spectrum.

For (A), (B) and (F), data are representative of at least n = 4 independent experiments. For (C), n = 3 independent experiments for anti-IgM and n = 2 independent experiments for anti-IgD. For (D) and (E), n = 7 and n = 4, respectively, WT, *IgM*$^{-/-}$, and *IgD*$^{-/-}$ mice. Welch's t test was used to calculate p values, and mean + SEM is displayed. ***$p < 0.001$.

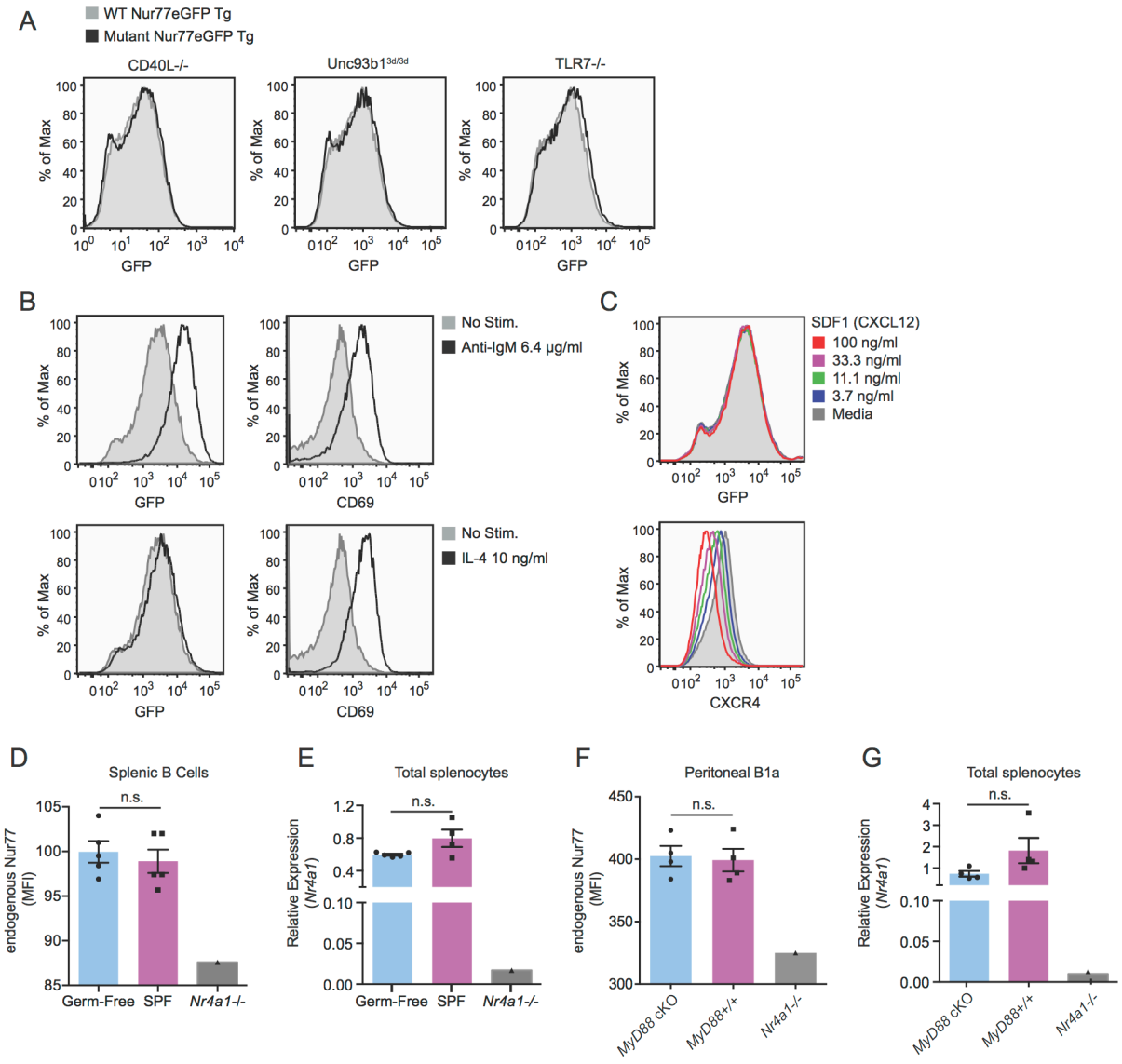
A
WT Nur77eGFP Tg
Mutant Nur77eGFP Tg
CD40L-/-
Unc93b1 3d/3d
TLR7-/-
% of Max
GFP
B
No Stim.
Anti-IgM 6.4 µg/ml
CD69
IL-4 10 ng/ml
C
SDF1 (CXCL12)
100 ng/ml
33.3 ng/ml
11.1 ng/ml
3.7 ng/ml
Media
CXCR4
D
Splenic B Cells
endogenous Nur77 (MFI)
n.s.
Germ-Free
SPF
Nr4a1-/-
E
Total splenocytes
Relative Expression (Nr4a1)
F
Peritoneal B1a
MyD88 cKO
MyD88+/+
G
Total splenocytes

Figure 2.2. Regulation of Nur77 and Nur77-eGFP reporter expression.

(A) Nur77-eGFP expression in mature Fo (B220+CD93-CD23+) B cells from mice with mutations in various signaling pathways (*CD40L*$^{-/-}$, *Unc93b1*$^{3d/3d}$,*TLR7*$^{-/-}$). This Unc93b1 mutation abolishes signaling through TLR3, TLR7, and TLR9.

(B) Nur77-eGFP and CD69 induction in B220+ splenocytes from Nur77-eGFP reporter mice stimulated with either anti-IgM or IL-4 *in vitro* for 24 hours.

(C) Splenic B cells were stimulated with CXCR4 ligand (SDF-1) *in vitro* for 18 hours and Nur77-eGFP expression and CXCR4 downregulation were assessed.

(D-E) Splenocytes from N=5 Germ-free and SPF mice were taken directly *ex vivo* and either permeabilized and stained to detect B220+ cells and endogenous Nur77 by intracellular staining (D), or total *Nr4a1* transcript by qPCR (E).

(F) PerC (peritoneal cavity) cells from n = 4 *MB1 Cre*$^{+}$ *MyD88*$^{fl/fl}$ and controls were permeabilized and stained immediately *ex vivo* to detect B1a cells and endogenous Nur77 by intracellular staining. In D-E, *Nr4a1*$^{-/-}$ splenocytes serve as a control both for Ab and primer specificity.

(G) Splenocytes from mice analyzed in (F) were harvested directly *ex vivo* to detect total *Nr4a1* transcript by qPCR.

Data in (A) and (C) are representative of n = 2 independent experiments. Data in (B) are representative of n = 3 independent experiments.

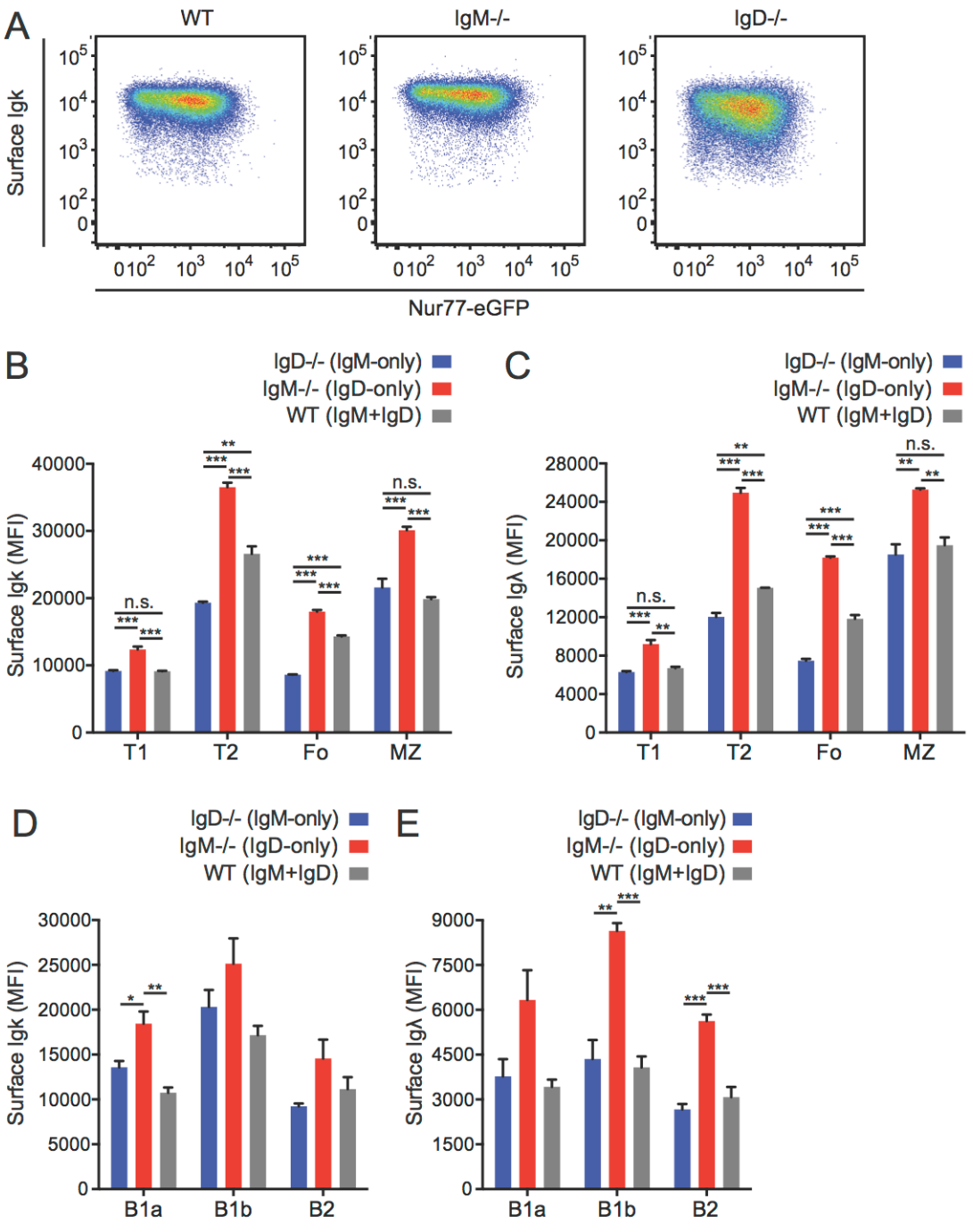
A
WT
IgM-/-
IgD-/-
Surface Igk
Nur77-eGFP
B
IgD-/- (IgM-only)
IgM-/- (IgD-only)
WT (IgM+IgD)
Surface Igk (MFI)
T1
T2
Fo
MZ
n.s.
C
Surface Igλ (MFI)
D
B1a
B1b
B2
E

Figure 2.3. Quantification of surface BCR expression on B cell subsets.

(A) Surface Igκ expression relative to Nur77-eGFP reporter in Fo B cells from WT, *IgM*$^{-/-}$, and *IgD*$^{-/-}$ mice.

(B) Mean surface Igκ was calculated for splenic B cell (B220+) subsets in WT, *IgM*$^{-/-}$, and *IgD*$^{-/-}$ mice. T1 (CD93+CD23-); T2 (CD93+CD23+); Fo (CD93-CD23+); MZ (CD21hiCD23lo).

(C) Surface Igλ on B cell subsets described in (B)

(D) Surface Igκ MFI of Igκ+ cells in peritoneal B cell (CD19+) subsets. B1a (CD5+CD23-); B1b (CD5-CD23-); B2 (CD5-CD23+).

(E) Surface Igλ MFI of Igλ+ cells in peritoneal B cell subsets described in (D).

Data in (A) are representative of n = 3 independent experiments. Values in (B-E) were calculated from n = 3 mice of each genotype. One-way ANOVA with Tukey's multiple comparisons test (B-E) was used to calculate p values, and mean + SEM is displayed. *$p < 0.05$, **$p < 0.01$, ***$p < 0.001$.

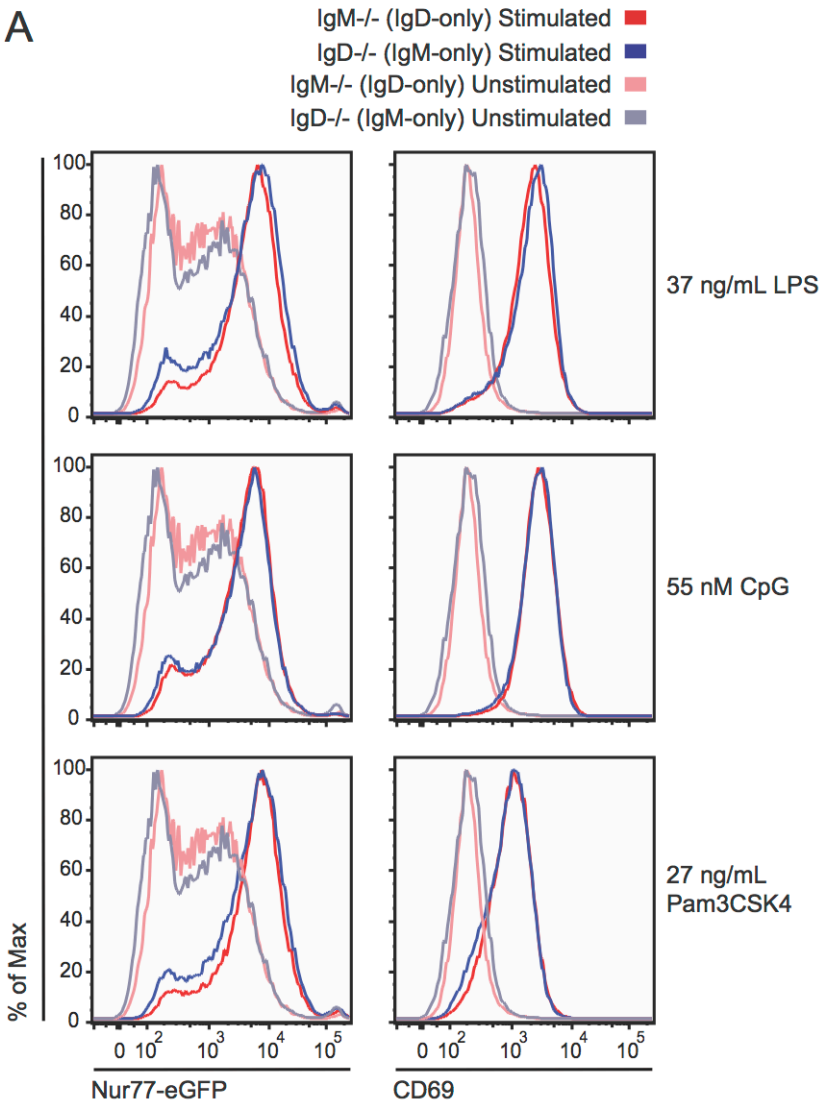
A
IgM-/- (IgD-only) Stimulated
IgD-/- (IgM-only) Stimulated
IgM-/- (IgD-only) Unstimulated
IgD-/- (IgM-only) Unstimulated
37 ng/mL LPS
55 nM CpG
27 ng/mL Pam3CSK4
% of Max
Nur77-eGFP
CD69

Figure 2.4. Induction of Nur77-eGFP and CD69 in TLR-stimulated *IgM*$^{-/-}$ and *IgD*$^{-/-}$ B cells. (A) Nur77-eGFP and CD69 upregulation in *IgM*$^{-/-}$ and *IgD*$^{-/-}$ splenic B cells stimulated with indicated doses of LPS, CpG DNA, and Pam3CSK4. Histograms compare unstimulated cells with cells incubated with indicated stimuli for 18 hours at 37C. Histograms are representative of two independent experiments.

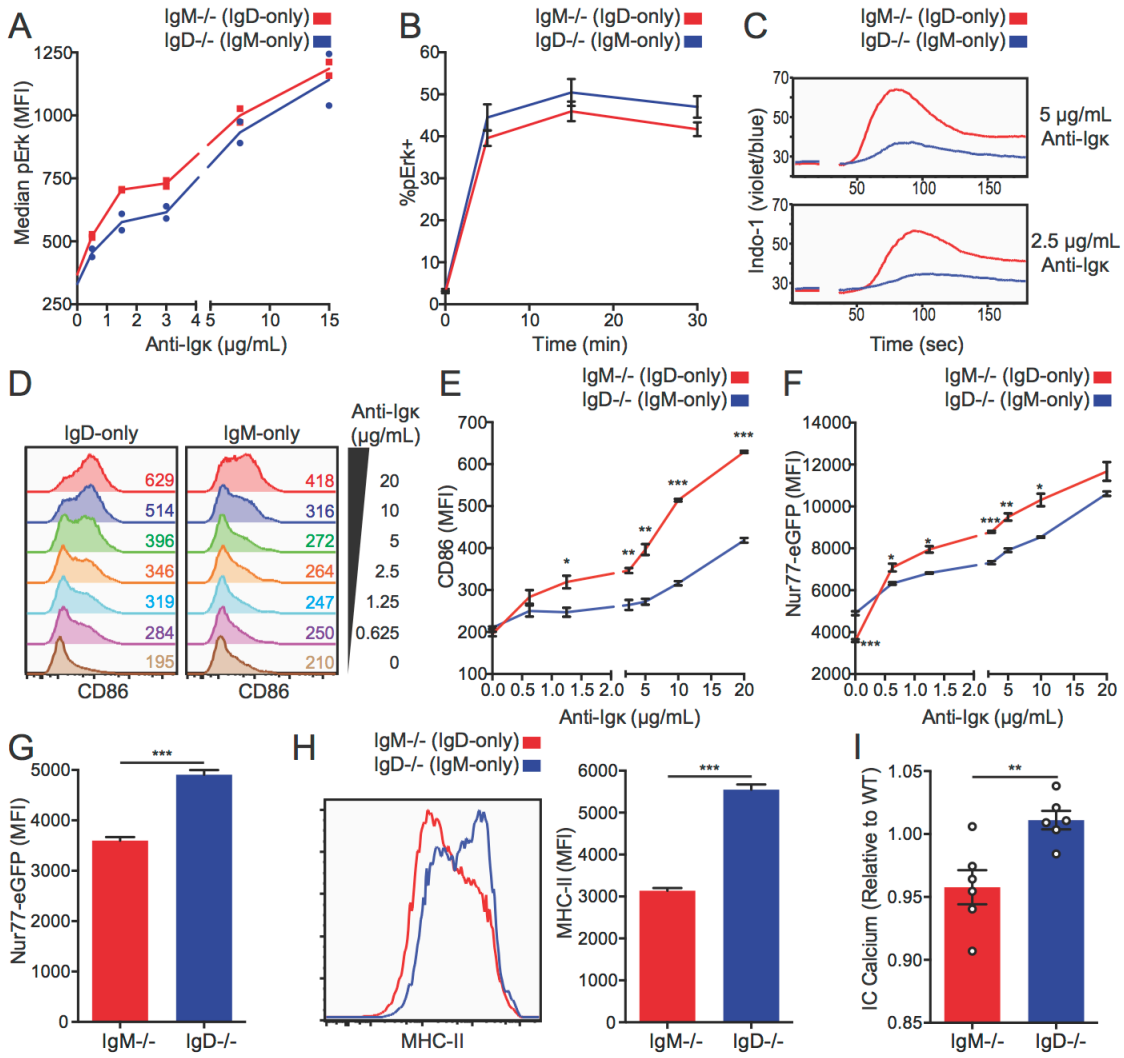
A
IgM-/- (IgD-only)
IgD-/- (IgM-only)
Median pErk (MFI)
Anti-Igκ (μg/mL)
B
%pErk+
Time (min)
C
Indo-1 (violet/blue)
5 μg/mL Anti-Igκ
2.5 μg/mL Anti-Igκ
Time (sec)
D
IgD-only
IgM-only
Anti-Igκ (μg/mL)
CD86
E
CD86 (MFI)
F
Nur77-eGFP (MFI)
G
H
MHC-II
MHC-II (MFI)
I
IC Calcium (Relative to WT)

Figure 2.5. IgD signals strongly *in vitro* but weakly *in vivo.*

(A) Median intracellular pErk in splenic Fo (B220+CD23+) B cells stimulated anti-Igκ for 15 minutes.

(B) Erk phosphorylation kinetics in Fo B cells stimulated with 15 μg/mL anti-Igκ.

(C) Splenocytes from *IgM*$^{-/-}$ and *IgD*$^{-/-}$ mice were loaded with Indo-1 and stimulated with 2.5 or 5 μg/mL anti-Igκ. (D) CD86 induction in CD23+ *IgM*$^{-/-}$ and *IgD*$^{-/-}$ splenocytes stimulated with anti-Igκ for 18 hours.

(E) Summary data for CD86 MFI in (D).

(F) Nur77-eGFP induction in cells from (D).

(G) Nur77-eGFP in cells from (D) incubated with medium alone (0 μg/mL anti-Igκ).

(H) Representative histograms and summary data for MHC-II induction in unstimulated cells from (D).

(I) Basal calcium in unstimulated *IgM*$^{-/-}$ and *IgD*$^{-/-}$ Fo (B220+CD23+CD93-) B cells was calculated by normalizing the geometric mean of [Indo-1(violet)/Indo-1(blue)] to WT B cells in the same experiment.

For (A), signaling in cells from n = 2 *IgM*$^{-/-}$ and *IgD*$^{-/-}$ mice is displayed, and results for 1.5, 3, and 15 μg/mL of anti-Igκ were replicated in n = 3 independent experiments. Data in (B) was compiled from n = 3 independent experiments with n = 3 mice of each genotype in each experiment. Data in (C) are representative of n = 4 independent experiments for 5 μg/mL and n = 2 independent experiments for 2.5 μg/mL. For (D-H), values were calculated for splenocytes from n = 3 mice of each genotype. For (I), basal calcium ratios from n = 6 independent experiments are compiled. Welch's t test was used to calculate p values, and mean ± SEM is displayed. *$p < 0.05$, **$p < 0.01$, ***$p < 0.001$.

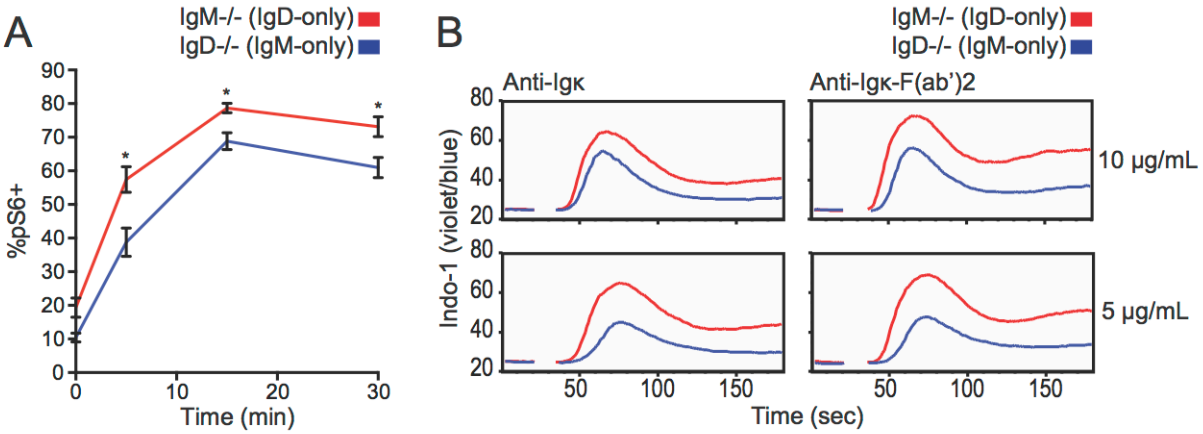
A
IgM-/- (IgD-only)
IgD-/- (IgM-only)
%pS6+
Time (min)
B
IgM-/- (IgD-only)
IgD-/- (IgM-only)
Anti-Igκ
Anti-Igκ-F(ab')2
10 μg/mL
5 μg/mL
Indo-1 (violet/blue)
Time (sec)

Figure 2.6. S6 and calcium signaling in *IgM*$^{-/-}$ and *IgD*$^{-/-}$ B cells.

(A) S6 phosphorylation kinetics in splenic CD23+ B cells following stimulation with 15 μg/mL anti-Igκ.

(B) Splenocytes from *IgM*$^{-/-}$ and *IgD*$^{-/-}$ mice were loaded with Indo-1 and stimulated with 10 or 5 μg/mL anti-Igκ or anti-Igκ F(ab')$_2$.

Data (A) and (B) are representative of n = 3 and n = 2 independent experiments, respectively. Welch's t test was used to calculate p values, and mean ± SEM is displayed. *$p < 0.05$.

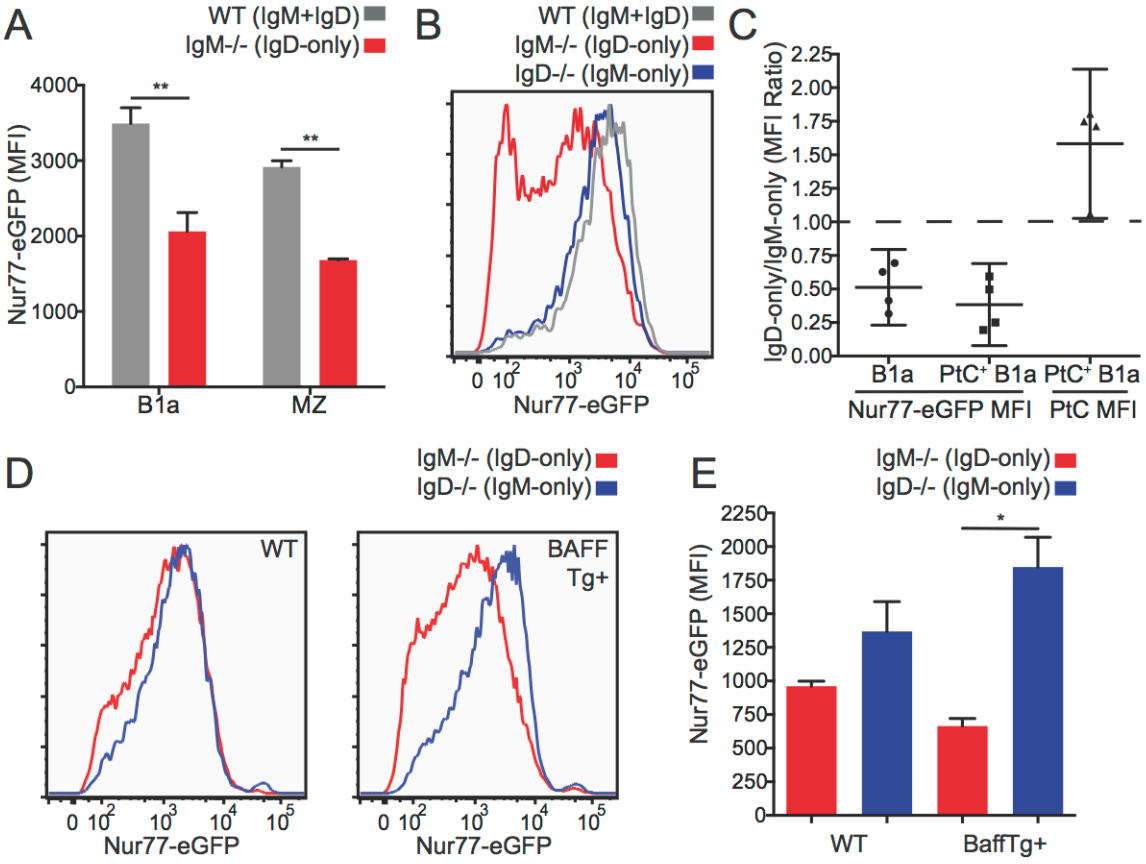
A
WT (IgM+IgD)
IgM-/- (IgD-only)
Nur77-eGFP (MFI)
4000
3000
2000
1000
0
**
**
B1a
MZ
B
WT (IgM+IgD)
IgM-/- (IgD-only)
IgD-/- (IgM-only)
0 10^2 10^3 10^4 10^5
Nur77-eGFP
C
IgD-only/IgM-only (MFI Ratio)
2.25
2.00
1.75
1.50
1.25
1.00
0.75
0.50
0.25
0.00
B1a
PtC+ B1a
PtC+ B1a
Nur77-eGFP MFI
PtC MFI
D
IgM-/- (IgD-only)
IgD-/- (IgM-only)
WT
BAFF Tg+
0 10^2 10^3 10^4 10^5
Nur77-eGFP
Nur77-eGFP
E
IgM-/- (IgD-only)
IgD-/- (IgM-only)
Nur77-eGFP (MFI)
2250
2000
1750
1500
1250
1000
750
500
250
0
*
WT
BaffTg+

Figure 2.7. Reduced *in vivo* antigen sensing by IgD in innate-like B cells.

(A) Nur77-eGFP in peritoneal B1a (CD19+CD5+CD23-) and splenic MZ (B220+CD21hiCD23lo) B cells from WT and $IgM^{-/-}$ mice.

(B) Nur77-eGFP in PtC-binding peritoneal B1a cells from WT, $IgM^{-/-}$, and $IgD^{-/-}$ mice.

(C) Nur77-eGFP and PtC MFIs were calculated for total B1a and PtC-binding B1a cells. The ratio of the $IgM^{-/-}$ (IgD-only) MFI to the $IgD^{-/-}$ (IgM-only) MFI is displayed with a 95% confidence interval.

(D) Representative histograms of Nur77-eGFP in $IgM^{-/-}$ and $IgD^{-/-}$ splenic MZ B cells from mice without (left) and with (right) a BAFF overexression transgene.

(E) Quantification of Nur77-eGFP in MZ B cells from (D).

For (A) and (E), n = 3 mice of each genotype were analyzed. For (B), histograms are representative of n = 4 mice of each genotype. For (C), ratios are pooled for n = 4 mice of each genotype from three independent experiments. For (D), histograms are representative of n = 3 mice of each genotype. Welch's t test (A and E) was used to calculate p values, and mean + SEM is displayed (except in C). *$p < 0.05$.

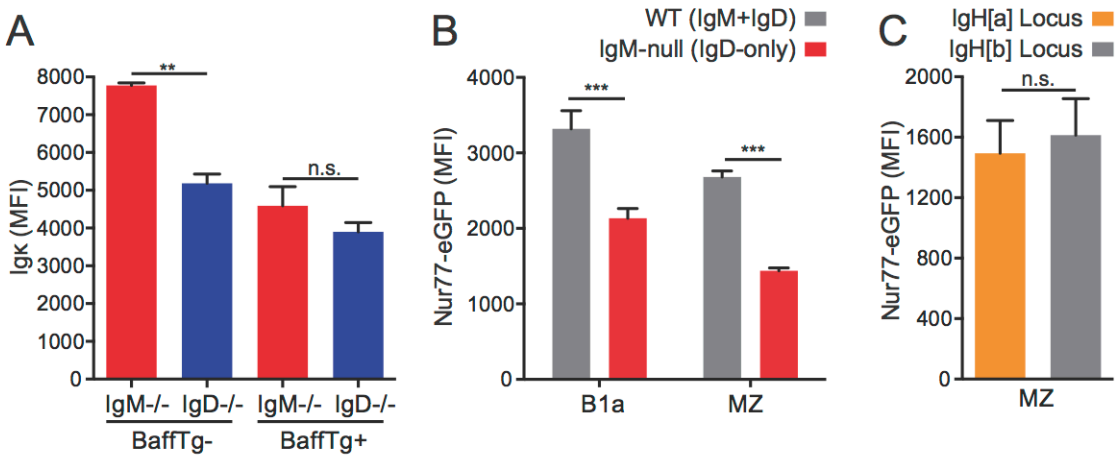
A
**
n.s.
Igκ (MFI)
8000
7000
6000
5000
4000
3000
2000
1000
0
IgM-/-
IgD-/-
IgM-/-
IgD-/-
BaffTg-
BaffTg+
B
WT (IgM+IgD)
IgM-null (IgD-only)
***
***
Nur77-eGFP (MFI)
4000
3000
2000
1000
0
B1a
MZ
C
IgH[a] Locus
IgH[b] Locus
n.s.
Nur77-eGFP (MFI)
2000
1600
1200
800
400
0
MZ

Figure 2.8. The effect of BAFF, competition, and allotype on Igκ and Nur77-eGFP expression.

(A) Surface Igκ expression on *IgM*$^{-/-}$ and *IgD*$^{-/-}$ splenic MZ B cells from mice without (left) and with (right) a BAFF overexpression transgene.

(B) Nur77-eGFP expression in peritoneal B1a and splenic MZ B cells from IgM-null (IgD[a]+) and WT (IgM[b]+) loci in *IgM*$^{-/-}$ mice.

(C) Nur77-eGFP expression in IgM[a]+ and IgM[b]+ splenic MZ B cells in 6-month-old *IgH*$^{a/b}$ mice with a BAFF overexpression transgene.

Values (A) were calculated from n = 3 mice of each genotype. Values in (B) and (C) were calculated in n = 6 and n = 4 mice, respectively. Welch's t test (A) and a paired t test (B-C) were used to calculate p values, and mean + SEM is displayed. **p < 0.01, ***p < 0.001.

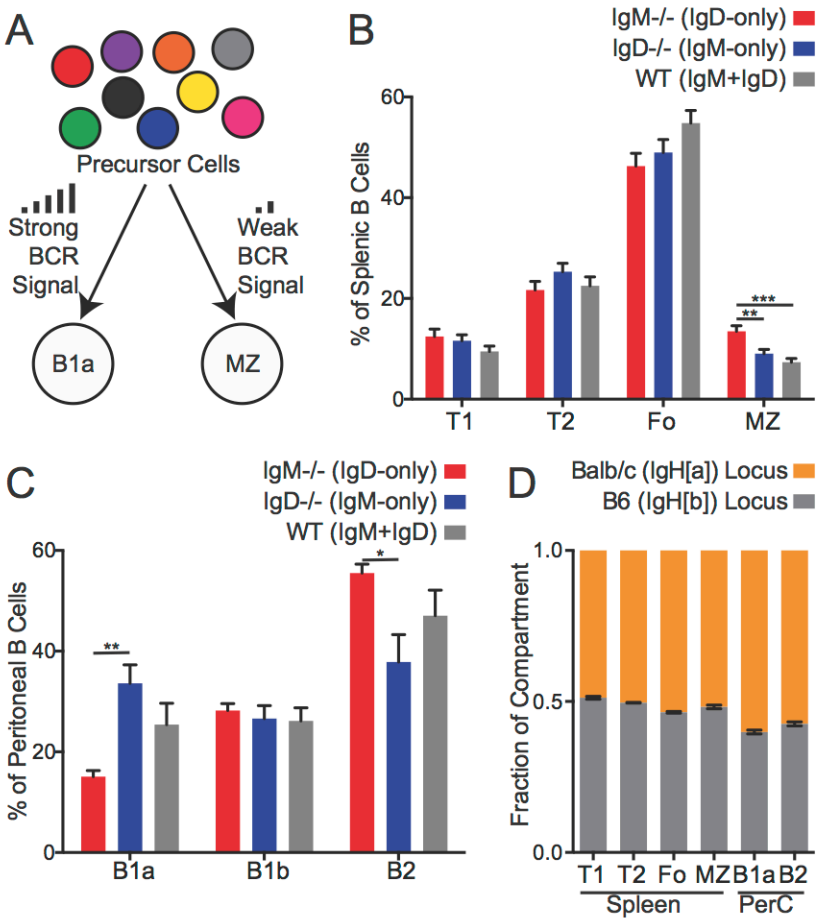
A
Precursor Cells
Strong BCR Signal
Weak BCR Signal
B1a
MZ
B
IgM-/- (IgD-only)
IgD-/- (IgM-only)
WT (IgM+IgD)
% of Splenic B Cells
60
40
20
0
T1
T2
Fo
MZ
***
**
C
IgM-/- (IgD-only)
IgD-/- (IgM-only)
WT (IgM+IgD)
% of Peritoneal B Cells
60
40
20
0
**
*
B1a
B1b
B2
D
Balb/c (IgH[a]) Locus
B6 (IgH[b]) Locus
Fraction of Compartment
1.0
0.5
0.0
T1 T2 Fo MZ B1a B2
Spleen
PerC

Figure 2.9. B cell subset development in *IgM*$^{-/-}$, *IgD*$^{-/-}$, WT, and *IgH*$^{a/b}$ mice.

(A) Signal strength model of B1a and MZ B cell development. While B1a and MZ cells originate from different precursor populations, their development is thought to be signal strength-dependent.

(B) B cell compartments as a percentage of total B220+ splenic B cells. T1 (CD93+CD23-); T2 (CD93+CD23+); Fo (CD93-CD23+); MZ (CD21^{hi}CD23^{lo}).

(C) B cell compartments as a percentage of total CD19+ peritoneal B cells. B1a (CD5+CD23-); B1b (CD5-CD23-); B2 (CD5-CD23+).

(D) Relative competition between IgM[a]+ and IgM[b]+ B cells in Balb/c-B6 F1 mice was calculated for splenic and peritoneal compartments described in (B-C).

For (B), n = 10-12 mice of each genotype were analyzed. For (C), n = 6 mice of each genotype were analyzed. For (D), n = 3 mice were analyzed. Mice in (D) were 6-14 weeks old. One-way ANOVA with Tukey's multiple comparisons test (B-C) was used to calculate p values, and mean ± SEM is displayed. *$p < 0.05$, **$p < 0.01$, ***$p < 0.001$.

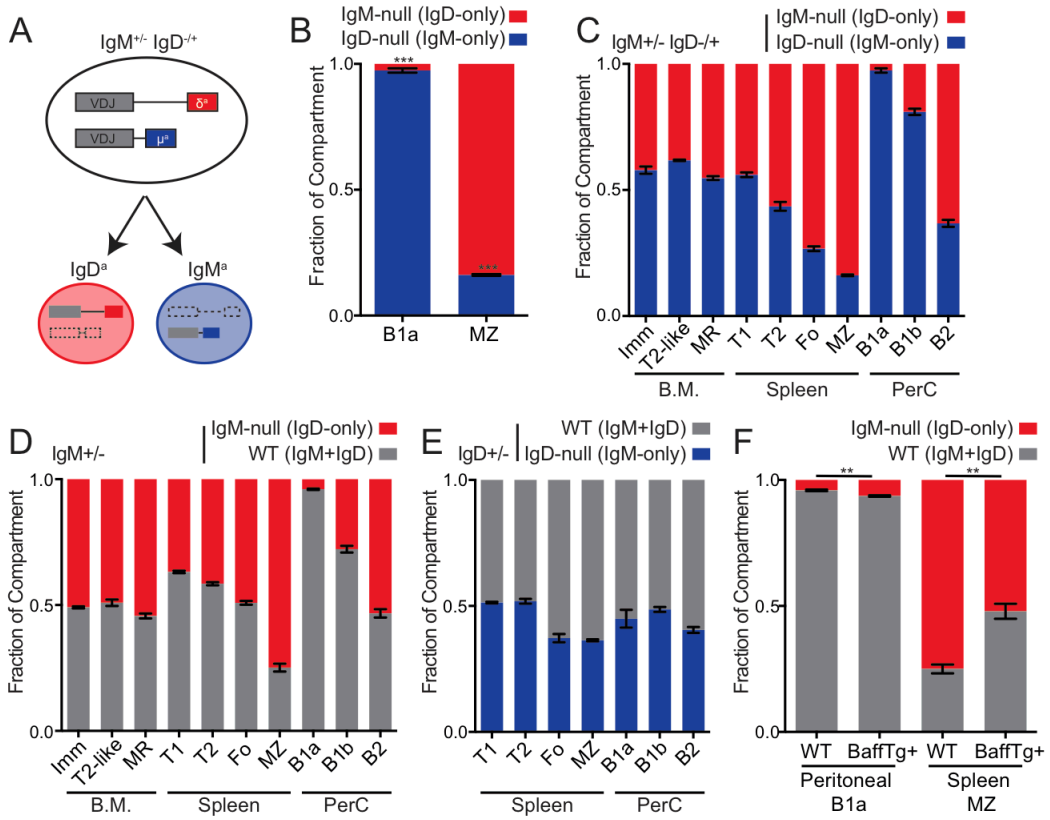
A
IgM+/- IgD-/+
VDJ
δa
VDJ
μa
IgDa
IgMa
B
IgM-null (IgD-only)
IgD-null (IgM-only)
Fraction of Compartment
1.0
0.5
0.0
***
***
B1a
MZ
C
IgM+/- IgD-/+
IgM-null (IgD-only)
IgD-null (IgM-only)
Fraction of Compartment
Imm
T2-like
MR
T1
T2
Fo
MZ
B1a
B1b
B2
B.M.
Spleen
PerC
D
IgM+/-
IgM-null (IgD-only)
WT (IgM+IgD)
Fraction of Compartment
Imm
T2-like
MR
T1
T2
Fo
MZ
B1a
B1b
B2
B.M.
Spleen
PerC
E
IgD+/-
WT (IgM+IgD)
IgD-null (IgM-only)
Fraction of Compartment
T1
T2
Fo
MZ
B1a
B1b
B2
Spleen
PerC
F
IgM-null (IgD-only)
WT (IgM+IgD)
Fraction of Compartment
**
**
WT
BaffTg+
WT
BaffTg+
Peritoneal B1a
Spleen MZ

Figure 2.10. Cell-intrinsic skewing of B cell developmental decisions by IgM and IgD BCRs.

(A) Allelic exclusion leads to a 1:1 mixture of IgM-only and IgD-only B cells in $IgM^{+/-}$ $IgD^{-/+}$ mice.

(B) Proportion of peritoneal B1a (CD19+CD5+CD23-) and splenic MZ (B220+$CD21^{hi}CD23^{lo}$) B cells originating from each Ig locus in $IgM^{+/-}$ $IgD^{-/+}$ mice.

(C) Relative competition between IgM+ and IgD+ B cells in $IgM^{+/-}$ $IgD^{-/+}$ mice was calculated for bone marrow, splenic, and peritoneal B cell compartments. Results include data from (B) for reference. Immature (CD23-CD93+); T2-like (CD23+CD93+); mature recirculating (CD23+CD93-); T1 (CD93+CD23-); T2 (CD93+CD23+); Fo (CD93-CD23+); MZ ($CD21^{hi}CD23^{lo}$); B1a (CD5+CD23-); B1b (CD5-CD23-); B2 (CD5-CD23+).

(D) Relative competition between WT (IgM[b]+) and IgM-null (IgD[a]+) B cells in $IgM^{+/-}$ mice was determined as in (C).

(E) Relative competition between WT (IgM[b]+) and IgD-null (IgM[a]+) B cells in $IgD^{+/-}$ mice was determined for splenic and peritoneal compartments as described in (C).

(F) Competition in peritoneal B1a and splenic MZ compartments in $IgM^{+/-}$ mice with or without a BAFF overexpression transgene. Results include data from (D) for reference.

For (B) and (C), n = 3-5 mice were analyzed. For (D), n = 3-8 mice were analyzed. For (E), n = 5 mice were analyzed. For (F), n = 4-5 mice of each genotype were analyzed. Welch's t test was used to calculate p values, and mean ± SEM is displayed. **$p < 0.01$, ***$p < 0.001$.

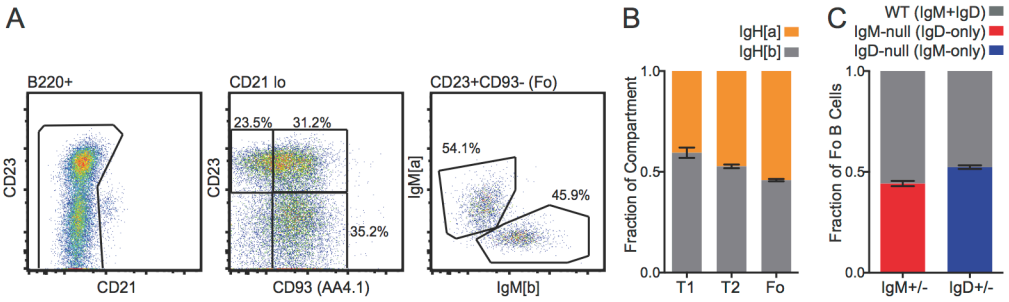
A
B220+
CD23
CD21
CD21 lo
23.5%
31.2%
35.2%
CD93 (AA4.1)
CD23+CD93- (Fo)
54.1%
45.9%
IgM[a]
IgM[b]
B
IgH[a]
IgH[b]
Fraction of Compartment
1.0
0.5
0.0
T1
T2
Fo
C
WT (IgM+IgD)
IgM-null (IgD-only)
IgD-null (IgM-only)
Fraction of Fo B Cells
IgM+/-
IgD+/-

Figure 2.11. Splenic B cell subsets in *IgH*$^{a/b}$, *IgM*$^{+/-}$, and *IgD*$^{+/-}$ *Lyn*$^{-/-}$ mice.

(A) Gating scheme for determining Ig locus of origin for splenic B cell subsets in 6-month-old *IgH*$^{a/b}$ *Lyn*$^{-/-}$ mice. CD21^{hi} cells did not express surface BCR and were not considered bona fide MZ B cells.

(B) Quantification of compartments in (A). T1 (CD93+CD23-); T2 (CD93+CD23+); Fo (CD93-CD23+).

(C) Percentage of Fo B cells originating from each Ig locus in *IgM*$^{+/-}$ and *IgD*$^{+/-}$ mice on the *Lyn*$^{-/-}$ background.

Percentages in (A-C) were calculated using n = 5-6 mice of each genotype, and mean + SEM is displayed.

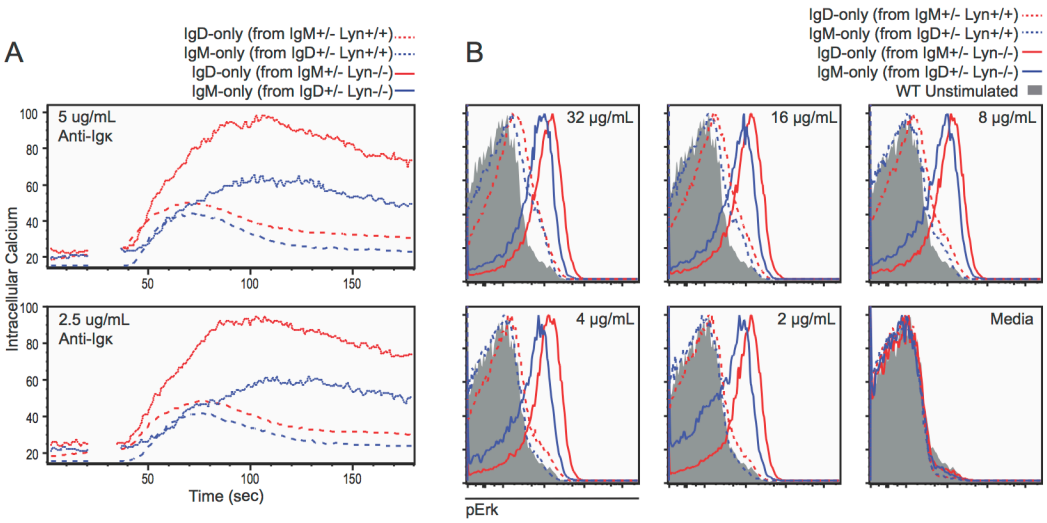
A
IgD-only (from IgM+/- Lyn+/+)
IgM-only (from IgD+/- Lyn+/+)
IgD-only (from IgM+/- Lyn-/-)
IgM-only (from IgD+/- Lyn-/-)
5 ug/mL
Anti-Igκ
2.5 ug/mL
Anti-Igκ
Intracellular Calcium
Time (sec)
B
IgD-only (from IgM+/- Lyn+/+)
IgM-only (from IgD+/- Lyn+/+)
IgD-only (from IgM+/- Lyn-/-)
IgM-only (from IgD+/- Lyn-/-)
WT Unstimulated
32 µg/mL
16 µg/mL
8 µg/mL
4 µg/mL
2 µg/mL
Media
pErk

Figure 2.12. Signaling in *IgM*$^{+/-}$ and *IgD*$^{+/-}$ *Lyn*$^{-/-}$ B cells.

(A) *IgM*$^{+/-}$ and *IgD*$^{+/-}$ mice on either *Lyn*$^{+/+}$ or *Lyn*$^{-/-}$ backgrounds were loaded with Indo-1 and stimulated with anti-Igκ. WT (IgM[b]+) B cells were gated out to isolate IgM-null (IgD-only) and IgD-null (IgM-only) cells. Mature (CD19+CD23+) B cells are displayed.

(B) Intracellular Erk phosphorylation in mature (B220+CD23+) B cells from mice in (A) stimulated with anti-Igκ for 5 minutes. Shaded histogram corresponds to IgM[b]+ cells from *IgD*$^{+/-}$ *Lyn*$^{-/-}$ mice incubated with medium alone.

(A) and (B) are representative of two independent experiments.

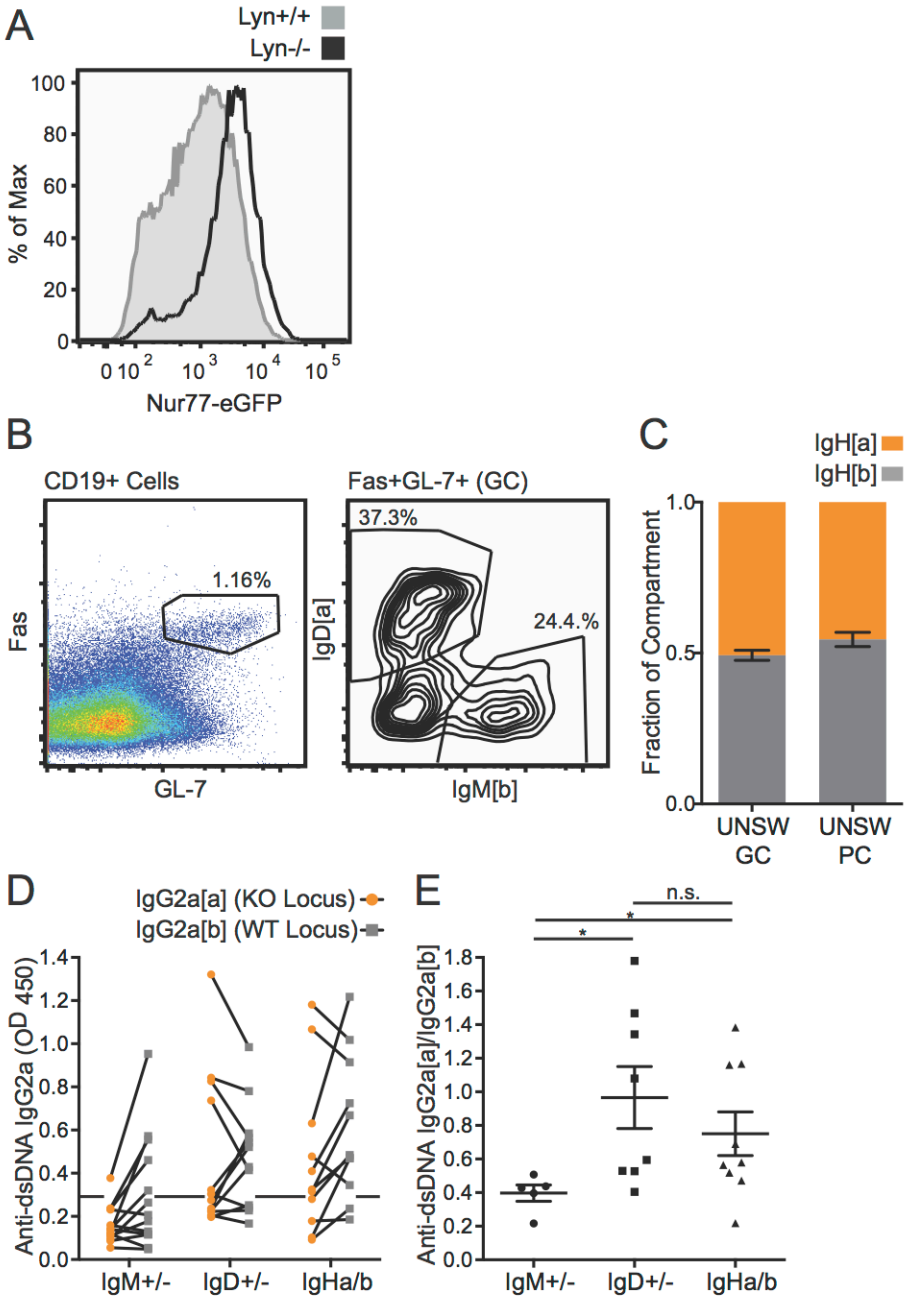
A
Lyn+/+
Lyn-/-
% of Max
Nur77-eGFP
B
CD19+ Cells
Fas+GL-7+ (GC)
1.16%
37.3%
24.4%
Fas
GL-7
IgD[a]
IgM[b]
C
IgH[a]
IgH[b]
Fraction of Compartment
UNSW GC
UNSW PC
D
IgG2a[a] (KO Locus)
IgG2a[b] (WT Locus)
Anti-dsDNA IgG2a (OD 450)
IgM+/-
IgD+/-
IgHa/b
E
n.s.
Anti-dsDNA IgG2a[a]/IgG2a[b]
IgM+/-
IgD+/-
IgHa/b

Figure 2.13. Nur77-eGFP in *Lyn*$^{-/-}$ B cells and the role of BCR allotype in *Lyn*$^{-/-}$ phenotypes.

(A) Nur77-eGFP expression in splenic mature follicular B cells from *Lyn*$^{+/+}$ and *Lyn*$^{-/-}$ mice.

(B) Gating scheme for determining the Ig locus of origin for germinal center B cells in 6-month-old *IgM*$^{+/-}$ *Lyn*$^{-/-}$ mice.

(C) Relative contribution of IgH[a]+ and IgH[b]+ B cells to the splenic unswitched GC (CD19+ Fas+ GL-7+ IgM+) and unswitched PC (CD138+ IgM+) compartments of 6-month-old *IgH*$^{a/b}$ *Lyn*$^{-/-}$ mice.

(D) Anti-dsDNA IgG2a from each Ig locus in 5-6 month old *IgM*$^{+/-}$, *IgD*$^{+/-}$, and *IgH*$^{a/b}$ mice on the *Lyn*$^{-/-}$ background was quantified by ELISA.

(E) The OD ratio of knockout (allotype a) to WT (allotype b) anti-dsDNA IgG2a was calculated for all mice in (D) in which either locus produced an OD > 0.3.

Histograms in (A) are representative of at least n = 3 mice of each genotype. Percentages in (B-C) were calculated using n = 5-6 mice of each genotype, and mean ± SEM is displayed. For (D), n = 10-13 mice of each genotype were analyzed. For (E), n = 5-9 autoantibody-positive mice were analyzed. Welch's t test (E) was used to calculate p values, and mean ± SEM is displayed. *$p < 0.05$.

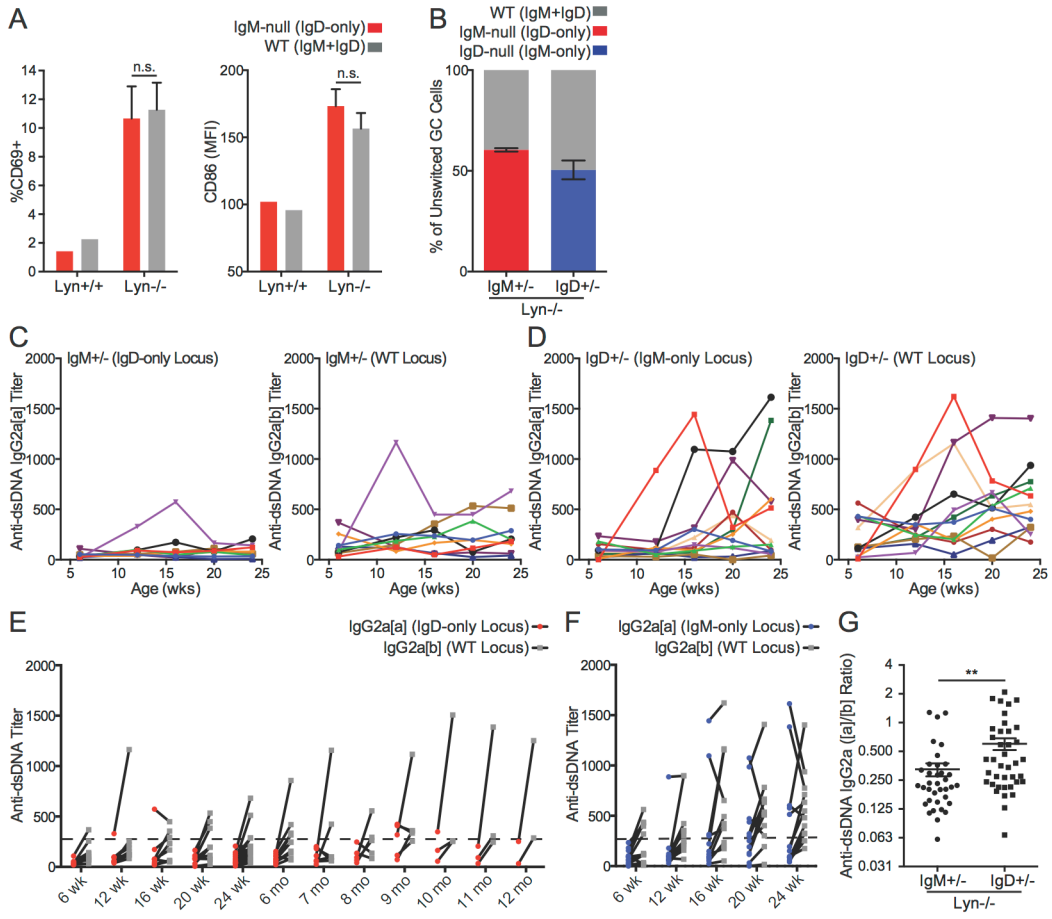
A
IgM-null (IgD-only)
WT (IgM+IgD)
%CD69+
n.s.
Lyn+/+
Lyn-/-
CD86 (MFI)
B
WT (IgM+IgD)
IgM-null (IgD-only)
IgD-null (IgM-only)
% of Unswitced GC Cells
IgM+/-
IgD+/-
Lyn-/-
C
IgM+/- (IgD-only Locus)
IgM+/- (WT Locus)
Anti-dsDNA IgG2a[a] Titer
Anti-dsDNA IgG2a[b] Titer
Age (wks)
D
IgD+/- (IgM-only Locus)
IgD+/- (WT Locus)
E
IgG2a[a] (IgD-only Locus)
IgG2a[b] (WT Locus)
Anti-dsDNA Titer
6 wk
12 wk
16 wk
20 wk
24 wk
6 mo
7 mo
8 mo
9 mo
10 mo
11 mo
12 mo
F
IgG2a[a] (IgM-only Locus)
IgG2a[b] (WT Locus)
G
Anti-dsDNA IgG2a ([a]/[b] Ratio)
**
IgM+/-
IgD+/-
Lyn-/-

Figure 2.14. IgD can drive polyclonal activation and germinal center entry, but not anti-dsDNA IgG2a production, in *Lyn*$^{-/-}$ mice.

(A) Surface CD69 and CD86 expression on CD23+ splenic B cells from each Ig locus in *IgM*$^{+/-}$ mice on *Lyn*$^{+/+}$ and *Lyn*$^{-/-}$ backgrounds.

(B) Percentage of unswitched germinal center (CD19+ Fas^{hi} GL-7^{hi} IgM/IgD+) B cells from each Ig locus in *IgM*$^{+/-}$ and *IgD*$^{+/-}$ mice on the *Lyn*$^{-/-}$ background.

(C) Anti-dsDNA IgG2a titers from each Ig locus in *IgM*$^{+/-}$ *Lyn*$^{-/-}$ mice were calculated by ELISA using pooled *IgH*$^{a/b}$ autoimmune serum with high-titer autoantibodies from each locus as a reference (titer set at 1000).

(D) Anti-dsDNA IgG2a titers in *IgD*$^{+/-}$ *Lyn*$^{-/-}$ mice were calculated as in (C).

(E) Paired anti-dsDNA titers from each locus in *IgM*$^{+/-}$ *Lyn*$^{-/-}$ mice from (C) with additional mice from 24 weeks to 12 months.

(F) Paired anti-dsDNA titers from each locus in *IgD*$^{+/-}$ *Lyn*$^{-/-}$ mice from (D).

(G) Ratio of anti-dsDNA IgG2a[a] to IgG2a[b] from all samples in (E) and (F) with an anti-dsDNA IgG2a titer > 250 from either locus; cutoff defined by titers in young WT mice.

For (A), n = 4 *IgM*$^{+/-}$ *Lyn*$^{-/-}$ mice are compared to a reference *IgM*$^{+/-}$ *Lyn*$^{+/+}$ mouse. Qualitatively similar results were obtained in two independent experiments. For (B) n = 5-6 mice of each genotype were analyzed. For (C) and (D), n = 9 and n = 12 mice were tracked. For (G), n = 36 *IgM*$^{+/-}$ *Lyn*$^{-/-}$ and n = 39 *IgD*$^{+/-}$ *Lyn*$^{-/-}$ anti-dsDNA IgG2a+ samples were compared. Welch's t test was used to calculate p values, and mean ± SEM is displayed. **$p < 0.01$.

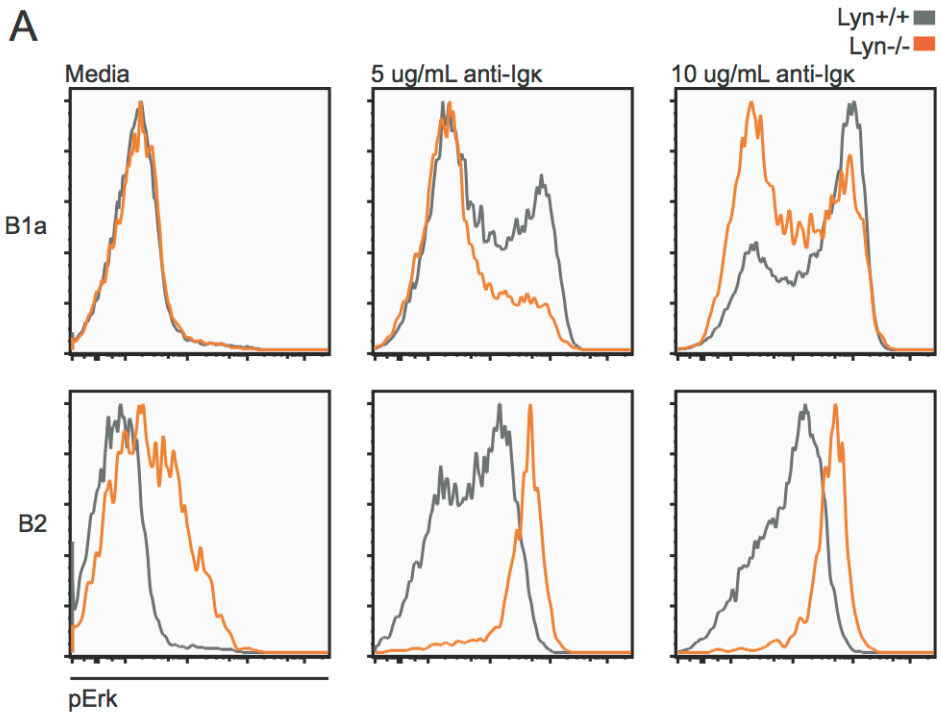
A
Lyn+/+
Lyn-/-
Media
5 ug/mL anti-Igκ
10 ug/mL anti-Igκ
B1a
B2
pErk

Figure 2.15. BCR signaling in *Lyn*$^{-/-}$ peritoneal B cell subsets.

(A) Intracellular Erk phosphorylation in peritoneal B220+ B cells stimulated with anti-Igκ for 5 minutes. B1a (CD5+CD23-); B2 (CD5-CD23+).

Histograms in (A) are representative of cells from n = 2 WT and *Lyn*$^{-/-}$ mice.

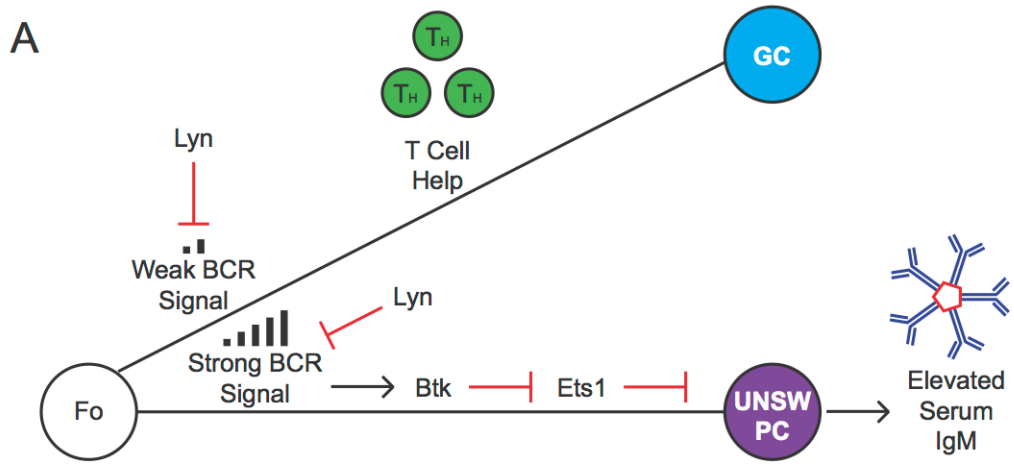
A
TH
TH
TH
GC
T Cell
Help
Lyn
Weak BCR
Signal
Lyn
Strong BCR
Signal
Fo
Btk
Ets1
UNSW
PC
Elevated
Serum
IgM

Figure 2.16. Model of how Lyn restrains follicular B cells.

(A) Lyn restrains BCR signaling in Fo B cells. Loss of Lyn leads to Btk-dependent repression of Ets1 and expansion of unswitched (IgM+) plasma cells.

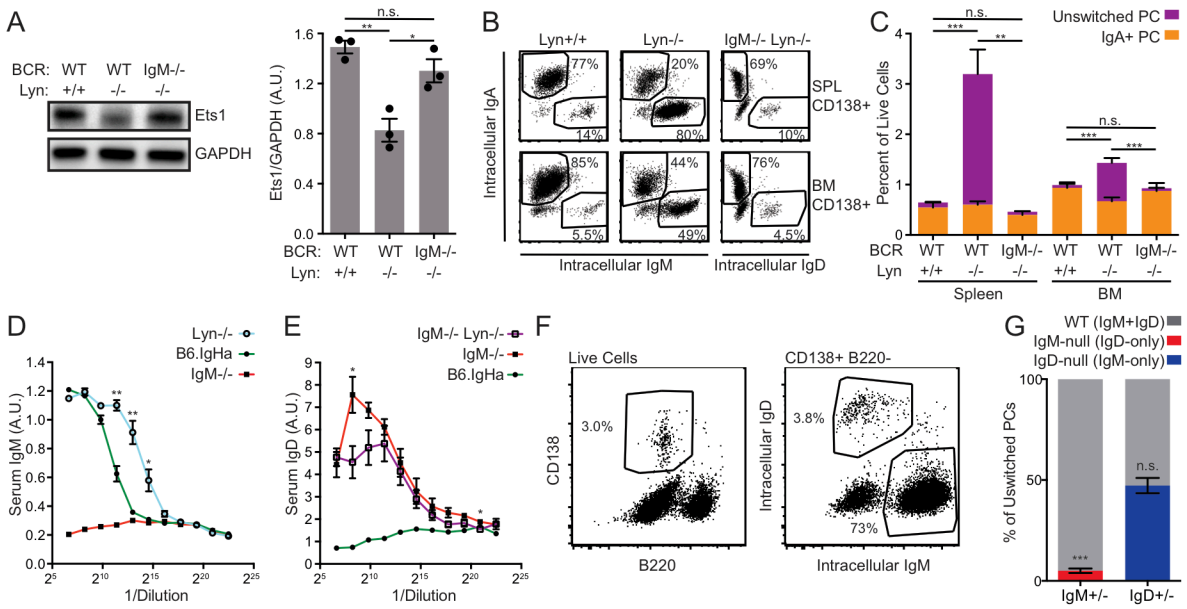
A
BCR: WT WT IgM-/-
Lyn: +/+ -/- -/-
Ets1
GAPDH
Ets1/GAPDH (A.U.)
n.s.
**
*
BCR: WT WT IgM-/-
Lyn: +/+ -/- -/-
B
Lyn+/+
Lyn-/-
IgM-/- Lyn-/-
Intracellular IgA
77%
14%
20%
80%
69%
10%
SPL CD138+
85%
5.5%
44%
49%
76%
4.5%
BM CD138+
Intracellular IgM
Intracellular IgD
C
Unswitched PC
IgA+ PC
Percent of Live Cells
n.s.
***
**
n.s.
***
***
BCR WT WT IgM-/- WT WT IgM-/-
Lyn +/+ -/- -/- +/+ -/- -/-
Spleen
BM
D
Lyn-/-
B6.IgHa
IgM-/-
Serum IgM (A.U.)
1/Dilution
E
IgM-/- Lyn-/-
IgM-/-
B6.IgHa
Serum IgD (A.U.)
1/Dilution
F
Live Cells
CD138
B220
3.0%
CD138+ B220-
Intracellular IgD
Intracellular IgM
3.8%
73%
G
WT (IgM+IgD)
IgM-null (IgD-only)
IgD-null (IgM-only)
% of Uswitched PCs
***
n.s.
IgM+/-
IgD+/-

Figure 2.17. Cell-intrinsic IgM expression is required for unswitched plasma cell expansion in *Lyn*$^{-/-}$ mice.

(A) Representative blot and quantification of Ets1 and GAPDH protein in purified splenic B cells from WT, *Lyn*$^{-/-}$, and *IgM*$^{-/-}$ *Lyn*$^{-/-}$ mice.

(B) Composition of the CD138+ plasma cell compartments in the spleens and bone marrow of WT, *Lyn*$^{-/-}$, and *IgM*$^{-/-}$ *Lyn*$^{-/-}$ mice was determined by intracellular staining of IgM, IgD, and IgA.

(C) Percentages in (B) multiplied by the fraction of live cells positive for CD138 in each tissue. Unswitched cells are positive for either IgM or IgD. Statistics correspond to unswitched plasma cell percentages; differences in IgA+ cells were not significant.

(D) Serum IgM in 16-week-old mice was quantified for B6.IgHa (WT) and *Lyn*$^{-/-}$ mice by ELISA. A sample from an *IgM*$^{-/-}$ mouse is shown for reference.

(E) Serum IgD in 16-week-old mice was quantified for *IgM*$^{-/-}$ and *IgM*$^{-/-}$ *Lyn*$^{-/-}$ mice by ELISA. A sample from a WT mouse is shown for reference.

(F) Gating scheme for quantifying the unswitched splenic plasma cell composition of *IgM*$^{+/-}$ *Lyn*$^{-/-}$ mice.

(G) Percentage of unswitched splenic plasma cells (CD138+B220^{lo}IgM/IgD+) from each locus in *IgM*$^{+/-}$ and *IgD*$^{+/-}$ mice on the *Lyn*$^{-/-}$ background.

For (B) and (C), figures are representative of n = 4-5 mice of each genotype. For (D), values from n = 3 WT and n = 4 *Lyn*$^{-/-}$ mice are averaged. For (E), values from n = 3 *IgM*$^{-/-}$ and n = 4 *IgM*$^{-/-}$ *Lyn*$^{-/-}$ mice are averaged. For (F) and (G), n = 4-5 mice of each genotype were used. Welch's t test was used to calculate p values, and mean ± SEM is displayed. *$p < 0.05$, **$p < 0.01$, ***$p < 0.001$.

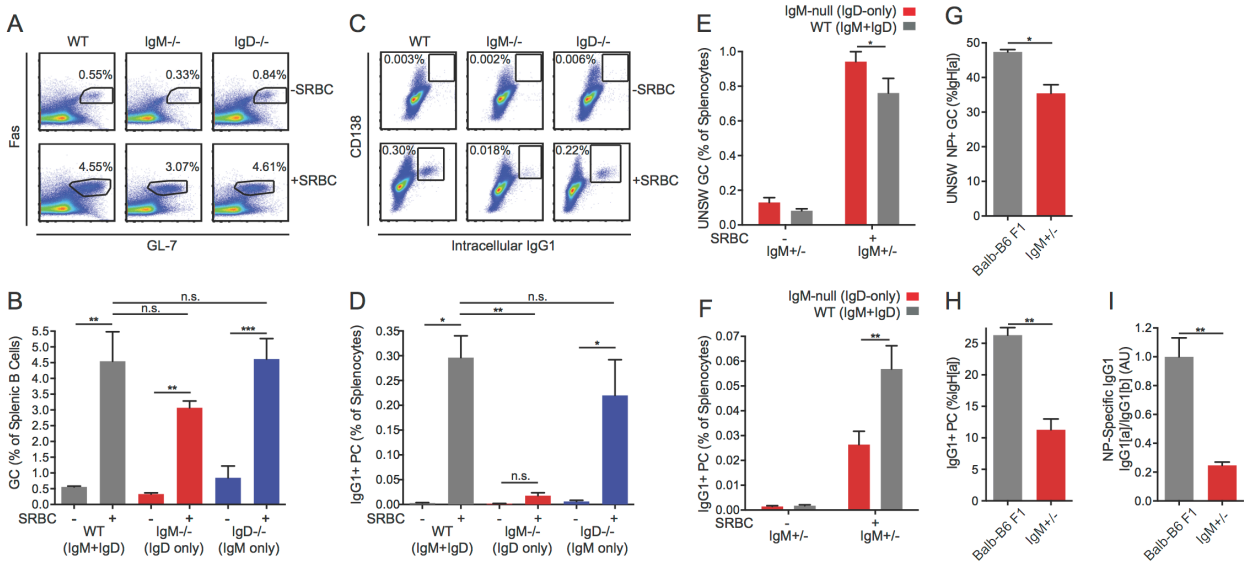
A
WT
IgM-/-
IgD-/-
0.55%
0.33%
0.84%
-SRBC
4.55%
3.07%
4.61%
+SRBC
Fas
GL-7
C
WT
IgM-/-
IgD-/-
0.003%
0.002%
0.006%
-SRBC
0.30%
0.018%
0.22%
+SRBC
CD138
Intracellular IgG1
E
IgM-null (IgD-only)
WT (IgM+IgD)
UNSW GC (% of Splenocytes)
SRBC
IgM+/-
IgM+/-
G
UNSW NP+ GC (%IgH[a])
Balb-B6 F1
IgM+/-
B
GC (% of Splenic B Cells)
n.s.
n.s.
SRBC
WT (IgM+IgD)
IgM-/- (IgD only)
IgD-/- (IgM only)
D
IgG1+ PC (% of Splenocytes)
n.s.
n.s.
SRBC
WT (IgM+IgD)
IgM-/- (IgD only)
IgD-/- (IgM only)
F
IgM-null (IgD-only)
WT (IgM+IgD)
IgG1+ PC (% of Splenocytes)
SRBC
IgM+/-
IgM+/-
H
IgG1+ PC (%IgH[a])
Balb-B6 F1
IgM+/-
I
NP-Specific IgG1
IgG1[a]/IgG1[b] (AU)
Balb-B6 F1
IgM+/-

Figure 2.18. IgD-only cells have intact germinal center responses but impaired IgG1+ plasma cell responses.

(A) Splenic B (CD19+) cells from unimmunized and WT, *IgM*$^{-/-}$, and *IgD*$^{-/-}$ mice 5 days after i.p. immunization with 200 μL of 10% SRBCs.

(B) Quantification of germinal center (Fas^{hi} GL-7^{hi}) cells in (A).

(C) Splenocytes from unimmunized and WT, *IgM*$^{-/-}$, and *IgD*$^{-/-}$ mice 5 days after i.p. immunization with 200 μL of 10% SRBCs.

(D) Quantification of CD138+ IgG1+ plasma cells in (C).

(E) WT (IgM[b]+) and IgM-null (IgD[a]+) germinal center B cells as a percentage of live splenocytes in unimmunized and *IgM*$^{+/-}$ mice 5 days after i.p. immunization with 200 μL of 10% SRBCs.

(F) WT (IgG1[b]+) and IgM-null (IgG1[a]+) switched plasma cells (CD138+IgG1+) as a percentage of live splenocytes in unimmunized and *IgM*$^{+/-}$ mice 5 days after i.p. immunization with 200 μL of 10% SRBCs.

(G) Fraction of unswitched NP-specific germinal center cells (CD19+ Fas^{hi} GL-7^{hi} IgM/IgD+) from the IgH[a] locus in the spleens of Balb/c-B6 F1 and *IgM*$^{+/-}$ mice 7-8 days after i.p. immunization with 100 μg NP-RSA.

(H) Fraction of IgG1+ CD138+ plasma cells from the IgH[a] locus in Balb/c-B6 F1 and *IgM*$^{+/-}$ mice 7-8 days after i.p. immunization with 100 μg NP-RSA.

(I) NP-specific IgG1[a] and IgG1[b] titers at OD = 0.2 were calculated for the mice in (G-H) by ELISA. The IgG1[a] to IgG1[b] titer ratio was calculated for each mouse, and all ratios were normalized such that the average IgG1[a]/IgG1[b] ratio in Balb/c-B6 F1 samples = 1.0.

For (A-D), statistics from n = 4 umimmunized mice of each genotype and n = 3 WT, n = 6 *IgM*$^{-/-}$

, and n = 7 *IgD*$^{-/-}$ immunized mice were pooled. For (E-F), n = 5 unimmunized and n = 5 immunized mice are shown. For (G-I), n = 5 Balb/c-B6 F1 mice and n = 3 *IgM*$^{+/-}$ mice are shown. One-way ANOVA with Tukey's multiple comparisons test (B and D), a paired t test (E-F), and Welch's t test (G-I) were used to calculate p values, and mean + SEM is displayed. *$p < 0.05$, **$p < 0.01$, ***$p < 0.001$.

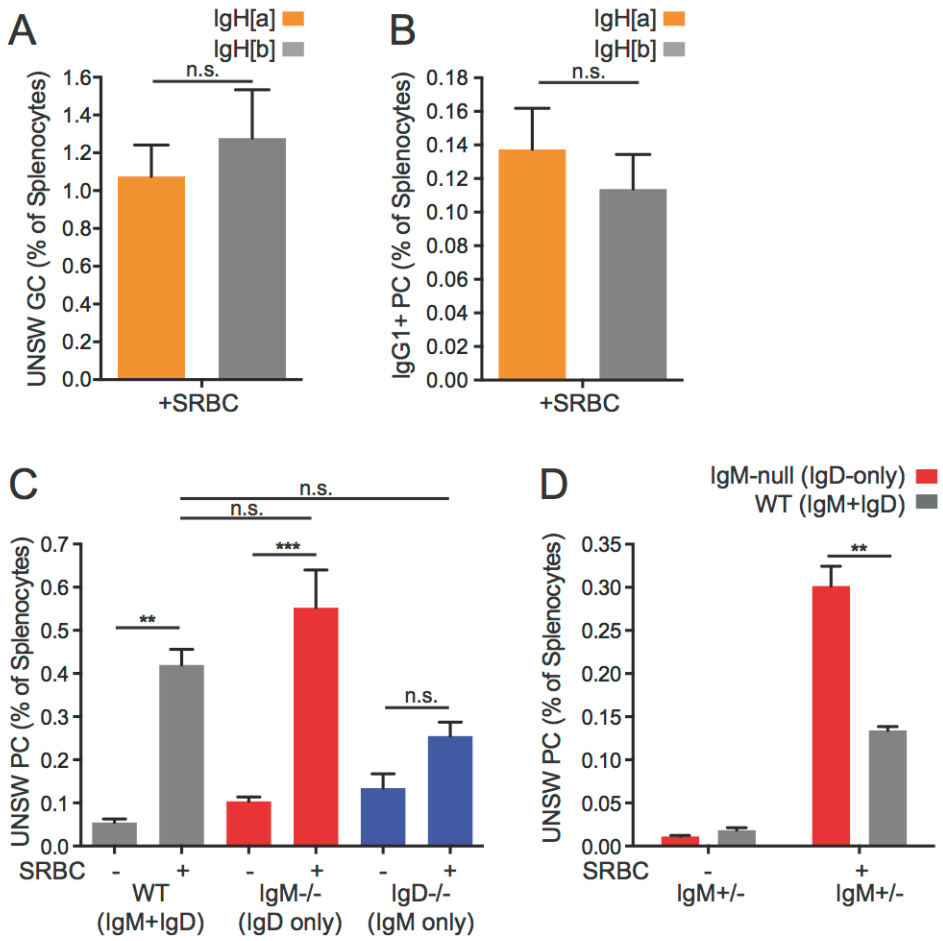
A
IgH[a]
IgH[b]
n.s.
UNSW GC (% of Splenocytes)
1.6
1.4
1.2
1.0
0.8
0.6
0.4
0.2
0.0
+SRBC
B
IgH[a]
IgH[b]
n.s.
IgG1+ PC (% of Splenocytes)
0.18
0.16
0.14
0.12
0.10
0.08
0.06
0.04
0.02
0.00
+SRBC
C
n.s.
n.s.
***
**
n.s.
UNSW PC (% of Splenocytes)
0.7
0.6
0.5
0.4
0.3
0.2
0.1
0.0
SRBC - + - + - +
WT (IgM+IgD)
IgM-/- (IgD only)
IgD-/- (IgM only)
D
IgM-null (IgD-only)
WT (IgM+IgD)
**
UNSW PC (% of Splenocytes)
0.35
0.30
0.25
0.20
0.15
0.10
0.05
0.00
SRBC - +
IgM+/-
IgM+/-

Figure 2.19. Role of BCR allotype and generation of unswitched plasma cells in SRBC-immunized mice.

(A) Quantification of IgM[a]+ and IgM[b]+ germinal center B cells (CD19+ Fas^{hi} GL-7^{hi}) as a percentage of live splenocytes in $IgH^{a/b}$ mice 5 days after i.p. immunization with 200 μL of 10% SRBCs.

(B) Quantification of IgM[a]+ and IgM[b]+ plasma cells (CD138+) as a percentage of live splenocytes in $IgH^{a/b}$ mice 5 days after i.p. immunization with 200 μL of 10% SRBCs.

(C) Quantification of splenic unswitched (IgM+ or IgD+) CD138+ plasma cells from unimmunized and WT, $IgM^{-/-}$, and $IgD^{-/-}$ mice 5 days after i.p. immunization with 200 μL of 10% SRBCs.

(D) WT (IgM[b]+) and IgM-null (IgD[a]+) unswitched plasma cells (CD138+) as a percentage of live splenocytes in unimmunized and $IgM^{+/-}$ mice 5 days after i.p. immunization with 200 μL of 10% SRBCs.

For (A) and (B), n = 3 mice were analyzed. Paired t tests (A-B and D) and one-way ANOVA with Tukey's multiple comparisons test were used to calculate p values, and mean + SEM is displayed. For (C), cell numbers from n = 4 umimmunized mice of each genotype and n = 3 WT, n = 6 $IgM^{-/-}$, and n = 7 $IgD^{-/-}$ immunized mice were analyzed. For (D), n = 5 unimmunized and n = 5 immunized were analyzed. **$p < 0.01$, ***$p < 0.001$.

A

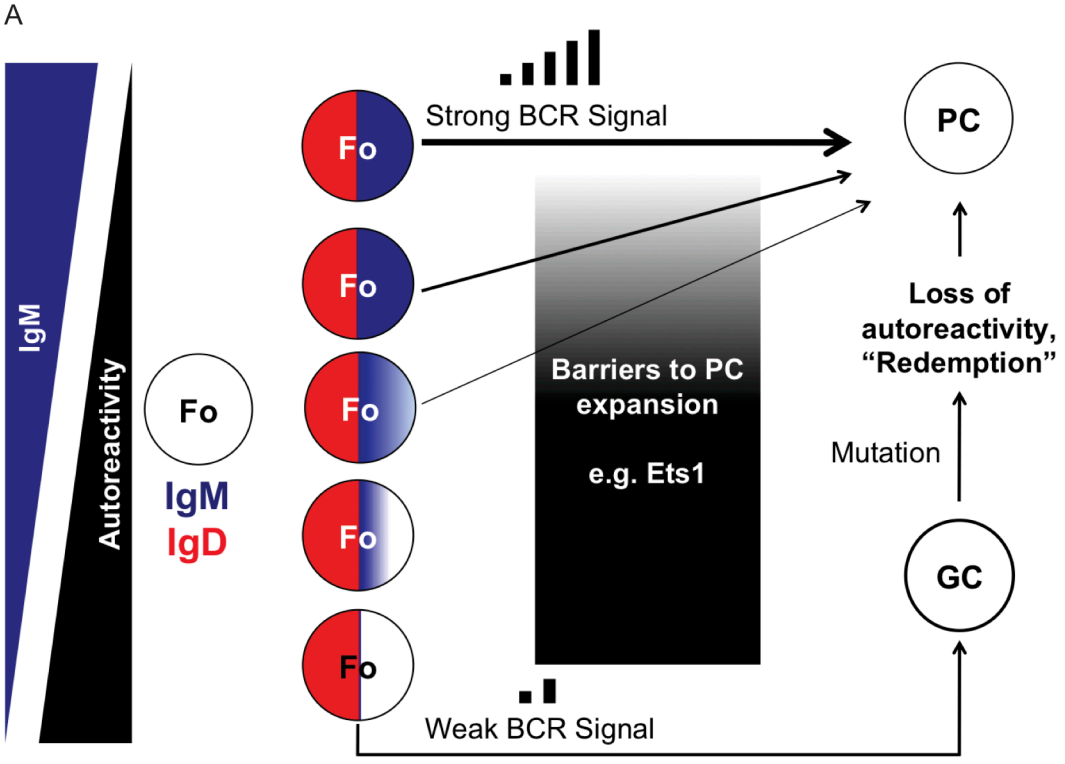
IgM
Autoreactivity
Fo
IgM
IgD
Strong BCR Signal
Fo
Fo
Fo
Fo
Fo
Barriers to PC expansion
e.g. Ets1
Weak BCR Signal
PC
Loss of autoreactivity, "Redemption"
Mutation
GC

Figure 2.20. Role of IgM and IgD in regulating rapid antibody responses.

(A) Model: Control of peripheral B cell tolerance by IgM and IgD. Selective downregulation of IgM is a well-described feature of autoreactive B cells, and this study demonstrates how loss of IgM could desensitize B cells towards self-antigens. High and invariant IgD expression provides survival signals to allow these autoreactive cells to be maintained in the repertoire. Upon activation by foreign antigen, the least autoreactive cells receive strong signals through IgM and can quickly differentiate into plasma cells with little danger of autoimmunity. In contrast, the most autoreactive B cells are activated through IgD, which is less efficient at transducing signals *in vivo*. This weak signaling forces IgD^{hi} IgM^{lo} cells into the germinal center where they can be "redeemed" via somatic hypermutation, as proposed by Goodnow and colleagues. In this way, dual expression of IgM and IgD expression facilitates repertoire diversity and balances immune responsiveness with autoimmune potential.

Discussion

We and others previously hypothesized that a major tolerance strategy employed by autoreactive Fo B cells is selective downregulation of IgM. However, since all Fo B cells express a high and invariant amount of surface IgD, it was unclear whether and how loss of IgM expression could affect B cell responses to antigenic stimulation. It was recently reported that IgM, but not IgD, is uniquely responsive to monomeric antigens due to a short and inflexible linker region coupling the Fab and Fc portions of IgM (Ubelhart et al., 2015). This could account for selective quiescence of mildly autoreactive B cells to monovalent endogenous antigens. However, the identity and structural characteristics of endogenous antigens are not well understood, and include cell-surface antigens on the surface of red cells and B cells (Quach et al.,

2011; Reed et al., 2016). Moreover, recent work from Goodnow and colleagues showed that HEL-specific IgD BCR, when expressed on primary mouse splenocytes, can indeed mobilize calcium *in vitro* and can mediate gene expression changes *in vivo* in response to monovalent cognate antigen (Sabouri et al., 2016).

How do our observations help move beyond and reconcile the seemingly contradictory published work on antigen sensing by IgM and IgD? *In vitro* signaling studies of HEL-specific BCRs by the Jumaa and Goodnow labs differ in several important ways; the former work assesses calcium signaling in pre-B cells that lack Slp-65 expression, while the latter studies splenic B cells with a considerably more mature phenotype. In addition, differences in reagents or strength of stimulus may also contribute to opposing conclusions. Our data suggests that the reduced sensitivity of IgD to bona fide endogenous antigen may lie somewhere between these two extremes; we find that IgD can sense endogenous antigens, just less efficiently than IgM. Consistent with this conclusion, both HEL-specific IgM and IgD BCRs can mediate B cell anergy and drive a common gene expression program in response to chronic high affinity soluble antigen exposure *in vivo* (Brink et al., 1992; Sabouri et al., 2016).

Here we show that B cells expressing IgD BCR alone inefficiently sense endogenous antigens, and exhibit impaired *in vivo* cell fate decisions that are dependent upon BCR signal strength. This is epitomized by dramatic skewing of IgD-only B cells away from the B1a and towards the MZ fate in a competitive setting. Importantly, signal transduction mediated by the IgD BCR in response to anti-Igκ stimulation *in vitro* is intact for all assayed parameters, suggesting that antigen sensing and signal initiation rather than signal transduction downstream of IgD is impaired. We propose that this impaired sensing is conferred by structural properties of

IgD, either through direct binding of antigen and signal transduction through the BCR or through differential pairing with co-receptors that directly modulate the BCR signaling pathway.

Characterization of bona fide endogenous antigens that drive Nur77-eGFP expression in the polyclonal repertoire is necessary in order to further dissect the biophysical basis for reduced antigen sensing by IgD *in vivo*. These antigens may not be exclusively restricted to those that are germline-encoded or generated by host enzymes; rather they may include non-inflammatory antigens taken up through the gastrointestinal tract and recognized by specific BCRs. At least some relevant endogenous antigens may be membrane-bound (Quach et al., 2011; Reed et al., 2016), and recent studies have illustrated the importance of membrane spreading, contraction, and stiffness discrimination in BCR signaling (Fleire et al., 2006; Shaheen et al., 2017). We propose that relevant endogenous antigens are presented in contexts that do not efficiently trigger signaling through the flexible structure of IgD. This might explain the discrepancy between weak responsiveness of IgD to endogenous antigens *in vivo* and strong signaling in response to crosslinking antibodies *in vitro*.

An alternative mechanism is that differential clustering of co-receptors with IgD and IgM might influence how BCR signals are integrated *in vivo*. It has long been proposed that there are not only quantitative, but also qualitative differences between IgM and IgD signaling. Early studies of IgM and IgD signaling in cell lines suggested that kinetics but not quality of signaling triggered by each isotype differed (Kim and Reth, 1995b). However, we have been unable to identify a difference in kinetics of BCR signaling in primary IgM- or IgD-deficient B cells *in vitro*. More recently, studies using TIRF, dSTORM, and PLA (proximity ligation assay) showed that IgD is more densely clustered on the cell surface than IgM, and these distinct IgM- and IgD-containing “islands” are differentially associated with co-receptors such as CD19 in resting and

activated B cells (Chandra Maity et al., 2015; Klasener et al., 2014; Mattila et al., 2013). Since function of the ITIM-containing inhibitory co-receptor CD22 depends on its ability to efficiently access the BCR, differences in cluster density of IgM and IgD might render them differentially sensitive to such inhibitory tone (Gasparrini et al., 2016). It is possible that differential association with such co-receptors contributes to differences in the function of the IgM and IgD BCRs *in vivo* by modulating BCR signal strength, or by selectively perturbing specific downstream signaling events.

In addition to B cell co-receptors that have long been known to directly modulate canonical BCR signaling, a growing list of immunoreceptors expressed on B cells have more recently been shown to require expression of the BCR for optimal function; Becker et al. have shown that expression of the IgD BCR is critical for CXCR4-dependent signaling (Becker et al., 2017). This may influence the biology of B cells expressing only IgM; indeed, CXCR4-deficient B cells exhibit reduced plasma cell migration from spleen to bone marrow (but intact splenic SLPC responses) (Nie et al., 2004). Importantly, defective CXCR4 signaling in IgM-only B cells could not account for reduced Nur77-eGFP expression in IgD-only B cells because reporter expression is insensitive to CXCR4 signaling (Figure 2.2C). Nor would it account for skewed cell fate decisions by IgD-only B cells in competition with wild type B cells, both of which retain intact CXCR4 signaling. B cell responses to TLR4 ligands also require expression of the BCR, but importantly canonical TLR ligands do not exhibit selective dependence on either the IgM or the IgD isotypes (Figure 2.4A). Finally, recent work establishes a role for the Fc-receptor for IgM in modulating B cell responses, and could therefore play a role downstream of serum IgM that is absent in *IgM*$^{-/-}$ mice (Nguyen et al., 2017a; Nguyen et al., 2017b). We control for this

effect by confirming that all phenotypes in this study are cell-intrinsic and independent of secreted IgM.

Accumulating evidence suggests that strong BCR signals favor SLPC over GC fate (Chan et al., 2009; Nutt et al., 2015; Paus et al., 2006). This is thought to be transcriptionally mediated at least in part by loss of Ets1 expression and induction of Irf4 in a BCR signal-strength dependent manner (Nutt et al., 2015). Here we show that IgM and IgD are each sufficient to drive GC responses, but IgD is less efficient at promoting SLPC fate in response to endogenous antigens, implying that IgD^{hi} IgM^{lo} B cells may similarly be shunted away from SLPC responses. This discrepancy is unlikely to be attributable to differences in antigen capture and presentation by the IgM and IgD BCRs, as GC entry is highly T cell-help dependent. Instead, we provide evidence to suggest that reduced antigen-dependent BCR signals are transduced *in vivo* by IgD. We show that, in the absence of Lyn, Ets1 downregulation and unswitched PC expansion require the IgM BCR. $IgM^{-/-}Lyn^{-/-}$ mice phenocopy $Btk^{lo}Lyn^{-/-}$ mice; both strains are protected from Ets1-downregulation, PC expansion, and anti-dsDNA autoantibody production *in vivo* (Mayeux et al., 2015; Whyburn et al., 2003). This suggests that robust Btk-dependent Ets-1 downregulation in response to endogenous antigens relies upon efficient antigen sensing by the IgM BCR and is important to drive unswitched PC expansion in the absence of Lyn. It will be important to explore whether a similar mechanism accounts for impaired $IgG1^{+}$ SLPC responses by Lyn-sufficient B cells with low or absent IgM expression.

We propose that the purpose (and consequence) of IgM downregulation on B cells reactive to endogenous antigens is to limit their direct differentiation into SLPCs in response to chronic endogenous antigen stimulation, and prevent secretion of auto-antibodies in the context of an acute humoral immune response (Figure 2.20A). However, IgD is sufficient to drive

germinal center differentiation without the contribution of IgM. This has been well-demonstrated both in the present study as well as prior work (Lutz et al., 1998). Indeed, not only are IgD^{hi} IgM^{lo} B cells that are reactive to endogenous antigens competent to enter the germinal center, they appear to do so with greater efficiency, perhaps due in part to improved survival (Sabouri et al., 2016; Sabouri et al., 2014). It is worth emphasizing that selection pressures and tolerance mechanisms operating within the germinal center must independently ensure that somatic hypermutation both abolishes germ-line-encoded autoreactivity and prevents *de novo* acquisition of autoreactivity. Goodnow and colleagues recently showed that autoreactive BCRs can indeed be "redeemed" by somatic hypermutation, providing proof-of-principle that entry of autoreactive B cells into the GC does not necessarily pose a risk to the organism (Sabouri et al., 2014).

Why, though, are autoreactive B cells preserved in the periphery and not deleted? Why is IgD necessary at all? One suggestion is that such BCRs are retained in the pre-immune B cell compartment to fill holes in the repertoire, and that IgD is essential for their survival; indeed, it has been shown that loss of IgD expression, with or without compensatory upregulation of IgM, leads to loss of mature naïve B cells in competition (Roes and Rajewsky, 1993; Sabouri et al., 2016). We similarly find that IgD-only B cells have a profound competitive advantage in the follicular B cell compartment relative to IgM-only (but not WT) B cells, implying an obligate survival function for the IgD isotype BCR. This is consistent with a well-appreciated pro-survival function of the BCR as demonstrated by Rajewsky and colleagues (Kraus et al., 2004; Lam et al., 1997). Since IgD expression is needed to keep IgM^{lo} B cells alive, this may explain why IgD expression facilitates a broad dynamic range of IgM expression across the B cell repertoire (Figure 2.1B-C), allowing B cells to fine-tune the intensity of their SLPC responses according to their autoreactivity. IgD expression on IgM^{lo} cells could serve to mediate antigen

capture and participation in T-dependent immune responses, while simultaneously limiting SLPC responses as we show here.

We demonstrate here for the first time that IgD BCRs sense endogenous antigen more weakly than IgM BCRs *in vivo*, are inefficient at driving SLPC responses to endogenous antigens, and thereby may function to divert autoreactive follicular B cells from direct PC differentiation. We propose that this property of the IgD BCR limits generation of auto-reactive antibodies in the context of immediate humoral immune responses. Taken together with recent work from the Jumaa and Goodnow groups, we propose a unified model of how IgM downregulation in the face of high IgD expression regulates the fate of naïve autoreactive B cells *in vivo* while retaining their contribution to the mature BCR repertoire.

Acknowledgements

We thank Anthony DeFranco for valuable feedback and suggestions for this manuscript, and Al Roque for help with mouse husbandry. We thank Renuka Nayak, Anne-Katrin Proebstel, and Eric Wigton for sharing valuable mouse reagents. Funding for this project was provided by the Rheumatology Research Foundation (J.Z.), NIAMS K08 AR059723 and R01 A127648 (J.Z.), and NSF Graduate Research Fellowship 1650113 (M.N.).

Materials and Methods

Mice. Nur77-eGFP mice and *Lyn*$^{-/-}$ mice have been previously described (Chan et al., 1997; Zikherman et al., 2012b). BAFF Tg mice were originally generated in the Nemazee lab, in which BAFF is under the control of a myeloid promoter, human CD68 (Gavin et al., 2005) (source: MMRRC UC Davis). *IgD*$^{-/-}$ and *IgM*$^{-/-}$ mice were previously described, and the former were generously shared by Dr. Hasan Jumaa (Lutz et al., 1998; Nitschke et al., 1993). *TLR7*$^{-/-}$, *CD40L*$^{-}$

$^{/-}$, *Unc93b1*$^{3d/3d}$, *Nr4a1*$^{-/-}$, and MB1-Cre *MyD88*$^{fl/fl}$ mice were previously described (Hobeika et al., 2006; Hou et al., 2008; Lee et al., 1995; Lund et al., 2004; Renshaw et al., 1994; Tabeta et al., 2006). All strains were backcrossed to the C57BL/6 genetic background for at least six generations. Mice were used at 5-12 weeks of age for all functional and biochemical experiments unless otherwise noted. Germ-free (GF) and specific pathogen free (SPF) C57BL/6 mice used for direct comparison were purchased from Taconic and Jackson Laboratory and kept in microisolators under GF or SPF (ISOcage P-Bioexclusion System, Tecniplast) conditions. All GF mice were housed in closed caging systems and provided with standard irradiated chow diet, acidified water and housed under a 12-hour light cycle; 7-week-old males mice were used. GF and control mice were generously provided by Drs. Sergio Baranzini and Anne-Katrin Proebstel at UCSF. All other mice used in our studies were housed in a specific pathogen free facility at UCSF according to the University Animal Care Committee and National Institutes of Health (NIH) guidelines.

Antibodies and Reagents. Fluorescently-conjugated or biotin-conjugated antibodies to B220, CD5, CD19, CD21, CD23, CD69, CD86, CD93 (AA4.1), CD95 (Fas), CD138, CXCR4, IgA, IgM, IgM[a], IgM[b], IgD, IgD[a], IgG1[a], IgG1[b], Igκ, Igλ, GL-7, MHC Class II, and fluorescently-conjugated streptavidin were from Biolegend, eBiosciences, BD Biosciences, Tonbo, or Life Technologies. NP-PE was from Biosearch Technologies. 100 nm Rhodamine PtC liposomes were from FormuMax. Antibodies for intra-cellular staining, pErk Ab (clone 194g2) and pS6 Ab (2F9), were from Cell Signaling Technologies, and Nur77 Ab (clone 12.14) conjugated to PE was from eBioscience. Goat anti-mouse IgM F(ab')$_2$ was from Jackson Immunoresearch. Goat anti-mouse Igκ and goat F(ab')$_2$ anti-mouse Igκ were from Southern

Biotech. Anti-IgD was from MD Biosciences. CXCR4 ligand (CXCL12/hSDF-1α) was from Peprotech. LPS (Cat. L8274) was from Sigma. CpG DNA (ODN 1826 Biotin; Cat. tlrl-1826b) and Pam3CSK4 (Cat. tlrl-pms) were from InvivoGen.

Flow Cytometry and Data Analysis. Cells were stained with indicated antibodies and analyzed on a Fortessa (Becton Dickson) as previously described (Hermiston et al., 2005). Data analysis was performed using FlowJo (v9.7.6) software (Treestar Incorporated, Ashland, OR). Statistical analysis and graphs were generated using Prism v6 (GraphPad Software, Inc). Figures were prepared using Illustrator CS6 v16.0.0. Median Igk levels (Figure 2.1F) were calculated for 200 equally sized "bins" spanning the Nur77-eGFP spectrum using Canopy v1.4.1 (Enthought); source code is provided, and parameters can be modified to condense any 2D FACS plot for comparisons of multiple samples.

Statistics and Replicates. We define biological replicates as independent analyses of cells isolated from different mice of the same genotype, and we define technical replicates as analyses of cells isolated from the same mouse and used in the same experiment. When technical replicates were used, we averaged them to calculate a value for the biological replicate. All reported values and statistics correspond to biological replicates only, and all "n" values reported reflect the number of biological replicates. Wherever MFIs are directly compared, we collected all samples in a single experiment to avoid potential error that could arise from fluctuations in our flow cytometers. In some instances, MFI ratios were compiled from different experiments for statistical purposes, but qualitative findings were consistent experiment to experiment. As our panels reproducibly generated flow plots with well-defined populations, population sizes were

calculated from data compiled from different experiments. When comparing two groups, we employed Welch's t test, which is more stringent than Student's t test and does not assume that the groups have the same standard deviation. We used paired difference t tests when studying parameters in allotype-heterozygous mice that are sensitive to cell-extrinsic factors (e.g. dose of immunogen or severity of autoimmune disease). When comparing three genotypes (e.g. receptor levels on WT vs. $IgM^{-/-}$ vs. $IgD^{-/-}$), we used one-way ANOVA and Tukey's multiple comparison test to calculate p values.

Intracellular Nur77, pErk and pS6 Staining. *Ex vivo* or following stimulation, cells were fixed in 2% paraformaldehyde, permeabilized with 100% methanol, and stained with anti-Nur77, anti-pErk or anti-pS6 followed by lineage markers and secondary antibodies if needed.

Intracellular Plasma Cell Staining. Cells were fixed in 2% paraformaldehyde and permeabilized in BD Perm/Wash. Stains for antibody isotypes and allotypes were prepared in BD Perm/Wash.

Intracellular Calcium Flux. Cells were loaded with 5 μg/mL Indo-1 AM (Life Technologies) and stained with lineage markers. Cells were rested at 37 C for 2 minutes, and Indo-1 fluorescence was measured immediately prior to stimulation to calculate basal calcium.

In vitro B Cell Stimulation. Splenocytes or lymphocytes were harvested into single cell suspension, subjected to red cell lysis using ACK buffer, and plated at a concentration of 7.5 x 10^5 cells/200 μL in round bottom 96 well plates in complete RPMI media with stimuli for 18

hours prior to analysis. *In vitro* cultured cells were stained using fixable near IR live/dead stain (Life technologies) per manufacturer's instructions.

ELISA. Serum antibody titers for total IgM, total IgD, anti-dsDNA IgG2a, and NP-specific IgG1 were measured by ELISA. For total IgM and total IgD, 96-well plates (Costar) were coated with 1 μg/mL anti-IgM $F(ab')_2$ (Jackson) or 1 μg/mL anti-IgD (BD 553438), respectively. Sera were diluted serially, and total IgM and total IgD were detected with anti-IgM-biotin (eBioscience) and SA-HRP (Southern Biotech) or anti-IgD-HRP (American Research Products). dsDNA plates were generated by serially coating plates with 100 μg/mL poly-L-lysine (SigmaAldrich) and 0.2 U/mL poly dA-dT (SigmaAldrich) in 0.1 M Tris-HCL pH 7.6. Sera were diluted serially on dsDNA plates, and autoantibodies were detected with IgG2[a]-biotin, IgG2a[b]-biotin, and SA-HRP. NP plates were generated by coating 96-well plates with 1 μg/mL NP-BSA (Biosearch, conjugation ratio 23) in PBS. Sera from NP-RSA immunized and unimmunized mice were diluted serially, and NP-specific IgG1 was detected with IgG1[a]-biotin, IgG1[b]-biotin, and SA-HRP. All ELISA plates were developed with TMB (Sigma) and stopped with 2N sulfuric acid. Absorbance was measured at 450 nm. For total IgM, total IgD, and dsDNA IgG2a, OD values or OD ratios were calculated and displayed. For NP-specific IgG1, titers were calculated at OD = 0.2 and normalized such that the average IgG1[a]/IgG1[b] ratio in immunized Balb/c-B6 F1 mice equals 1.0.

B Cell Purification and Western Blots. Splenic B cells were purified by negative selection with a MACS kit according to manufacturer's protocol (Miltenyi Biotech, cat# 130-090-862). Purified B cells were lysed in 2N 4X SDS and boiled at 95C for 5 minutes. 500,000 cells per lane were

loaded onto NuPAGE 4-12% Bis-Tris gels (Invitrogen NP0335), run for 50 minutes at 200V, and transferred onto PVDF membranes using XCell II Blot Module (Invitrogen). Membranes were blocked with 3% BSA. Proteins were detected with rabbit monoclonal anti-Ets1 (Epitomics, custom lot provided by Lee Ann Garrett-Sinha), mouse anti-mouse GAPDH (Santa Cruz Biotechnology 32233), and HRP-conjugated secondary antibodies goat anti-rabbit IgG (H+L) and goat anti-mouse IgG (H+L) (SouthernBiotech). Membranes were developed with Western Lightning Plus ECL (Perkin Elmer 0RT2651 and 0RT2751) and imaged using a ChemiDoc Touch Imaging System (Bio-Rad). Quantifications were performed using Image Lab v. 5.2.14 (Bio-Rad).

Immunizations. Mice were immunized i.p. with 200 uL of 10% sheep red blood cells (Rockland R406-0050) diluted in PBS. Mice were sacrificed 5 days after immunization, and serum and spleens were harvested. Mice were immunized i.p. with 100 ug of NP-conjugated rabbit serum album (NP-RSA, Biosearch N-5054-10, conjugation ratio 10) prepared in PBS with Alhydrogel 1% adjuvant (Accurate Chemical and Scientific Corp. 21645-51-2). NP-RSA immunized mice were sacrificed 7-8 days following immunization, and serum and spleens were harvested. To ensure that our calculated values accurately reflect the magnitude and variability of immune response induced by immunization, we analyzed all mice that had larger plasma cell and germinal center compartments than unimmunized mice. One $IgM^{+/-}$ mouse immunized with SRBCs (Figure 2.18E-F) was excluded because it did not display an expanded plasma cell compartment; no other mice were excluded from analysis.

Quantitative PCR. Splenocytes were lysed in TRIzol (Invitrogen) and stored at -80 C. cDNA was prepared using a SuperScriptIII kit (Invitrogen). Quantitative PCR reactions were run on a QuantStudio 12K Flex thermal cycler (Applied Biosystems) with FastStart Universal SYBR Green Master Mix (Roche). Nr4a1 (forward: gcctagcactgccaaattg; reverse: ggaaccagagagcaagtcat) and GAPDH (forward: aggtcggtgtgaacggatttg; reverse: tgtagaccatgtagttgaggtca) primers were used at 250 nM each.

CHAPTER 3: DISCUSSION

The results outlined in Chapter 2, interpreted in light of the literature, provide useful insight into the mystery of dual expression of IgM and IgD. This chapter will reintroduce and then build upon many of the points raised in the discussion section of Chapter 2. This chapter will also address remaining questions and how they might be answered with currently available technologies and mouse models.

Why is IgM downregulated and IgD maintained on autoreactive B cells?

B cells require surface BCR expression for survival. This was clearly demonstrated by a series of BCR deletion studies in the Rajewsky lab (Kraus et al., 2004; Lam et al., 1997; Srinivasan et al., 2009), and by a study in the Tybulewicz lab that showed that BAFF signaling requires the BCR (Schweighoffer et al., 2013). More recently, the finding that B cells lacking surface IgD expression without compensatory IgM upregulation (*dmit*) have poor survival provides additional evidence in favor of IgD's role in promoting B cell survival (Sabouri et al., 2016). The competition data in Chapter 2 also paint a broader picture of IgD's survival function. Notably, IgD-deficient B cells compete efficiently into the T1 compartment but compete poorly where IgD expression is normally the highest: in the mature-follicular compartment. IgD-deficient B cells also compete poorly into the MZ compartment, which may be due to their putative origin in the IgD-expressing T2 compartment. IgM-deficient B cells do not display a disadvantage against WT cells for entry into the Fo compartment, which suggests that IgD alone can promote survival in this compartment. Mechanistically, IgD's pro-survival function may arise from its close association with CD19 on resting B cells (Klasener et al., 2014). Given CD19's ability to promote PI3K signaling, which was shown to rescue cell death in the face of BCR deletion (Srinivasan et al., 2009), it is likely that an IgD-CD19-PI3K axis promotes the survival of Fo B cells. Exactly where BAFF signaling feeds into this axis could be dissected

using the tools described in Chapter 1. PLA, dSTORM, and other imaging techniques could determine whether BAFFR is preferentially associated with either BCR isotype and whether its mobility is affected by cytoskeletal disruption or BCR signaling. These techniques can also determine whether differential co-localization with relevant co-receptors requires dual expression of IgM and IgD. For example, does the distance between IgM and CD19 clusters shrink on IgD-deficient B cells? And if so, how much of this is due to the elevated surface IgM expression on these cells?

In contrast to the high level of IgD on all follicular B cells, IgM is downregulated on autoreactive B cells. The Nur77-eGFP and developmental data presented in Chapter 2 strongly suggest that IgM is more sensitive to endogenous antigens than IgD is. At the most basic level, selective IgM downregulation might serve to desensitize autoreactive B cells towards self antigens. However, there is also a broad range of surface IgM expression at every level of Nur77-eGFP. The fact that follicular B cells do not fall into a tightly-clustered line on an IgM vs. Nur77-eGFP plot indicates that variability is a feature of the system. Furthermore, the dynamic range of surface IgM expression is strongly restricted on IgD-deficient B cells. This suggests that IgD provides survival signals that enable greater variation in surface IgM expression. However, it remains unclear whether IgM^{lo} B cells are completely eliminated from the repertoire of $IgD^{-/-}$ mice, or whether these cells increase their surface IgM expression. Answering this question could require taking several complementary approaches. Most directly, one could sequence heavy chain sequences of B cells at different levels of Nur77-eGFP in WT (129/Sv) and $IgD^{-/-}$ mice. Interpretation of sequence data may be problematic, however, because the diversity of the follicular compartment is astronomical (Yang et al., 2015). On the other hand, sequence information could be used to generate knock-in mice that recognize bona fide endogenous

antigens and analyze how IgD deficiency influences their Nur77-eGFP and surface IgM expression. Alternatively, inducibly IgD-deficient mice could be generated by flanking C_δ with loxP sites and introducing a tamoxifen-responsive Cre. In this system, any changes in Nur77-eGFP, surface IgM, or cell viability would substantially inform our understanding of how surface IgM variability is generated and maintained.

Why are autoreactive B cells maintained within the repertoire?

The breadth of Nur77-eGFP and IgM expression on follicular B cells raises the question of why autoreactive B cells are maintained in the repertoire instead of being purged. As outlined in Chapter 1, certain broadly-neutralizing anti-HIV antibodies arise from precursors that are normally purged from the repertoire due to their autoreactivity (Verkoczy and Diaz, 2014). Furthermore, two well-characterized broadly-neutralizing anti-HIV antibodies also cross-react with the endogenous phospholipid cardiolipin (Haynes et al., 2005). This means that in some cases, protective antibodies require autoreactive precursors to serve as a "backbone" for further mutation, and others recognize self antigens. It could be that some degree of autoreactivity is tolerated within or selected into the B cell repertoire because autoreactivity implies recognition of biological patterns. While generating antibodies that *strongly* cross-react with self antigens may be harmful to the host, weakly autoreactive precursors might require fewer mutations to recognize foreign antigens than "blank slate" precursors. As mutation within the germinal center is a random event and pathogens can multiply very rapidly, a starting population that only requires a few mutations to acquire foreign reactivity could mean the difference between life and death for the host.

Moreover, autoreactivity/polyreactivity is a predominant feature of the natural antibody repertoire (Lacroix-Desmazes et al., 1998). Because of this autoreactivity, the cells responsible

for natural antibody production, B1 cells, reveal interesting aspects of IgM and IgD function. Notably, the role of IgD in the survival of B1a cells stands in marked contrast to its role the follicular compartment. In the B1a compartment, IgM-deficient B cells compete poorly, suggesting that generation and/or survival of B1a cells requires signals that only the IgM BCR can efficiently provide. As the data in Chapter 2 clearly demonstrate, the IgM BCR is much more sensitive to endogenous antigens than the IgD BCR, and this sensing may play a role in maintaining proper B1a function. Perhaps not coincidentally, the B1a compartment produces polyreactive antibodies that play a role in clearing cell debris. In a way, the role of autoreactivity in the B1a compartment blurs the line between antigen-dependent and "tonic" BCR signaling. Another unique feature of B1a cells is their capacity for self-renewal (Martin and Kearney, 2001). Whether IgM provides unique signals that drive self-renewal remains to be addressed. Further investigation could also determine whether IgM and IgD differ in their ability to maintain the balance between B1a self-renewal and differentiation into antibody secreting cells.

How are autoreactive B cells excluded from rapid antibody responses?

The original defining feature of anergic B cells in IgHEL/sHEL model systems was a lack of antibody secretion upon immunization (Brink et al., 1992; Goodnow et al., 1988; Goodnow et al., 1989). Blunted antibody responses are also a notable characteristic of anergic B cells in other transgenic models of B cell tolerance (Cambier et al., 2007). Subsequent investigation provides clues as to where the block(s) in antibody production may occur. In the HEL model, it was shown that, on a per-receptor basis, IgM and IgD are equally efficient at upregulating the costimulatory markers CD80 and CD86 (Brink et al., 1995). This, along with studies of *IgM*$^{-/-}$ and *IgD*$^{-/-}$ mice (Lutz et al., 1998; Nitschke et al., 1993; Roes and Rajewsky, 1993), would imply that IgM and IgD are both competent to mediate at least a subset of B cell-T

cell interactions. However, the subsequent fate of the B cells may be shaped by their autoreactivity. For non-tolerized HEL-specific B cells, interaction with T cells normally leads to proliferation and antibody secretion, but chronic HEL exposure converts this interaction into Fas-mediated apoptosis (Rathmell et al., 1995). While this is a dramatic example, more subtle shifts in cell fate could shape the immune response of more mildly autoreactive B cells. It was previously shown that cAMP-dependent signals are required for optimal germinal center entry of cells stimulated through IgD (Chaturvedi et al., 2002). However, the authors of that study did not look at other cell fates, particularly plasma cell differentiation.

Given the skewing of IgD-only cells away from the $IgG1^+$ SLPC fate upon immunization (described in Chapter 2), it is especially enticing to think that cAMP signaling discourages rapid SLPC generation from IgD-only cells. A crude experiment would be to treat immunized mice with PKA inhibitors or cAMP and see whether this influences SLPC generation in $IgM^{-/-}$, $IgD^{-/-}$, and WT mice. Intriguingly, cAMP supplementation enhances antibody responses in the absence of T cells but inhibits antibody responses when T cells are present (Kammer, 1988). However, it is unclear whether the concentrations of cAMP the B cells experienced are comparable to the cAMP increase generated by IgD stimulation, and it is underdetermined how much of the phenotype was driven by alterations in T cells, myeloid cells, and stromal cells. To control for these cell-extrinsic factors, it would be necessary to develop an *ex vivo* stimulation strategy that promotes rapid PC induction following reintroduction into a host. In this system, one could supplement IgM-only cells with dibutyrl cAMP or treat IgD-only cells with PI-PLC and see whether this influences their propensity to differentiate into $IgG1^+$ PCs.

While the $IgG1^+$ SLPC defect in IgD-only mice was profound, it was partially ameliorated in $IgM^{+/-}$ that contain serum IgM. In this case, the defect appears to be more

quantitative than absolute. Similarly, IgM-only and IgD-only B cells respond to anti-Igκ but differ in their relative abilities to induce pERK, calcium increase, pCD22, pSHP-1, and activation marker upregulation (Figures 2.5 and 3.1). The exact balance of triggered biochemical second messengers and activation markers expressed on the surface of B cells interacting with T cells could influence their fate. A more comprehensive examination of activation marker upregulation on IgM-only and IgD-only cells could identify potential targets that drive the SLPC/GC skewing in immunized mice. Alternatively, unbiased transcriptional or biochemical analysis might identify new candidates that are differentially expressed or activated.

Despite the recurrent theme of defective plasma cell responses by IgD-only cells, IgD-only cells were perfectly competent to enter the germinal center in all situations examined in Chapter 2. Given that GC B cells (eventually) give rise to antibody-secreting cells, additional tolerance mechanisms must restrain autoreactive B cells that enter the GC. GC tolerance models that rely entirely on antigen presentation to T cells (or lack thereof) are incomplete because B cells and T cells need not recognize the same epitope for a productive interaction; a B cell could recognize an autoantigen linked to a foreign antigen and present a foreign peptide to nearby T cells. Therefore, GC tolerance mechanisms that consider the intrinsic self reactivity of the BCR are particularly relevant. The original MD-4/ML-5 study examined anti-HEL antibody secretion 24 days after HEL/CFA immunization and after a recall challenge with HEL-SRBCs (Goodnow et al., 1988). These experiments did not examine GC entry and utilized a BCR transgene integrated outside of the BCR locus, which may preclude high levels of SHM and studies of physiological GC responses. A related model system, SW_{HEL}, which integrates a HEL-specific BCR into the endogenous BCR locus, was used to uncover the strong negative selective pressure B cells face when they encounter autoantigen in the GC (Chan et al., 2012). This led to a model

in which GC B cells that recognize ubiquitous autoantigens are deleted, but GC B cells that cross-react with tissue-restricted autoantigens pose a danger to the host (Chan and Brink, 2012; Brink, 2014). However, ubiquitous autoreactivity does not necessarily condemn a B cell to death once it enters the GC. Two recent papers demonstrated that germinal center B cells participate in a process called clonal redemption where they acquire mutations that abolish their self reactivity (Reed et al., 2016; Sabouri et al., 2014).

Given the selective downregulation of IgM on autoreactive B cells, strong signaling through IgD and weak signaling through IgM might be a way that these cells "know" they need to be redeemed. Once these cells enter the GC, however, it's unclear how they know whether their autoreactivity has been lost. This is a particular challenge in light of the finding that BCR signaling is suppressed in GC B cells (Khalil et al., 2012). Nevertheless, a subset of germinal center cells do actively signal through their BCRs (Mueller et al., 2015), but the fate of those cells is less clear. Intriguingly, GC B cells turn off IgD expression and primarily express IgM (unless they have class switched). In other words, they express the isotype that is more sensitive to self antigens. In this way, the balance between BCR signaling (autoreactivity + foreign reactivity) and T cell help (foreign reactivity alone) could guide the evolution of germinal center B cells. A better understanding of the context in which GC B cells see self antigens would be instrumental in further developing and testing this model.

How do the phenotypes in *Lyn*$^{-/-}$ mice relate to human disease?

The finding that IgM-deficient B cells are excluded from unswitched SLPC responses in *Lyn*$^{-/-}$ mice suggests that IgM downregulation might be sufficient to enforce tolerance in a well-characterized autoimmune mouse model. The IgM-null cells also contributed significantly less to the anti-dsDNA IgG2a/c response than IgM-sufficient cells did. However, it is unclear whether

these two phenomena are linked because the cellular and secreted antibody isotypes differ. Reliable quantification of IgG2a/c plasma cells was difficult because these cells are rare in the spleen and bone marrow, and the compartment size varies substantially (data not shown). On the other hand, the rapid fluctuation in antibody titers suggests that at least some of the anti-dsDNA IgG2a/c comes from short-lived plasma cells. Sequencing of antibody secreting cells generated during SLE flares indicates that a substantial fraction of them arise directly from the naïve follicular B cell repertoire without acquiring SHM, implying generation outside of the germinal center (Tipton et al., 2015). A subset of SLE patients also display clinical improvement after B cell depletion (Looney et al., 2004). Because plasma cells lack many of the markers used in B cell depletion therapy, this would suggest that depleting their precursors can have a therapeutic effect in a subset of patients. Therefore, the tolerance mechanisms employed by mature-naïve B cells may have clinical relevance in human disease. Whether IgM and IgD play a similar role in enforcing tolerance and modulating fate decisions in human B cells remains to be understood, and it is unknown whether this process is dysregulated in patients with rheumatological disease. Further investigation is necessary to determine whether selective downregulation (or blocking) of IgM on human B cells could restrain autoimmune responses without having to ablate the entire compartment.

Remaining unanswered questions

What properties of IgM and IgD confer the phenotypes described in Chapter 2?

Based on existing evidence, IgM and IgD could mediate their non-redundant phenotypes through two (non-mutually exclusive) mechanisms: direct binding of antigen or differential association with co-receptors. In the favor of the direct binding hypothesis is the finding that the hinge of IgD renders it unresponsive to monovalent antigens (Ubelhart et al., 2015). While an

independent study found that this defect is not absolute (Sabouri et al., 2016), the phenotypes were clean and dramatic in the model system Ubelhart used. Sabouri found that IgM and IgD can drive similar gene expression patterns in the IgHEL/sHEL model, but this system features a very strong BCR-antigen interaction. The Vh125/Vκ125 (insulin) and the Ars/A1 (ssDNA/Ars hapten) model systems could be modified to see whether IgM and IgD equivalently drive anergic phenotypes in models with low affinity BCR-antigen interactions. In each case, it would be prudent to first validate the phenomenology in TKO cells before generating new mouse lines. It is also possible to explore the role of IgD's hinge in shaping polyclonal repertoires. Many of the phenotypes described in Chapter 2 are very robust and could be probed in $IgM^{-/-}$ mice with a shortened IgD hinge. While reproducible, Nur77-eGFP phenotypes in IgD-only B cells were mild and quantitative, but the skewing of B1a/MZ development was striking, cell-intrinsic, and would be easy to probe in $IgM^{+/-}$ ($IgD^{+/\Delta hinge}$) mice. Once these mice are generated, they can be crossed onto $Lyn^{-/-}$ for quantification of unswitched SLPC generation.

The other proposed mechanism, differential association of IgM and IgD with co-receptors, can be tested in several ways. An epistasis-based approach would involve crossing $IgM^{-/-}$ and $IgD^{-/-}$ mice onto backgrounds that lack relevant co-receptors such as CD22, CD45, CD19, and Siglec-G. CD45 is of particular interest because of its role in regulating SFK activity and the absolute requirement for SFKs in B cell responses to monomeric antigens (Mukherjee et al., 2013). $IgM^{+/-}$ mice were crossed an allelic series of CD45 (Zikherman et al., 2012a), and signaling and developmental competition were examined (Figure 3.2 A-C). Notably, $CD45^{-/-}$ IgD-only cells competed poorly into the splenic follicular and peritoneal B2 compartments, suggesting impaired survival or positive selection of IgD-only cells in the absence of CD45. $CD45^{-/-}$ IgD-only B cells also lost much of their competitive advantage in the marginal zone

compartment, possibly because reduced signaling enabled entry of more WT cells into the massively expanded compartment (Figure 3.2D). In the peritoneal compartment, superphysiological levels of CD45 (H/+) promoted an expansion of the B1a compartment at the expense of the B2 compartment (Figure 3.2E-G). This was accompanied by modest increase in the competitive fitness of IgD-only B1a cells, although they were still strongly disfavored (Figure 3.3C).

CD22 is another reasonable candidate for mediating differences between IgM and IgD signaling because *CD22*$^{-/-}$ cells display strong enhancement of anti-IgM signaling but less enhancement of anti-IgD signaling (Figure 3.3A). However, this phenotype could be an artifact of the anti-IgM and anti-IgD stimulatory antibodies because although they produced dramatic signaling phenotypes in *CD45*$^{-/-}$ B cells (Figure 3.3B), anti-Igκ produced identical signaling in IgD-only and WT (IgM + IgD) *CD45*$^{-/-}$ B cells (Figure 3.2A). Nevertheless, crossing IgM and IgD mutants onto *CD19*$^{-/-}$ could unmask new survival phenotypes, and crossing them onto *Siglec-G*$^{-/-}$ could uncover how the isotypes function in B1a cells.

Other approaches could selectively mutate the BCR and/or co-receptors to abolish or enforce their association. This approach was taken with the IgD TM-S mutant to abolish its ability to oligomerize and with BiFC stabilization to force oligomerization (Yang and Reth, 2010b). With regards to co-receptors, the path forward is murkier. One could take a systematic approach and mutate different domains and glycosylation sites on the receptors and see whether this alters their co-localization with the BCR. However, it's hard to know where to start without crystal structures showing interactions between the BCR isotypes and relevant co-receptors. Complicating matters further, mutations in IgD's hinge could influence its ability to interact with co-receptors, a possibility Ubelhart et al. did not address. Because of these caveats and

complications, understanding the mechanistic basis of the phenotypes observed in IgM-only and IgD-only mice will require parallel and orthogonal approaches.

How is IgM selectively downregulated?

Selective downregulation of IgM is likely mediated post-translationally because total IgM (intracellular + surface) varies much less than surface IgM across the Nur77-eGFP repertoire (Figure 3.4). The Igα/β complex is an obvious potential mediator of selective IgM downregulation on autoreactive B cells. It is already known that IgM absolutely requires Igα/β for surface expression, but IgD can be expressed in its absence (Venkitaraman et al., 1991). However, it is underdetermined whether or how Igα/β expression is changed in autoreactive B cells. Anything from changes in total expression, to dimerization, to glycosylation could modulate its ability to mediate surface BCR transport. Furthermore, IgD's hinge or differential pairing with other co-receptors could influence how efficiently it is transported to the surface or contribute to its lack of downregulation on autoreactive B cells. There is also the possibility that variation in surface IgM is stochastically generated early in development, and the cells receiving the right amount of signaling persist within the repertoire. The proposed experiments with inducibly IgD-deficient B cells (described earlier) would help address this possibility.

What is the nature of the endogenous antigens that mature-naïve B cells recognize?

The study of B cell autoimmunity brings up a question that veers from the scientific to the philosophical: what is self? In one sense, "self" is something produced by an organism that can be attacked during the progression of autoimmune disease. These targets include many of the molecules described earlier: dsDNA, ssDNA, and cardiolipin. Some SLE patients have circulating antibodies that bind B220, a CD45 isoform expressed on B cells (Cappione et al., 2004). The identity of the "self" seen by Nur77-eGFP^{hi} B cells is less clear. It's most likely not

encountered passively or non-specifically (e.g. in response to TLR ligands) because IgHEL B cells can respond to many TLR ligands yet do not constitutively express high levels of Nur77-eGFP (Figure 3.5). “Self” could also include antigens not encoded in the host genome, including enzymatically generated and modified molecules or even food antigens. One could clone BCR specificities found in Nur77-eGFP^{hi} B cells and see what they bind in antigen arrays, or develop biochemical techniques to elute antigens from the BCRs of individual B cells. It is also possible (likely) that a given B cell could recognize multiple self antigens, with different affinities for each interaction. These many possibilities will make B cell biology an exciting field for years to come.

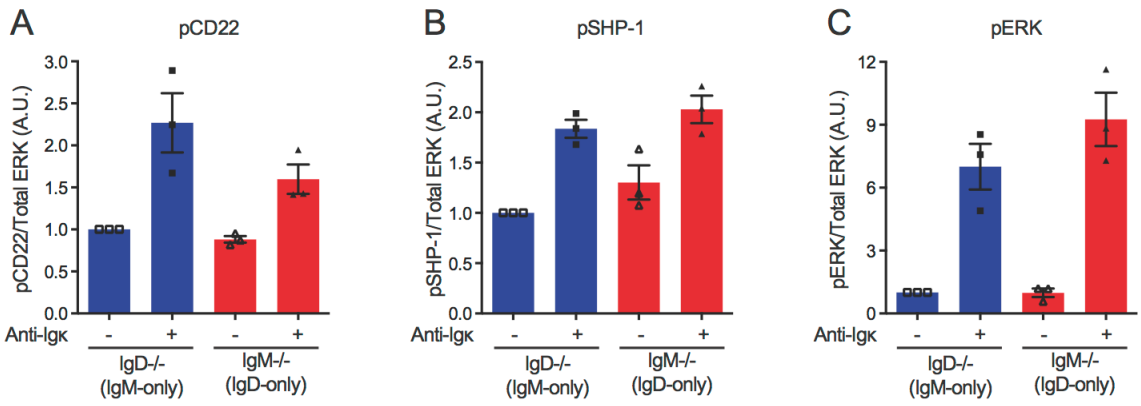
A
pCD22
pCD22/Total ERK (A.U.)
3.0
2.5
2.0
1.5
1.0
0.5
0.0
Anti-Igκ
-
+
-
+
IgD-/-
(IgM-only)
IgM-/-
(IgD-only)
B
pSHP-1
pSHP-1/Total ERK (A.U.)
2.5
2.0
1.5
1.0
0.5
0.0
Anti-Igκ
-
+
-
+
IgD-/-
(IgM-only)
IgM-/-
(IgD-only)
C
pERK
pERK/Total ERK (A.U.)
12
9
6
3
0
Anti-Igκ
-
+
-
+
IgD-/-
(IgM-only)
IgM-/-
(IgD-only)

Figure 3.1. Anti-Igκ-stimulated IgD-only B cells display reduced CD22 phosphorylation relative to other pathways.

Splenic B cells from *IgM*$^{-/-}$ and *IgD*$^{-/-}$ mice were MACS enriched by negative selection according to manufacturer's protocol (Miltenyi). Purified B cells were incubated with PBS or stimulated with 10 μg/mL anti-Igκ for 5 minutes and then lysed with SDS and reduced with DTT. Lysates were ultracentrifuged, run on a 4-12% gradient NuPAGE Tris-Bis gel (Invitrogen), and transferred to PVDF membranes. Following blocking, membranes were probed for pCD22 Y822 (EPITOMICS), pSHP-1 Y564 (Cell Signaling), pERK1/2 p44/42 (Cell Signaling), and total ERK1/2 (Santa Cruz) and developed with ECL substrate (Perkin Elmer). Blots were quantified with Image Lab v. 5.2.14 (Bio-Rad), and PBS-treated *IgM*$^{-/-}$ cells assigned a value of 1.0 for all parameters. Protein phosphorylation normalized to total ERK was compiled from three independent experiments.

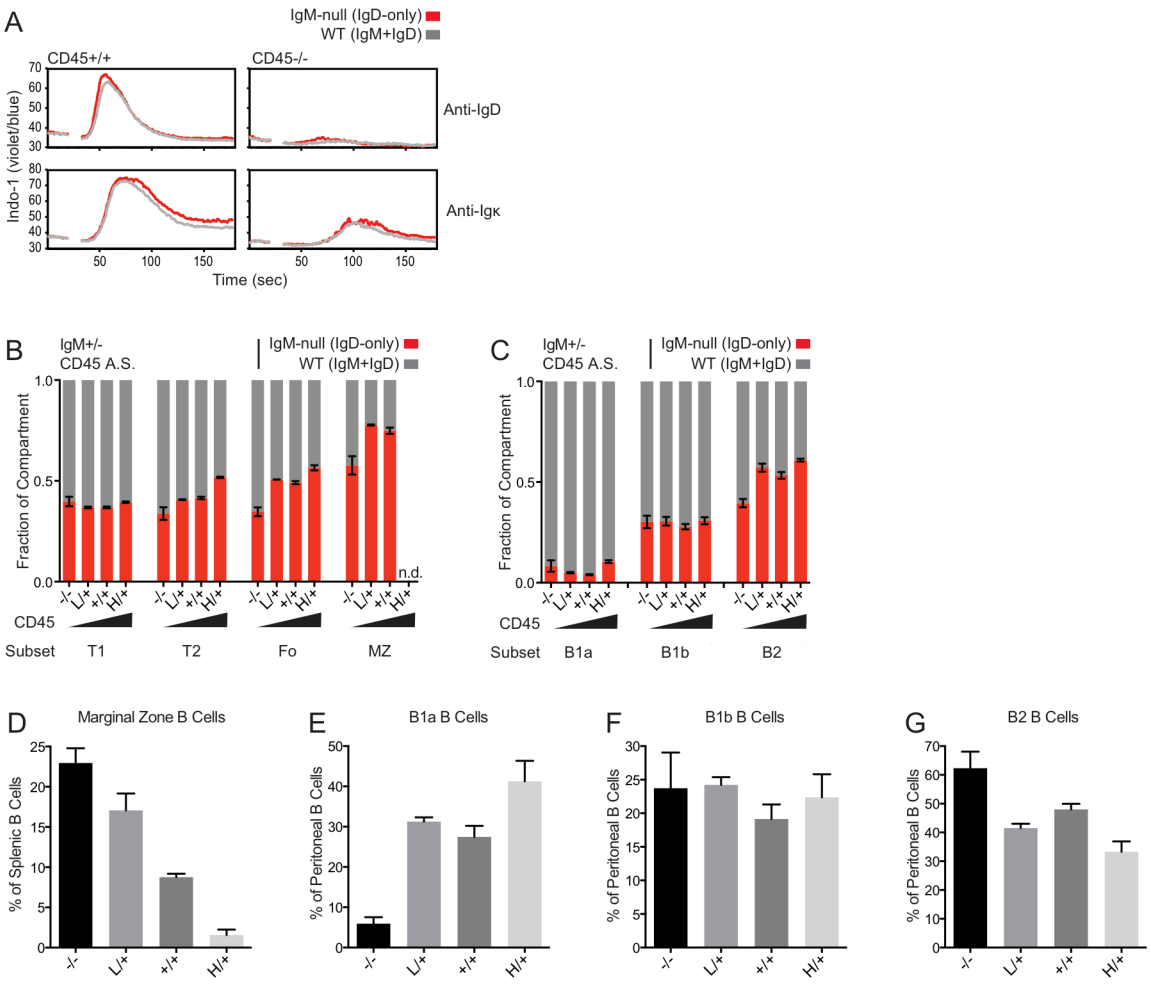
A
IgM-null (IgD-only)
WT (IgM+IgD)
CD45+/+
CD45-/-
Anti-IgD
Anti-Igκ
Indo-1 (violet/blue)
Time (sec)
B
IgM+/-
CD45 A.S.
IgM-null (IgD-only)
WT (IgM+IgD)
Fraction of Compartment
n.d.
CD45
Subset
T1
T2
Fo
MZ
C
IgM+/-
CD45 A.S.
IgM-null (IgD-only)
WT (IgM+IgD)
Fraction of Compartment
CD45
Subset
B1a
B1b
B2
D
Marginal Zone B Cells
% of Splenic B Cells
E
B1a B Cells
% of Peritoneal B Cells
F
B1b B Cells
% of Peritoneal B Cells
G
B2 B Cells
% of Peritoneal B Cells

Figure 3.2. The role of CD45 in signaling and development of IgD-only B cells.

(A) *IgM*$^{+/-}$ *CD45*$^{+/+}$ (BaffTg^{+}) and *IgM*$^{+/-}$ *CD45*$^{-/-}$ cells were loaded with Indo-1, and stimulated with varying doses of anti-IgD and anti-Igκ. IgM-null and WT cells were differentiated using anti-IgM-F_{ab} staining, and calcium signaling in mature (CD19+CD23+) B cells is displayed. 1:400 anti-IgD and 5 μg/mL anti-Igκ and are shown. Results represent a single preliminary experiment.

(B) Relative competition between WT and IgM-null (IgD-only) B cells in *IgM*$^{+/-}$ mice was calculated for splenic B cell compartments on backgrounds expressing varying levels of CD45. Mouse lines used in the CD45 allelic series were previously described (Zikherman et al., 2012a). Subset definitions: T1 (CD93+CD23-); T2 (CD93+CD23+); Fo (CD93-CD23+); MZ (CD21^{hi}CD23^{lo})

(C) Relative competition in the peritoneal B cell compartments of mice described in (B). Subset definitions: B1a (CD5+CD23-); B1b (CD5-CD23-); B2 (CD5-CD23+).

(D-G) Quantification of B cell subsets in (B) and (C) as a fraction of total B cells in each tissue. (B) and (C) contain data from Figure 2.10 for reference. (B-F) display mean ± SEM for n = 3-8 mice per genotype.

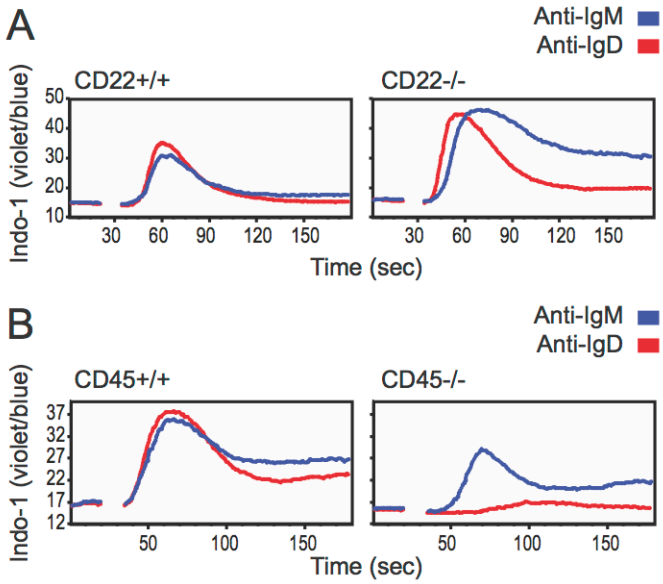
A
Anti-IgM
Anti-IgD
CD22+/+
CD22-/-
Indo-1 (violet/blue)
50
40
30
20
10
30
60
90
120
150
Time (sec)
B
Anti-IgM
Anti-IgD
CD45+/+
CD45-/-
Indo-1 (violet/blue)
37
32
27
22
17
12
50
100
150
Time (sec)

Figure 3.3. IgM and IgD signaling in $CD22^{-/-}$ and $CD45^{-/-}$ B cells.

(A) *$CD22^{-/-}$* and BoyJ (*$CD22^{+/+}$*) cells were mixed, loaded with Indo-1, and stimulated with varying doses of anti-IgM and anti-IgD. Genotypes were differentiated on the basis of CD45.1 expression, and calcium signaling in mature (CD19+CD23+) B cells is displayed. 10 μg/mL anti-IgM-F(ab')$_2$ and 5 μg/mL anti-IgD (clone 11-26) produced equivalent responses in *$CD22^{+/+}$* B cells, and these doses are displayed for *$CD22^{-/-}$* B cells. Surface BCR expression in *$CD22^{+/+}$* (IgM MFI: 549, IgD MFI: 2343) and *$CD22^{-/-}$* (IgM MFI: 232, IgD MFI: 1759) B cells was quantified in a parallel stain. Results are representative of three independent experiments, though polyclonal anti-IgD was used in one experiment.

(B) *$CD45^{-/-}$* B cells were compared to BoyJ (*$CD45^{+/+}$*) as in (A), and 5 μg/mL anti-IgM-F(ab')$_2$ and 1:200 anti-IgD (clone 11-26) produced equivalent responses in *$CD45^{+/+}$* B cells. Surface BCR expression in *$CD45^{+/+}$* (IgM MFI: 12622, IgD MFI: 2017) and *$CD45^{-/-}$* (IgM MFI: 40008, IgD MFI: 1740) B cells was quantified in a parallel stain. Results represent a single preliminary experiment.

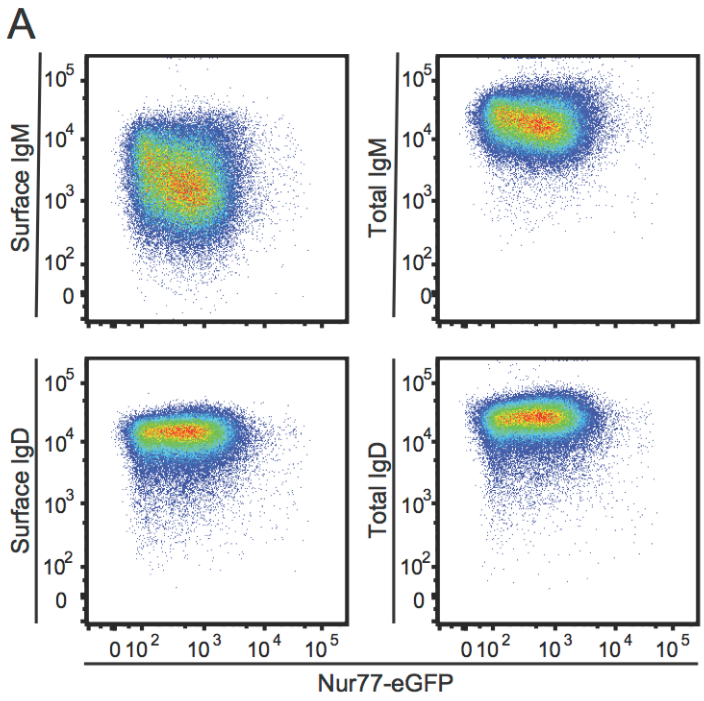
A
Surface IgM
Total IgM
Surface IgD
Total IgD
0
10^2
10^3
10^4
10^5
Nur77-eGFP

Figure 3.4. Regulation of surface IgM across the Nur77-eGFP repertoire is primarily post-translational.

Splenocytes were stained with saturating concentrations of fluorophore-conjugated anti-IgM and anti-IgD either before (left) or after (right) permeabilizing cells with BD Perm Wash. Surface and total IgM and IgD on Nur77-eGFP reporter mature $CD23^{+}$ B cells is displayed. Data are representative of two independent experiments.

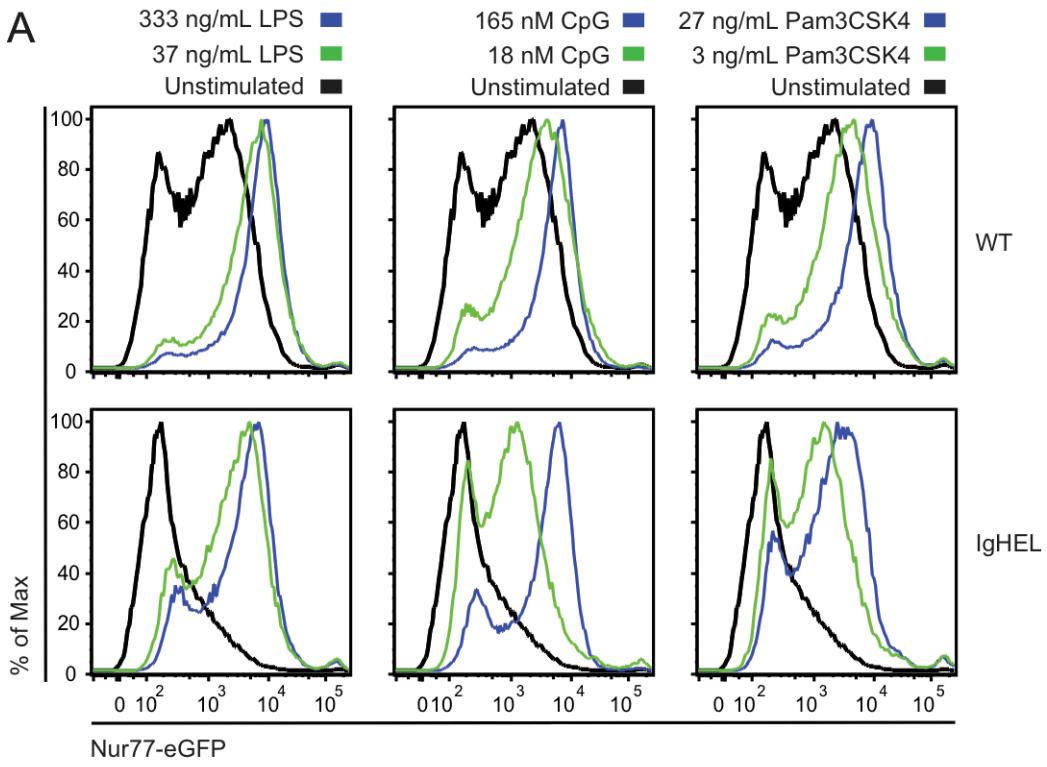
A
333 ng/mL LPS
37 ng/mL LPS
Unstimulated
165 nM CpG
18 nM CpG
Unstimulated
27 ng/mL Pam3CSK4
3 ng/mL Pam3CSK4
Unstimulated
WT
IgHEL
% of Max
Nur77-eGFP

Figure 3.5. Naïve B cells are competent to upregulate Nur77-eGFP in response to canonical TLR ligands even in the absence of endogenous antigen.

Splenocytes from non-BCR Tg and IgHEL BCR Tg reporter mice were stimulated overnight with low and high doses of ligands for TLR4 / rp105 (**left**), TLR9 (**center**), and TLRs1/2 (**right**). Histograms depict GFP fluorescence in B220+ splenocytes. Nur77-eGFP expression is low in the absence of endogenous antigen (IgHEL BCR Tg), but these cells are nevertheless responsive to a broad range of TLR ligands.

APPENDIX

The role of V(D)J locus in autoantibody production in BAFF-transgenic mice

While investigating the role of IgM and IgD in driving autoimmune disease, we generated *IgM*$^{+/-}$ and *IgD*$^{+/-}$ mice on a BAFF-overexpressing background. The original intent was to study an autoimmune disease model driven by perturbations outside of the BCR signaling cascade, in contrast to *Lyn*$^{-/-}$ mice. Mice with transgene-driven BAFF overexpression develop an autoimmune disease characterized by anti-DNA autoantibodies and immune complex deposition in the kidneys (Mackay et al., 1999). However, unlike *Lyn*$^{-/-}$ mice, BAFF-overexpressing mice have a massively expanded B cell compartment (Gavin et al., 2005; Mackay et al., 1999). In addition to promoting expansion of the B cell compartment in general, BAFF overexpression rescues autoreactive B cells that are normally deleted or otherwise pruned from the repertoire on the basis of their poor competitive fitness (Ota et al., 2010).

The autoimmune disease that develops in BAFF overexpressing mice is mechanistically complex due to the many cell types involved and the multiple receptors BAFF can bind. In addition to BAFFR, BAFF also binds to TACI and BCMA, and this can be influenced by BAFF's multimerization state and association with another TNF family member, APRIL (Mackay et al., 2007). BAFF transgenic mice can develop disease in the absence of T cells, but they require MyD88 to develop disease (Groom et al., 2007). Groom et al. identified a feed-forward loop in which BAFF increases expression of TLR7 and TLR9 on B cells, and TLR7/9 signaling upregulates TACI expression on B cells. However, the exact identity of the B cells that drive autoantibody production in BAFF transgenic mice remains controversial. One model proposes that BAFF rescues autoreactive MZ and B1 cells, allowing them to produce autoantibodies (Groom and Mackay, 2008). Another model proposes that excess BAFF promotes the expansion of TACI^{+} transitional B cells that spontaneously secrete class-switched autoantibodies (Jacobs et al., 2016). Regardless, many SLE patients have elevated serum BAFF

levels (Cancro et al., 2009), and this pathway is targeted in existing and proposed treatments for SLE (Liu and Davidson, 2011).

When we collected serum *IgM*$^{+/-}$ and *IgD*$^{+/-}$ *BaffTg*$^{+}$ mice, we were struck by the high penetrance of the disease, which is present even in 6-week-old mice (Figure A1A-D). While WT B cells generated extremely high titers of ANA and anti-dsDNA IgG2a, IgD-only B cells appeared to be completely protected (Figures A1A and A1C). IgM-only B cells were also partially protected from ANA IgG2a generation and completely protected from anti-dsDNA IgG2a generation (Figures A1B and A1D). It is worth emphasizing that autoantibody titers were measured in isotype-heterozygous mice using allotype-specific detection antibodies. Thus, the phenotypes were cell-intrinsic. However, the phenotype was entirely driven by the V(D)J background of the IgM-null and IgD-null B cells. *IgH*$^{a/b}$ mice crossed onto the BaffTg background only developed autoantibodies from the IgH^{b} (B6) locus and did not develop any from the IgH^{a} (Balb/c) locus (Figure A1E). Because the IgH^{a} B cells in these mice express both IgM and IgD, we concluded that the lack of autoantibody by IgM-null and IgD-null B cells was due to their V(D)J background and not perturbations in isotype expression.

These results suggest that the autoantibodies generated in BaffTg mice are germline-encoded. Future investigation could use this information to more definitively identify the B cell compartment(s) that generate(s) autoantibodies in this model. BCR repertoire sequencing of the MZ, B1, and transitional B cell subsets and IgG2a^{+} plasma cells in these mice could provide a more definitive link between each compartment and autoantibody generation.

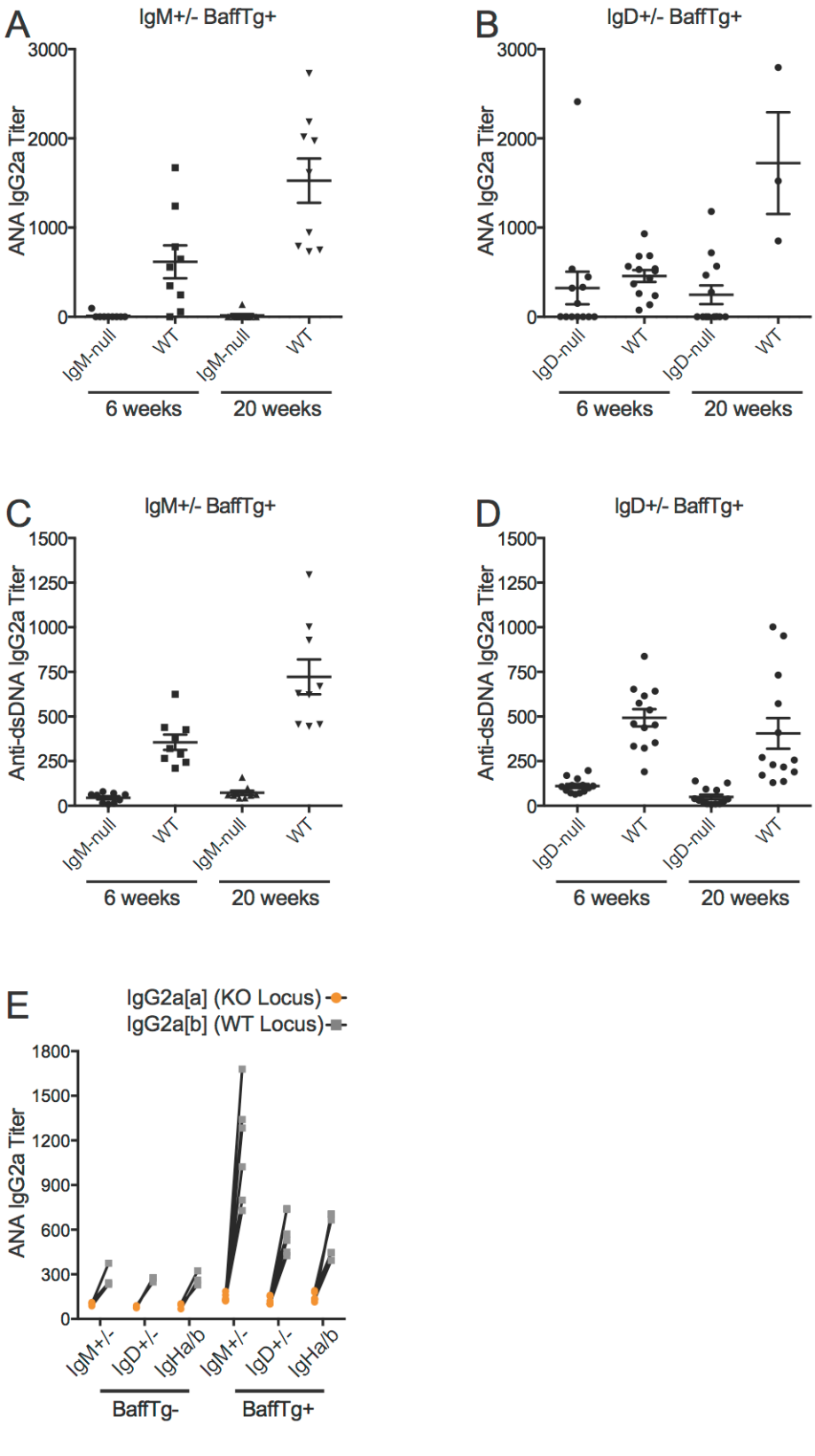
A
IgM+/- BaffTg+
ANA IgG2a Titer
3000
2000
1000
0
IgM-null
WT
IgM-null
WT
6 weeks
20 weeks
B
IgD+/- BaffTg+
ANA IgG2a Titer
3000
2000
1000
0
IgD-null
WT
IgD-null
WT
6 weeks
20 weeks
C
IgM+/- BaffTg+
Anti-dsDNA IgG2a Titer
1500
1250
1000
750
500
250
0
IgM-null
WT
IgM-null
WT
6 weeks
20 weeks
D
IgD+/- BaffTg+
Anti-dsDNA IgG2a Titer
1500
1250
1000
750
500
250
0
IgD-null
WT
IgD-null
WT
6 weeks
20 weeks
E
IgG2a[a] (KO Locus)
IgG2a[b] (WT Locus)
ANA IgG2a Titer
1800
1500
1200
900
600
300
0
IgM+/-
IgD+/-
IgHa/b
IgM+/-
IgD+/-
IgHa/b
BaffTg-
BaffTg+

Figure A1. Autoantibodies on the BaffTg background preferentially arise from the allotype [b] Ig locus.

Allotype-specific IgG2a/c titers against lysed 293T cells (A-B) and dsDNA (C-D) were calculated by ELISA for $IgM^{+/-}$ and $IgD^{+/-}$ mice overexpressing transgenic BAFF. Pooled serum from 6-month autoimmune $IgH^{a/b}$ mice was assigned an arbitrary value of 1000 and used as a standard.

(E) Allotype-specific ANA IgG2a/c titers in 6 month old $IgM^{+/-}$, $IgD^{+/-}$, and $IgH^{a/b}$ mice with and without the BAFF overexpression transgene. $BaffTg^{-}$ $IgH^{a/b}$ mice were 12 weeks old.

REFERENCES:

Achatz, G., Lamers, M., and Crameri, R. (2008). Membrane bound IgE: the key receptor to restrict high IgE levels. Open Immunol. J. *1*, 25-32.

Achatz, G., Nitschke, L., and Lamers, M. (1997). Effect of transmembrane and cytoplasmic domains of IgE on the IgE response. Science *276*, 409-411.

Akahori, Y., and Kurosawa, Y. (1997). Nucleotide sequences of all the γ gene loci of murine immunoglobulin heavy chains. Genomics *41*, 100-104.

Akinleye, A., Chen, Y., Mukhi, N., Song, Y., and Liu, D. (2013). Ibrutinib and novel BTK inhibitors in clinical development. J. Hematol. Oncol. *6*, 59.

Allman, D., and Pillai, S. (2008). Peripheral B cell subsets. Curr. Opin. Immunol. *20*, 149-157.

Alt, F.W., Bothwell, A.L.M., Knapp, M., Siden, E., Mather, E., Koshland, M., and Baltimore, D. (1980). Synthesis of secreted and membrane-bound immunoglobulin mu heavy chains is directed by mRNAs that differ at their 3' ends. Cell *20*, 293-301.

Amezcua Vesely, M.C., Schwartz, M., Bermejo, D.A., Montes, C.L., Cautivo, K.M., Kalergis, A.M., Rawlings, D.J., Acosta-Rodriguez, E.V., and Gruppi, A. (2012). FcγRIIb and BAFF differentially regulate peritoneal B1 cell survival. J. Immunol. *188*, 4792-4800.

Au-Yeung, B.B., Smith, G.A., Mueller, J.L., Heyn, C.S., Jaszczak, R.G., Weiss, A., and Zikherman, J. (2017). IL-2 modulates the TCR signaling threshold for CD8 but not CD4 T cell proliferation on a single-cell level. J. Immunol. *198*, 2445-2456.

Bachmann, M.F., Kalinke, U., Althage, A., Freer, G., Burkhart, C., Roost, H.P., Aguet, M., Hengartner, H., and Zinkernagel, R.M. (1997). The role of antibody concentration and avidity in antiviral protection. Science *276*, 2024-2027.

Bai, L., Chen, Y., He, Y., Dai, X., Lin, X., Wen, R., and Wang, D. (2007). Phospholipase Cγ2 contributes to light-chain gene activation and receptor editing. Mol. Cell. Biol. *27*, 5957-5967.

Baumgarth, N. (2011). The double life of a B-1 cell: self-reactivity selects for protective effector functions. Nat. Rev. Immunol. *11*, 34-46.

Becker, M., Hobeika, E., Jumaa, H., Reth, M., and Maity, P.C. (2017). CXCR4 signaling and function require the expression of the IgD-class B-cell antigen receptor. Proc. Natl. Acad. Sci. USA *114*, 5231-5236.

Benschop, R.J., Aviszus, K., Zhang, X., Manser, T., Cambier, J.C., and Wysocki, L.J. (2001). Activation and anergy in bone marrow B cells of a novel immunoglobulin transgenic mouse that is both hapten specific and autoreactive. Immunity *14*, 33-43.

Berridge, M.J. (1993). Inositol triphosphate and calcium signaling. Nature *361*, 315-325.

Bertocci, B., De Smet, A., Weill, J., and Reynaud, C. (2006). Nonoverlapping functions of DNA polymerases mu, lambda, and terminal deoxynucleotidyltransferase during immunoglobulin V(D)J recombination in vivo. Immunity *25*, 31-41.

Blum, J.H., Stevens, T.L., and Defranco, A.L. (1992). Role of the mu immunoglobulin heavy chain transmembrane and cytoplasmic domains in B cell antigen receptor expression and signal transduction. J. Biol. Chem. *268*, 27236-27245.

Boes, M., Esau, C., Fischer, M.B., Schmidt, T., Carroll, M., and Chen, J. (1998). Enhanced B-1 cell development, but impaired IgG antibody responses in mice deficient in secreted IgM. J. Immunol. *160*, 4776-4787.

Boes, M., Schmidt, T., Linkemann, K., Beaudette, B.C., Marshak-Rothstein, A., and Chen, J. (2000). Accelerated development of IgG autoantibodies and autoimmune disease in the absence of secreted IgM. Proc. Natl. Acad. Sci. USA *97*, 1184-1189.

Bolland, S., and Ravetch, J.V. (2000). Spontaneous autoimmune disease in FcγRIIB-deficient mice results from strain-specific epistasis. Immunity *13*, 277-285.

Braet, F., De Zanger, R., Jans, D., Spector, I., and Wisse, E. (1996). Microfilament-disrupting agent latrunculin A induces an increased number of fenestrae in rat liver sinusoidal endothelial cells: comparison with cytochalasin B. Hepatology *24*, 627-635.

Brezski, R.J., and Georgiou, G. (2016). Immunoglobulin isotype knowledge and application to Fc engineering. Curr. Opin. Immunol. *40*, 62-69.

Brink, R. (2014). The imperfect control of self-reactive germinal center B cells. Cur. Opin. Immunol. *28*, 97-101.

Brink, R., Goodnow, C.C., and Basten, A. (1995). IgD expression on B cells is more efficient than IgM but both receptors are functionally equivalent in up-regulation CD80/CD86 co-stimulatory molecules. Eur. J. Immunol. *25*, 1980-1984.

Brink, R., Goodnow, C.C., Crosbie, J., Adams, E., Eris, J., Mason, D.Y., Hartley, S.B., and Basten, A. (1992). Immunoglobulin M and D antigen receptors are both capable of mediating B lymphocyte activation, deletion, or anergy after interaction with specific antigen. J. Exp. Med. *176*, 991-1005.

Browne, C.D., Del Nagro, C.J., Cato, M.H., Dengler, H.S., and Rickert, R.C. (2009). Suppression of phosphatidylinositol 3,4,5-trisphosphate production is a key determinant of B cell anergy. Immunity *31*, 749-760.

Buhl, A.M., Pleiman, C.M., Rickert, R.C., and Cambier, J.C. (1997). Qualitative regulation of B Cell antigen receptor signaling by CD19: selective requirement for PI3-kinase activation, inositol-1,4,5-trisphosphate production and Ca2+ mobilization. J. Exp. Med. *186*, 1897-1910.

Butcher, E.C., Rouse, R.V., Coffman, R.L., Nottenburg, C., Hardy, R.R., and Weissman, I. (1982). Surface phenotype of Peyer's patch germinal center cells: implications for the role of germinal centers in B cell differentiation. J. Immunol. *1982*, 2698-2707.

Cambier, J.C., Gauld, S.B., Merrell, K.T., and Vilen, B.J. (2007). B-cell anergy: from transgenic models to naturally occurring anergic B cells? Nat. Rev. Immunol. *7*, 633-643.

Cancro, M.P., D'Cruz, D.P., and Khamashta, M.A. (2009). The role of B lymphocyte stimulator (BLyS) in systemic lupus erythematosus. J. Clin. Invest. *119*, 1066-1073.

Cappione, A.J., Pugh-Bernard, A.E., Anolik, J.H., and Sanz, I. (2004). Lupus IgG VH4.34 Antibodies bind to a 220-kDa glycoform of CD45/B220 on the surface of human B lymphocytes. J. Immunol. *172*, 4298-4307.

Cariappa, A., and Pillai, S. (2002). Antigen-dependent B-cell development. Curr. Opin. Immunol. *14*, 241-249.

Casola, S., Otipoby, K.L., Alimzhanov, M., Humme, S., Uyttersprot, N., Kutok, J.L., Carroll, M.C., and Rajewsky, K. (2004). B cell receptor signal strength determines B cell fate. Nat. Immunol. *5*, 317-327.

Chan, T.D., and Brink, R. (2012). Affinity-based selection and the germinal center response. Immunol. Rev. *247*, 11-23.

Chan, T.D., Gatto, D., Wood, K., Camidge, T., Basten, A., and Brink, R. (2009). Antigen affinity controls rapid T-dependent antibody production by driving the expansion rather than the

differentiation or extrafollicular migration of early plasmablasts. J. Immunol. *183*, 3139-3149.

Chan, T.D., Wood, K., Hermes, J.R., Butt, D., Jolly, C.J., Basten, A., and Brink, R. (2012). Elimination of germinal-center-derived self-reactive B cells is governed by the location and concentration of self-antigen. Immunity *37*, 893-904.

Chan, V.W., Meng, F., Soriano, P., DeFranco, A.L., and Lowell, C.A. (1997). Characterization of the B lymphocyte populations in Lyn-deficient mice and the role of Lyn in signal initiation and down-regulation. Immunity *7*, 69-81.

Chandra Maity, P., Blount, A., Jumaa, H., Ronneberger, O., Lillemeier, B.F., and Reth, M. (2015). B cell antigen receptors of the IgM and IgD classes are clustered in different protein islands that are altered during B cell activation. Sci. Signal. *8*, ra93.

Chaturvedi, A., Siddiqui, Z., Bayiroglu, F., and Rao, K.V. (2002). A GPI-linked isoform of the IgD receptor regulates resting B cell activation. Nat. Immunol. *3*, 951-957.

Chen, J., McLean, P.A., Neel, B.G., Okunade, G., Shull, G.E., and Wortis, H.H. (2004). CD22 attenuates calcium signaling by potentiating plasma membrane calcium-ATPase activity. Nat. Immunol. *5*, 651-657.

Chen, K., and Cerutti, A. (2010). New insights into the enigma of immunoglobulin D. Immunol. Rev. *237*, 160-179.

Chen, K., Xu, W., Wilson, M., He, B., Miller, N.W., Bengten, E., Edholm, E.S., Santini, P.A., Rath, P., Chiu, A.*, et al.* (2009). Immunoglobulin D enhances immune surveillance by activating antimicrobial, proinflammatory and B cell-stimulating programs in basophils. Nat. Immunol. *10*, 889-898.

Chen, L., Morris, D.L., and Vyse, T.J. (2017). Genetic advances in systemic lupus erythematosus: an update. Curr. Opin. Rheumatol. *29*, 423-433.

Chen, Y., Zhang, J., Hwang, K.K., Bouton-Verville, H., Xia, S.M., Newman, A., Ouyang, Y.B., Haynes, B.F., and Verkoczy, L. (2013). Common tolerance mechanisms, but distinct cross-reactivities associated with gp41 and lipids, limit production of HIV-1 broad neutralizing antibodies 2F5 and 4E10. J. Immunol. *191*, 1260-1275.

Cheng, A.M., Rowley, B., Pao, W., Hayday, A., Bolen, J.B., and Pawson, T. (1995). Syk tyrosine kinase required for mouse viability and B-cell development. Nature *378*, 303-306.

Contreras, C.M., Halcomb, K.E., Randle, L., Hinman, R.M., Gutierrez, T., Clarke, S.H., and Satterthwaite, A.B. (2007). Btk regulates multiple stages in the development and survival of B-1 cells. Mol. Immunol. *44*, 2719-2728.

Cooke, M.P., Heath, A.W., Shokat, K.M., Zeng, Y., Finkelman, F.D., Linsley, P.S., Howard, M., and Goodnow, C.C. (1994). Immunoglobulin signal transduction guides the specificity of B cell-T cell interactions and is blocked in tolerant self-reactive B cells. J. Exp. Med. *179*, 425-438.

Cornall, R.J., Cyster, J.G., Hibbs, M.L., Dunn, A.R., Otipoby, K.L., Clark, E.A., and Goodnow, C.C. (1998). Polygenic autoimmune traits: Lyn, CD22, and SHP-1 are limiting elements of a biochemical pathway regulating BCR signaling and selection. Immunity *8*, 497-508.

Coughlin, S., Noviski, M., Mueller, J.L., Chuwonpad, A., Raschke, W., Weiss, A., and Zikherman, J. (2015). An extracatalytic function of CD45 in B cells is mediated by CD22. Proc. Natl. Acad. Sci. USA *112*, E6515-6524.

Cyster, J.G., and Goodnow, C.C. (1995). Antigen-induced exclusion from follicles and anergy are separate and complementary processes that influence peripheral B cell fate. Immunity *3*, 691-701.

Cyster, J.G., Healy, J.I., Kishihara, K., Mak, T.W., Thomas, M.L., and Goodnow, C.C. (1996). Regulation of B-lymphocyte negative and positive selection by tyrosine phosphatase CD45. Nature *381*, 325-328.

Das, J., Ho, M., Zikherman, J., Govern, C., Yang, M., Weiss, A., Chakraborty, A.K., and Roose, J.P. (2009). Digital signaling and hysteresis characterize Ras activation in lymphoid cells. Cell *136*, 337-351.

Ding, C., Liu, Y., Wang, Y., Park, B.K., Wang, C.Y., Zheng, P., and Liu, Y. (2007). Siglecg limits the size of B1a B cell lineage by down-regulating NFκB activation. PLoS One *2*, e997.

Dingjan, G.M., Middendorp, S., Dahlenborg, K., Maas, A., Grosveld, F., and Hendricks, R.W. (2001). Bruton's tyrosine kinase regulates the activation of gene rearrangements at the λ light chain locus in precursor B cells in the mouse. J. Exp. Med. *193*, 1169-1178.

Doyle-Cooper, C., Hudson, K.E., Cooper, A.B., Ota, T., Skog, P., Dawson, P.E., Zwick, M.B., Schief, W.R., Burton, D.R., and Nemazee, D. (2013). Immune tolerance negatively regulates B cells in knock-in mice expressing broadly neutralizing HIV antibody 4E10. J. Immunol. *191*, 3186-3191.

Duty, J.A., Szodoray, P., Zheng, N.Y., Koelsch, K.A., Zhang, Q., Swiatkowski, M., Mathias, M., Garman, L., Helms, C., Nakken, B.*, et al.* (2009). Functional anergy in a subpopulation of naive B cells from healthy humans that express autoreactive immunoglobulin receptors. J. Exp. Med. *206*, 139-151.

Ehrenstein, M.R., and Notley, C.A. (2010). The importance of natural IgM: scavenger, protector and regulator. Nat. Rev. Immunol. *10*, 778-786.

El Shikh, M.E., El Sayed, R.M., Szakal, A.K., and Tew, J.G. (2009). T-independent antibody responses to T-dependent antigens: a novel follicular dendritic cell-dependent activity. J. Immunol. *182*, 3482-3491.

Enders, A., Short, A., Miosge, L.A., Bergmann, H., Sontani, Y., Bertram, E.M., Whittle, B., Balakishnan, B., Yoshida, K., Sjollema, G.*, et al.* (2014). Zinc-finger protein ZFP318 is essential for expression of IgD, the alternatively spliced Igh product made by mature B lymphocytes. Proc. Natl. Acad. Sci. USA *111*, 4513-4518.

Engelman, J.A., Luo, J., and Cantley, L.C. (2006). The evolution of phosphatidylinositol 3-kinases as regulators of growth and metabolism. Nat. Rev. Genet. *7*, 606-619.

Engels, N., Konig, L.M., Heeman, C., Lutz, J., Tsubata, T., Griep, S., Schrader, V., and Wienands, J. (2009). Recruitment of the cytoplasmic adaptor Grb2 to surface IgG and IgE provides antigen receptor-intrinsic costimulation to class-switched B cells. Nat. Immunol. *10*, 1018-1025.

Fleire, S.J., Goldman, J.P., Carrasco, Y.R., Weber, M., Bray, D., and Batista, F.D. (2006). B cell ligand discrimination through a spreading and contraction response. Science *312*, 738-741.

Fu, C., Turck, C.W., Kurosaki, T., and Chan, A.C. (1998). BLNK: a central linker protein in B cell activation. Immunity *9*, 93-103.

Fukuyama, H., Nimmerjahn, F., and Ravetch, J.V. (2005). The inhibitory Fcγ receptor modulates autoimmunity by limiting the accumulation of immunoglobulin G^+ anti-DNA plasma cells. Nat. Immunol. *6*, 99-106.

Gardam, S., and Brink, R. (2014). Non-canonical NF-κB signaling initiated by BAFF influences B cell biology at multiple junctures. Front. Immunol. *4*, 509.

Gaspar, H.B., and Conley, M.E. (2000). Early B cell defects. Clin. Exp. Immunol. *119*.

Gasparrini, F., Feest, C., Bruckbauer, A., Mattila, P.K., Muller, J., Nitschke, L., Bray, D., and Batista, F.D. (2016). Nanoscale organization and dynamics of the siglec CD22 cooperate with the cytoskeleton in restraining BCR signalling. EMBO J. *35*, 258-280.

Gauld, S.B., Benschop, R.J., Merrell, K.T., and Cambier, J.C. (2005). Maintenance of B cell anergy requires constant antigen receptor occupancy and signaling. Nat. Immunol. *6*, 1160-1167.

Gavin, A.L., Duong, B., Skog, P., Ait-Azzouzene, D., Greaves, D.R., Scott, M.L., and Nemazee, D. (2005). ΔBAFF, a splice isoform of BAFF, opposes full-length BAFF activity in vivo in transgenic mouse models. J. Immunol. *175*, 319-328.

Gay, D., Saunders, T., Camper, S., and Weigert, M. (1993). Receptor editing: an approach by autoreactive B cells to escape tolerance. J. Exp. Med. *177*, 999-1008.

Genestier, L., Taillardet, M., Mondiere, P., Gheit, H., Bella, C., and Defrance, T. (2007). TLR agonists selectively promote terminal plasma cell differentiation of B cell subsets specialized in thymus-independent responses. J. Immunol. *178*, 7779-7786.

Genot, E., and Cantrell, D. (2000). Ras regulation and function in lymphocytes. Curr. Opin. Immunol. *12*, 289-294.

Getahun, A., Beavers, N.A., Larson, S.R., Shlomchik, M.J., and Cambier, J.C. (2016). Continuous inhibitory signaling by both SHP-1 and SHIP-1 pathways is required to maintain unresponsiveness of anergic B cells. J. Exp. Med. *213*, 751-769.

Goitsuka, R., Fujimura, Y., Mamada, H., Umeda, A., Morimura, T., Uetsuka, K., Doi, K., Tsuji, S., and Kitamura, D. (1998). Cutting edge: BASH, a novel signaling molecule preferentially expressed in B cells of the bursa of Fabricius. J. Immunol. *161*, 5804-5808.

Gold, M.R., Matsuuchi, L., Kelly, R.B., and Defranco, A.L. (1991). Tyrosine phosphorylation of components of the B-cell antigen receptors following receptor crosslinking. Proc. Natl. Acad. Sci. USA *88*, 3436-3440.

Gong, S., and Nussenzweig, M.C. (1996). Regulation of an early developmental checkpoint in the B cell pathway by Igβ. Science *272*, 411-414.

Goodnow, C.C., Brink, R., and Adams, E. (1991). Breakdown of self-tolerance in anergic B lymphocytes. Nature *352*, 532-536.

Goodnow, C.C., Crosbie, J., Adelstein, S., Lavoie, T.B., Smith-Gill, S.J., Brink, R.A., Pritchard-Briscoe, H., Wotherspoon, J.S., Loblay, R.H., and Raphael, K. (1988). Altered immunoglobulin expression and functional silencing of self-reactive B lymphocytes in transgenic mice. Nature *334*, 676-682.

Goodnow, C.C., Crosbie, J., Jorgensen, H., Brink, R.A., and Basten, A. (1989). Induction of self-tolerance in mature peripheral B lymphocytes. Nature *342*, 385-391.

Green, M.C., and Shultz, L.D. (1975). Motheaten, an immunodeficient mutant of the mouse. J. Hered. *66*, 250-258.

Groom, J., and Mackay, F. (2008). B cells flying solo. Immunol. Cell Biol. *86*, 40-46.

Groom, J.R., Fletcher, C.A., Walters, S.N., Grey, S.T., Watt, S.V., Sweet, M.J., Smyth, M.J., Mackay, C.R., and Mackay, F. (2007). BAFF and MyD88 signals promote a lupuslike disease independent of T cells. J. Exp. Med. *204*, 1959-1971.

Gross, A.J., Lyandres, J.R., Panigrahi, A.K., Prak, E.T., and DeFranco, A.L. (2009). Developmental acquisition of the Lyn-CD22-SHP-1 inhibitory pathway promotes B cell tolerance. J. Immunol. *182*, 5382-5392.

Gutierrez, T., Halcomb, K.E., Coughran, A.J., Li, Q.Z., and Satterthwaite, A.B. (2010). Separate checkpoints regulate splenic plasma cell accumulation and IgG autoantibody production in Lyn-deficient mice. Eur. J. Immunol. *40*, 1897-1905.

Haas, K.M., Poe, J.C., Steeber, D.A., and Tedder, T.F. (2005). B-1a and B-1b cells exhibit distinct developmental requirements and have unique functional roles in innate and adaptive immunity to S. pneumoniae. Immunity *23*, 7-18.

Halper-Stromberg, A., Lu, C.L., Klein, F., Horwitz, J.A., Bournazos, S., Nogueira, L., Eisenreich, T.R., Liu, C., Gazumyan, A., Schaefer, U.*, et al.* (2014). Broadly neutralizing antibodies and viral inducers decrease rebound from HIV-1 latent reservoirs in humanized mice. Cell *158*, 989-999.

Hardy, R.R. (2006). B-1 B cell development. J. Immunol. *177*, 2749-2754.

Hartley, S.B., Crosbie, J., Brink, R., Kantor, A.B., Basten, A., and Goodnow, C.C. (1991). Elimination from peripheral lymphoid tissues of self-reactive B lymphocytes recognizing membrane-bound antigens. Nature *353*, 765-769.

Haynes, B.F., Fleming, J., St. Clair, E.W., Katinger, H., Stiegler, G., Kunert, R., Robinson, J., Scearce, R.M., Plonk, K., Staats, H.F.*, et al.* (2005). Cardiolipin polyspecific autoreactivity in two broadly neutralizing HIV-1 antibodies. Science *308*, 1906-1908.

Healy, J.I., Dolmetsch, R.E., Timmerman, L.A., Cyster, J.G., Thomas, M.L., Crabtree, G.R., Lewis, R.S., and Goodnow, C.C. (1997). Different nuclear signals are activated by the B cell receptor during positive versus negative signaling. Immunity *6*, 419-428.

Hermiston, M.L., Tan, A.L., Gupta, V.A., Majeti, R., and Weiss, A. (2005). The juxtamembrane wedge negatively regulates CD45 function in B cells. Immunity *23*, 635-647.

Hermiston, M.L., Zikherman, J., and Zhu, J.W. (2009). CD45, CD148, and Lyp/Pep: critical phosphatases regulating Src family kinase signaling networks in immune cells. Immunol. Rev. *228*, 288-311.

Hertz, M., and Nemazee, D. (1997). BCR ligation induces receptor editing in $IgM^{+}IgD^{-}$ bone marrow B cells in vitro. Immunity *6*, 429-436.

Heyman, B., and Shulman, M.J. (2016). Structure, function, and production of immunoglobulin M (IgM). Encyclopedia of Immunobiology, 1-14.

Hibbs, M.L., Tarlinton, D.M., Armes, J., Grail, D., Hodgson, G., Maglitto, R., Stacker, S.A., and Dunn, A.R. (1995). Multiple defects in the immune system of Lyn-deficient mice, culminating in autoimmune disease. Cell *83*, 301-311.

Hobeika, E., Thiemann, S., Storch, B., Jumaa, H., Nielsen, P.J., Pelanda, R., and Reth, M. (2006). Testing gene function early in the B cell lineage in mb1-cre mice. Proc. Natl. Acad. Sci. USA *103*, 13789-13794.

Hoffmann, A., Kerr, S., Jellusova, J., Zhang, J., Weisel, F., Wellmann, U., Winkler, T.H., Kneitz, B., Crocker, P.R., and Nitschke, L. (2007). Siglec-G is a B1 cell-inhibitory receptor that controls expansion and calcium signaling of the B1 cell population. Nat. Immunol. *8*, 695-704.

Hombach, J., Tsubata, T., Leclercq, L., Stappert, H., and Reth, M. (1990). Molecular components of the B-cell antigen receptor complex of the IgM class. Nature *343*, 760-762.

Hou, B., Reizis, B., and DeFranco, A.L. (2008). Toll-like receptors activate innate and adaptive immunity by using dendritic cell-intrinsic and -extrinsic mechanisms. Immunity *29*, 272-282.

Hua, Z., Gross, A.J., Lamagna, C., Ramos-Hernandez, N., Scapini, P., Ji, M., Shao, H., Lowell, C.A., Hou, B., and DeFranco, A.L. (2014). Requirement for MyD88 signaling in B cells and dendritic cells for germinal center anti-nuclear antibody production in Lyn-deficient mice. J. Immunol. *192*, 875-885.

Ichiyoshi, Y., and Casali, P. (1994). Analysis of the structural correlates for antibody polyreactivity by multiple reassortments of chimeric human immunoglobulin heavy and light chain V segments. J. Exp. Med. *180*, 885-895.

Infantino, S., Jones, S.A., Walker, J.A., Maxwell, M.J., Light, A., O'Donnell, K., Tsantikos, E., Peperzak, V., Phesse, T., Ernst, M.*, et al.* (2014). The tyrosine kinase Lyn limits the cytokine responsiveness of plasma cells to restrict their accumulation in mice. Sci. Signal. *7*, ra77.

Ishiai, M., Sugawara, H., Kurosaki, M., and Kurosaki, T. (1999). Cutting edge: association of phospholipase C-γ2 Src homology 2 domains with BLNK is critical for B cell antigen receptor signaling. J. Immunol. *163*, 1746-1749.

Ishiura, N., Nakashima, H., Watanabe, R., Kuwano, Y., Adachi, T., Takahashi, Y., Tsubata, T., Okochi, H., Tamaki, K., Tedder, T.F., *et al*. (2010). Differential phosphorylation of functional tyrosines in CD19 modulates B-lymphocyte activation. Eur. J. Immunol. *40*, 1192-1204.

Jacobs, H.M., Thouvenel, C.D., Leach, S., Arkatkar, T., Metzler, G., Scharping, N.E., Kolhatkar, N.S., Rawlings, D.J., and Jackson, S.W. (2016). Cutting edge: BAFF promotes

autoantibody production via TACI-dependent activation of transitional B cells. J. Immunol. *196*, 3525-3531.

Jellusova, J., Duber, S., Guckel, E., Binder, C.J., Weiss, S., Voll, R., and Nitschke, L. (2010). Siglec-G regulates B1 cell survival and selection. J. Immunol. *185*, 3277-3284.

John, S.A., Clements, J.L., Russell, L.M., and Garrett-Sinha, L.A. (2008). Ets-1 regulates plasma cell differentiation by interfering with the activity of the transcription factor Blimp-1. J. Biol. Chem. *283*, 951-962.

Jun, J.E., Rubio, I., and Roose, J.P. (2013). Regulation of ras exchange factors and cellular localization of Ras activation by lipid messengers in T cells. Front. Immunol. *4*, 239.

Jung, D., Giallourakis, C., Mostoslavsky, R., and Alt, F.W. (2006). Mechanism and control of V(D)J recombination at the immunoglobulin heavy chain locus. Annu. Rev. Immunol. *24*, 541-570.

Kaisho, T., Schwenk, F., and Rajewsky, K. (1997). The Roles of γ1 heavy chain membrane expression and cytoplasmic tail in IgG1 responses. Science *276*, 412-415.

Kammer, G. (1988). The adenylate cyclase-cAMP-protein kinase A pathway and regulation of the immune response. Immunol. Today *9*, 222-229.

Kantor, A.B., Merrill, C.E., Herzenberg, L.A., and Hillson, J.L. (1997). An unbiased analysis of V(H)-D-J(H) sequences from B-1a, B-1b, and conventional B cells. J. Immunol. *158*, 1175-1186.

Kehry, M., Ewald, S., Douglas, R., Sibley, C., Raschke, W., Fambrough, D., and Hood, L. (1980). The immunoglobulin μ chains of membrane-bound and secreted IgM molecules differ in their C-terminal segments. Cell *21*, 393-406.

Kelesidis, T., Daikos, G., Boumpas, D., and Tsiodras, S. (2011). Does rituximab increase the incidence of infectious complications? A narrative review. Int. J. Infect. Dis. *15*, e2-16.

Kerner, J.D., Appleby, M.W., Mohr, R.N., Chien, S., Rawlings, D.J., Maliszewski, C.R., Witte, O.N., and Perlmutter, R.M. (1995). Impaired expansion of mouse B cell progenitors lacking Btk. Immunity *3*, 301-312.

Khalil, A.M., Cambier, J.C., and Shlomchik, M.J. (2012). B cell signal transduction in germinal center B cells is short-circuited by increased phosphatase activity. Science *336*, 1178-1181.

Khan, W.N., Alt, F.W., Gerstein, R.M., Malynn, B.A., Larsson, I., Rathbun, G., Davidson, L., Muller, S., Kantor, A.B., Herzenberg, L.A.*, et al.* (1995). Defective B cell development and function in Btk-deficient mice. Immunity *3*.

Kil, L.P., de Bruijn, M.J.W., van Nimwegen, M., Corneth, O.B.J., van Hamburg, J.P., Dingjan, G.M., Thaiss, F., Rimmelzwaan, G.F., Elewaut, D., Delsing, D.*, et al.* (2012). Btk levels set the threshold for B-cell activation and negative selection of autoreactive B cells in mice. Blood *119*, 3744-3756.

Kim, K., and Reth, M. (1995a). The B cell antigen receptor of class IgD induces a stronger and more prolonged protein tyrosine phosphorylation than that of class IgM. J. Exp. Med. *181*, 1005-1014.

Kim, K., and Reth, M. (1995b). Signaling differences between class IgM and IgD antigen receptors. Ann. N. Y. Acad. Sci. *766*, 81-88.

Kim, Y.M., Pan, J.Y., Korbel, G.A., Peperzak, V., Boes, M., and Ploegh, H.L. (2006). Monovalent ligation of the B cell receptor induces receptor activation but fails to promote antigen presentation. Proc. Natl. Acad. Sci. USA *103*, 3327-3332.

Kirchenbaum, G.A., St Clair, J.B., Detanico, T., Aviszus, K., and Wysocki, L.J. (2014). Functionally responsive self-reactive B cells of low affinity express reduced levels of surface IgM. Eur. J. Immunol. *44*, 970-982.

Kitamura, D., Roes, J., Kuhn, R., and Rajewsky, K. (1991). A B cell-deficient mouse by targeted disruption of the membrane exon of the immunoglobulin m chain gene. Nature *350*, 423-426.

Klasener, K., Maity, P.C., Hobeika, E., Yang, J., and Reth, M. (2014). B cell activation involves nanoscale receptor reorganizations and inside-out signaling by Syk. Elife *3*, e02069.

Knapp, W., Bolhuis, R.L.H., Radl, J., and Hijmans, W. (1973). Independent movement of IgD and IgM molecules on the surface of individual lymphocytes. J. Immunol. *111*, 1295-1298.

Kraal, G., Weissman, I.L., and Butcher, E.C. (1982). Germinal centre B cells: antigen specificity and changes in heavy chain class expression. Nature *298*, 377-379.

Kraus, M., Alimzhanov, M.B., Rajewsky, N., and Rajewsky, K. (2004). Survival of resting mature B lymphocytes depends on BCR signaling via the Igα/β heterodimer. Cell *117*, 787-800.

Kulkarni, A.B., and Karlsson, S. (1993). Transforming growth factor-β_1 knockout mice. A mutation in one cytokine gene causes a dramatic inflammatory disease. Am. J. Pathol. *143*, 3-9.

Kurosaki, T., Johnson, S.A., Pao, L., Sada, K., Yamamura, H., and Cambier, J. (1995). Role of the Syk autophosphorylation site and SH2 domains in B cell antigen receptor signaling. J. Exp. Med. *182*, 1815-1823.

Kurosaki, T., Kometani, K., and Ise, W. (2015). Memory B cells. Nat. Rev. Immunol. *15*, 149-159.

Lacroix-Desmazes, S., Kaveri, S.V., Mouthon, L., Ayouba, A., Malanchere, E., Coutinho, A., and Kazatchkine, M.D. (1998). Self-reactive antibodies (natural autoantibodies) in healthy individuals. J. Immunol. Methods *216*, 117-137.

Lam, K.P., Kuhn, R., and Rajewsky, K. (1997). In vivo ablation of surface immunoglobulin on mature B cells by inducible gene targeting results in rapid cell death. Cell *90*, 1073-1083.

Lamagna, C., Hu, Y., Defranco, A.L., and Lowell, C.A. (2014). B cell-specific loss of Lyn kinase leads to autoimmunity. J. Immunol. *192*, 919-928.

Lee, S.L., Wesselschmidt, R.L., Linette, G.P., Kanagawa, O., Russell, J.H., and Milbrandt, J. (1995). Unimpaired thymic and peripheral T cell death in mice lacking the nuclear receptor NGFI-B (Nur77). Science *269*, 532-535.

Lesley, R., Xu, Y., Kalled, S.L., Hess, D.M., Schwab, S.R., Shu, H.B., and Cyster, J.G. (2004). Reduced competitiveness of autoantigen-engaged B cells due to increased dependence on BAFF. Immunity *20*, 441-453.

Leslie, N.R., and Downes, C.P. (2002). PTEN: the down side of PI 3-kinase signalling. Cell. Signal. *14*, 285-295.

Liu, M., Yang, G., Wiehe, K., Nicely, N.I., Vandergrift, N.A., Rountree, W., Bonsignori, M., Alam, S.M., Gao, J., Haynes, B.F., and Kelsoe, G. (2015). Polyreactivity and autoreactivity among HIV-1 antibodies. J. Virol. *89*, 784-798.

Liu, Z., and Davidson, A. (2011). BAFF and selection of autoreactive B cells. Trends Immunol. *32*, 388-394.

Liu, Z., Zou, Y., and Davidson, A. (2011). Plasma cells in systemic lupus erythematosus: the long and short of it all. Eur. J. Immunol. *41*, 588-591.

Loh, D.Y., Bothwell, A.L.M., White-Scharf, M.E., Imanishi-Kari, T., and Baltimore, D. (1983). Molecular basis of a mouse strain-specific anti-hapten response. Cell *33*, 85-93.

Looney, R.J., Anolik, J.H., Campbell, D., Felgar, R.E., Young, F., Arend, L.J., Sloand, J.A., Rosenblatt, J., and Sanz, I. (2004). B cell depletion as a novel treatment for systemic lupus erythematosus: a phase I/II dose-escalation trial of rituximab. Arthritis Rheum. *50*, 2580-2589.

Løset, G.Å., Roux, K.H., Zhu, P., Michaelsen, T.E., and Sandlie, I. (2004). Differential segmental flexibility and reach dictate the antigen binding mode of chimeric IgD and IgM: implications for the function of the B cell receptor. J. Immunol. *172*, 2925-2934.

Lund, J.M., Alexopoulou, L., Sato, A., Karow, M., Adams, N.C., Gale, N.W., Iwasaki, A., and Flavell, R.A. (2004). Recognition of single-stranded RNA viruses by Toll-like receptor 7. Proc. Natl. Acad. Sci. USA *101*, 5598-5603.

Luo, W., Mayeux, J., Gutierrez, T., Russell, L., Getahun, A., Muller, J., Tedder, T., Parnes, J., Rickert, R., Nitschke, L.*, et al.* (2014). A balance between B cell receptor and inhibitory receptor signaling controls plasma cell differentiation by maintaining optimal Ets1 levels. J. Immunol. *193*, 909-920.

Lutz, C., Ledermann, B., Kosco-Vilbois, M.H., Ochsenbein, A.F., Zinkernagel, R.M., Kohler, G., and Brombacher, F. (1998). IgD can largely substitute for loss of IgM function in B cells. Nature *393*, 797-801.

Mackay, F., Silveira, P.A., and Brink, R. (2007). B cells and the BAFF/APRIL axis: fast-forward on autoimmunity and signaling. Curr. Opin. Immunol. *19*, 327-336.

Mackay, F., Woodcock, S.A., Lawton, P., Ambrose, C., Baetscher, M., Schneider, P., Tschopp, J., and Browning, J.L. (1999). Mice transgenic for BAFF develop lymphocytic disorders along with autoimmune manifestations. J. Exp. Med. *190*, 1697-1710.

MacLennan, I.C.M., Liu, Y.J., and Johnson, G.D. (1992). Maturation and dispersal of B-cell clones during T cell-dependent antibody responses. Immunol. Rev. *126*, 143-161.

MacLennan, I.C.M., Toellner, K.M., Cunningham, A.F., Serre, K., Sze, D.M.Y., Zuniga, E., Cook, M.C., and Vinuesa, C.G. (2003). Extrafollicular antibody responses. Immunol. Rev. *194*, 8-18.

Malbec, O., Fong, D.C., Turner, M., Tybulewicz, V.L., Cambier, J.C., Fridman, W.H., and Daeron, M. (1998). Fcε receptor I-associated Lyn-dependent phosphorylation of Fcγ receptor IIB during negative regulation of mast cell activation. J. Immunol. *160*, 1647-1658.

Manson, J.J., Mauri, C., and Ehrenstein, M.R. (2005). Natural serum IgM maintains immunological homeostasis and prevents autoimmunity. Springer Semin. Immun. *26*, 425-432.

Martin, F., and Kearney, J.F. (2001). B1 cells: similarities and differences with other B cell subsets. Curr. Opin. Immunol. *13*, 195-201.

Martin, F., and Kearney, J.F. (2002). Marginal-zone B cells. Nat. Rev. Immunol. *2*, 323-335.

Martin, F., Oliver, A.M., and Kearney, J.F. (2001). Marginal zone and B1 B cells unite in the early response against T-independent blood-borne particulate antigens. Immunity *14*, 617-629.

Mattila, P.K., Feest, C., Depoil, D., Treanor, B., Montaner, B., Otipoby, K.L., Carter, R., Justement, L.B., Bruckbauer, A., and Batista, F.D. (2013). The actin and tetraspanin

networks organize receptor nanoclusters to regulate B cell receptor-mediated signaling. Immunity *38*, 461-474.

Maxwell, M.J., Duan, M., Armes, J.E., Anderson, G.P., Tarlinton, D., and Hibbs, M.L. (2011). Genetic sgregation of inflammatory lung disease and autoimmune disease severity in SHIP-1$^{-/-}$ mice. J. Immunol. *186*, 7164-7175.

Mayeux, J., Skaug, B., Luo, W., Russell, L.M., John, S., Saelee, P., Abbasi, H., Li, Q.Z., Garrett-Sinha, L.A., and Satterthwaite, A.B. (2015). Genetic interaction between Lyn, Ets1, and Btk in the control of antibody levels. J. Immunol. *195*, 1955-1963.

McHeyzer-Williams, M.G., and Ahmed, R. (1999). B cell memory and the long-lived plasma cell. Curr. Opin. Immunol. *11*, 172-179.

Melchers, F., Karasuyama, H., Haasner, D., Bauer, S., Kudo, A., Sakaguchi, N., Jameson, B., and Rolink, A. (1993). The surrogate light chain in B-cell development. Immunol. Today *14*, 60-68.

Merrell, K.T., Benschop, R.J., Gauld, S.B., Aviszus, K., Decote-Ricardo, D., Wysocki, L.J., and Cambier, J.C. (2006). Identification of anergic B cells within a wild-type repertoire. Immunity *25*, 953-962.

Mestas, J., and Hughes, C.C.W. (2004). Of mice and not men: differences between mouse and human immunology. J. Immunol. *172*, 2731-2738.

Middendorp, S., and Hendricks, R.W. (2004). Cellular maturation defects in Bruton's tyrosine kinase-deficient immature B cells are amplified by premature B cell receptor expression and reduced by receptor editing. J. Immunol. *172*, 1371-1379.

Mills, R.E., Lam, V.C., Tan, A., Cresalia, N., Oksenberg, N., Zikherman, J., Anderson, M., Weiss, A., and Hermiston, M.L. (2015). Unbiased modifier screen reveals that signal

strength determines the regulatory role murine TLR9 plays in autoantibody production. J. Immunol. *194*, 3675-3686.

Minegishi, Y., Coustan-Smith, E., Rapalus, L., Ersoy, F., Campana, D., and Conley, M.E. (1999). Mutations in Igα (CD79a) result in a complete block in B-cell development. J. Clin. Invest. *104*, 1115-1121.

Mittelstadt, P.R., and Defranco, A.L. (1993). Induction of early response genes by cross-linking membrane Ig on B lymphocytes. J. Immunol. *150*, 4822-4832.

Mombaerts, P., Iacomini, J., Johnson, R.S., Herrup, K., Tonegawa, S., and Papaioannou, V.E. (1992). RAG-1-deficient mice have no mature B and T lymphocytes. Cell *68*, 869-877.

Mond, J.L., Lees, A., and Snapper, C.M. (1995). T cell-independent antigens type 2. Annu. Rev. Immunol. *13*, 655-692.

Moore, K.W., Rogers, J., Hunkapiller, T., Early, P., Nottenburg, C., Weissman, I., Bazin, H., Wall, R., and Hood, L.E. (1981). Expression of IgD may use both DNA rearrangement and RNA splicing mechanisms. Proc. Natl. Acad. Sci. USA *78*, 1800-1804.

Moran, A.E., Holzapfel, K.L., Xing, Y., Cunningham, N.R., Maltzman, J.S., Punt, J., and Hogquist, K.A. (2011). T cell receptor signal strength in Treg and iNKT cell development demonstrated by a novel fluorescent reporter mouse. J. Exp. Med. *208*, 1279-1289.

Mueller, J., Matloubian, M., and Zikherman, J. (2015). Cutting edge: an in vivo reporter reveals active B cell receptor signaling in the germinal center. J. Immunol. *194*, 2993-2997.

Mukherjee, S., Zhu, J., Zikherman, J., Parameswaran, R., Kadlecek, T.A., Wang, Q., Au-Yeung, B.B., Ploegh, H.L., Kuriyan, J., Das, J., and Weiss, A. (2013). Monovalent and

multivalent ligation of the B cell receptor exhibit differential dependence upon Syk and Src family kinases. Sci. Signal. *6*, ra1.

Nada, S., Okada, M., MacAuley, A., Cooper, J.A., and Nakagawa, H. (1991). Cloning of a complementary DNA for a protein-tyrosine kinase that specifically phosphorylates a negative regulator site of p60c-src. Nature *351*, 69-72.

Nemazee, D. (2006). Receptor editing in lymphocyte development and central tolerance. Nat. Rev. Immunol. *6*, 728-740.

Nemazee, D. (2017). Mechanisms of central tolerance for B cells. Nat. Rev. Immunol. *17*, 281-294.

Nemazee, D.A., and Burki, K. (1989). Clonal deletion of B lymphocytes in a transgenic mouse bearing anti-MHC class I antibody genes. Nature *337*, 562-566.

Newton, A.C. (2001). Protein Kinase C: Structural and spatial regulation by phosphorylation, cofactors, and macromolecular interactions. Chem. Rev. *101*, 2353-2364.

Ng, Y.S., Wardemann, H., Chelnis, J., Cunningham-Rundles, C., and Meffre, E. (2004). Bruton's tyrosine kinase is essential for human B cell tolerance. J. Exp. Med. *200*, 927-934.

Nguyen, T.T., Klasener, K., Zurn, C., Castillo, P.A., Brust-Mascher, I., Imai, D.M., Bevins, C.L., Reardon, C., Reth, M., and Baumgarth, N. (2017a). The IgM receptor FcμR limits tonic BCR signaling by regulating expression of the IgM BCR. Nat. Immunol. *18*, 321-333.

Nguyen, T.T.T., Graf, B.A., Randall, T.D., and Baumgarth, N. (2017b). sIgM-FcμR interactions regulate early B cell activation and plasma cell development after influenza virus infection. J. Immunol. *199*, 1635-1646.

Nie, Y., Waite, J., Brewer, F., Sunshine, M.J., Littman, D.R., and Zou, Y.R. (2004). The role of CXCR4 in maintaining peripheral B cell compartments and humoral immunity. J. Exp. Med. *200*, 1145-1156.

Nishizumi, H., Taniuchi, I., Yamanashi, Y., Kitamura, D., Ilic, D., Mori, S., Watanabe, T., and Yamamoto, T. (1995). Impaired proliferation of peripheral B cells and indication of autoimmune disease in Lyn-deficient mice. Immunity *3*, 549-560.

Nitschke, L. (2005). The role of CD22 and other inhibitory co-receptors in B-cell activation. Curr. Opin. Immunol. *17*, 290-297.

Nitschke, L. (2009). CD22 and Siglec-G: B-cell inhibitory receptors with distinct functions. Immunol. Rev. *230*, 128-143.

Nitschke, L., Carsetti, R., Ocker, B., Kohler, G., and Lamers, M.C. (1997). CD22 is a negative regulator of B-cell receptor signalling. Curr. Biol. *7*, 133-143.

Nitschke, L., Kosco, M.H., Kohler, G., and Lamers, M.C. (1993). Immunoglobulin D-deficient mice can mount normal immune responses to thymus-independent and -dependent antigens. Proc. Natl. Acad. Sci. USA *90*, 1887-1891.

Norvell, A., Mandik, L., and Monroe, J.G. (1995). Engagement of the antigen-receptor on immature murine B lymphocytes results in death by apoptosis. J. Immunol. *154*, 4404-4413.

Nutt, S.L., Hodgkin, P.D., Tarlinton, D.M., and Corcoran, L.M. (2015). The generation of antibody-secreting plasma cells. Nat. Rev. Immunol. *15*, 160-171.

Nyhoff, L.E., Clark, E.S., Barron, B.L., Bonami, R.H., Khan, W.N., and Kendall, P.L. (2018). Bruton's tyrosine kinase is not essential for B cell survival beyond early developmental stages. J. Immunol. DOI: 10.4049/jimmunol.1701489.

O'Neill, S.K., Getahun, A., Gauld, S.B., Merrell, K.T., Tamir, I., Smith, M.J., Dal Porto, J.M., Li, Q.Z., and Cambier, J.C. (2011). Monophosphorylation of CD79a and CD79b ITAM motifs initiates a SHIP-1 phosphatase-mediated inhibitory signaling cascade required for B cell anergy. Immunity *35*, 746-756.

O'Keefe, T.L., Williams, G.T., Batista, F.D., and Neuberger, M.S. (1999). Deficiency in CD22, a B cell-specific inhibitory receptor, is sufficient to predispose to development of high affinity autoantibodies. J. Exp. Med. *189*, 1307-1313.

Obukhanych, T.V., and Nussenzweig, M.C. (2006). T-independent type II immune responses generate memory B cells. J. Exp. Med. *203*, 305-310.

Ohashi, P.S., and Defranco, A.L. (2002). Making and breaking tolerance. Curr. Opin. Immunol. *14*, 744-759.

Okada, T., Maeda, A., Iwamatsu, A., Gotoh, K., and Kurosaki, T. (2000). BCAP: the tyrosine kinase substrate that connects B cell receptor to phosphoinositide 3-kinase activation. Immunity *13*, 817-827.

Ono, M., Bolland, S., Tempst, P., and Ravetch, J.V. (1996). Role of the inositol phosphatase SHIP in negative regulation of the immune system by the receptor FcγRIIB. Nature *383*, 263-266.

Ota, M., Duong, B.H., Torkamani, A., Doyle, C.M., Gavin, A.L., Ota, T., and Nemazee, D. (2010). Regulation of the B cell receptor repertoire and self-reactivity by BAFF. J. Immunol. *185*, 4128-4136.

Pabst, O. (2012). New concepts in the generation and functions of IgA. Nat. Rev. Immunol. *12*, 821-832.

Packard, T.A., and Cambier, J.C. (2013). B lymphocyte antigen receptor signaling: initiation, amplification, and regulation. F1000Prime Rep. *5*, 40.

Pao, L.I., Lam, K.P., Henderson, J.M., Kutok, J.L., Alimzhanov, M., Nitschke, L., Thomas, M.L., Neel, B.G., and Rajewsky, K. (2007). B cell-specific deletion of protein-tyrosine phosphatase Shp1 promotes B-1a cell development and causes systemic autoimmunity. Immunity *27*, 35-48.

Paus, D., Phan, T.G., Chan, T.D., Gardam, S., Basten, A., and Brink, R. (2006). Antigen recognition strength regulates the choice between extrafollicular plasma cell and germinal center B cell differentiation. J. Exp. Med. *203*, 1081-1091.

Pelanda, R., Schwers, S., Sonoda, E., Torres, R.M., Nemazee, D., and Rajewsky, K. (1997). Receptor editing in a transgenic mouse model: site, efficiency, and role in B cell tolerance and antibody diversification. Immunity *7*, 765-775.

Pfrengle, F., Macauley, M.S., Kawasaki, N., and Paulson, J.C. (2013). Copresentation of antigen and ligands of Siglec-G induces B cell tolerance independent of CD22. J. Immunol. *191*, 1724-1731.

Phan, T.G., Gardam, S., Basten, A., and Brink, R. (2005). Altered migration, recruitment, and somatic hypermutation in the early response of marginal zone B cells to T cell-dependent antigen. J. Immunol. *174*, 4567-4578.

Pioli, P.D., Debnath, I., Weis, J.J., and Weis, J.H. (2014). Zfp318 regulates IgD expression by abrogating transcription termination within the Ighm/Ighd locus. J. Immunol. *193*, 2546-2553.

Pisitkun, P., Deane, J.A., Difilippantonio, M.J., Tarasenko, T., Satterthwaite, A.B., and Bolland, S. (2006). Autoreactive B cell responses to RNA-related antigens due to TLR7 gene duplication. Science *312*, 1669-1672.

Poe, J.C., Fujimoto, M., Jansen, P.J., Miller, A.S., and Tedder, T.F. (2000). CD22 forms a quaternary complex with SHIP, Grb2, and Shc. A pathway for regulation of B lymphocyte antigen receptor-induced calcium flux. J. Biol. Chem. *275*, 17420-17427.

Preud'homme, J., Petit, I., Barra, A., Morel, F., Lecron, J., and Leliévre, E. (2000). Structural and functional properties of membrane and secreted IgD. Mol. Immunol. *37*, 871-887.

Quach, T.D., Manjarrez-Orduno, N., Adlowitz, D.G., Silver, L., Yang, H., Wei, C., Milner, E.C., and Sanz, I. (2011). Anergic responses characterize a large fraction of human autoreactive naive B cells expressing low levels of surface IgM. J. Immunol. *186*, 4640-4648.

Radaev, S., Zou, Z., Tolar, P., Nguyen, K., Nguyen, A., Krueger, P.D., Stutzman, N., Pierce, S., and Sun, P.D. (2010). Structural and functional studies of Igαβ and its assembly with the B cell antigen receptor. Structure *18*, 934-943.

Raff, M.C., Megson, M., Owen, J.J.T., and Cooper, M.D. (1976). Early production of intracellular IgM by B-lymphocyte precursors in mouse. Nature *259*, 224-226.

Randall, T.D., Brewer, J.W., and Corley, R.B. (1992). Direct evidence that J chain regulates the polymeric structure of IgM in antibody-secreting B cells. J. Biol. Chem. *267*, 18002-18007.

Rathmell, J.C., Cooke, M.P., Ho, W.Y., Grein, J., Townsend, S.E., Davis, M.M., and Goodnow, C.C. (1995). CD95 (Fas)-dependent elimination of self-reactive B cells upon interaction with $CD4^+$ T cells. Nature *376*, 181-184.

Reed, J.H., Jackson, J., Christ, D., and Goodnow, C.C. (2016). Clonal redemption of autoantibodies by somatic hypermutation away from self-reactivity during human immunization. J. Exp. Med. *213*, 1255-1265.

Renshaw, B.R., Fanslow, W.C.I., Armitage, R.J., Campbell, K.A., Liggitt, D., Wright, B., Davison, B.L., and Maliszewski, C.R. (1994). Humoral immune responses in CD40 ligand-deficient mice. J. Exp. Med. *180*, 1889-1900.

Reth, M. (1992). Antigen receptors in B lymphocytes. Annu. Rev. Immunol. *10*, 97-121.

Rhee, S.G., and Bae, Y.S. (1997). Regulation of phosphoinositide-specific phospholipase C isozymes. J. Biol. Chem. *272*, 15045-15048.

Rickert, R.C. (2013). New insights into pre-BCR and BCR signalling with relevance to B cell malignancies. Nat. Rev. Immunol. *13*, 578-591.

Rickert, R.C., Rajewsky, K., and Roes, J. (1995). Impairment of T-cell-dependent B-cell responses and B-l cell development in CD19-deficient mice. Nature *376*, 352-355.

Rispens, T., and Vidarsson, G. (2014). Human IgG subclasses. Antibody Fc, 159-177.

Roes, J., and Rajewsky, K. (1991). Cell autonomous expression of IgD is not essential for the maturation of conventional B cells. Int. Immunol. *3*, 1367-1371.

Roes, J., and Rajewsky, K. (1993). Immunoglobulin D (IgD)-deficient mice reveal an auxiliary receptor function for IgD in antigen-mediated recruitment of B cells. J. Exp. Med. *177*, 45-55.

Rogers, J., Early, P., Calame, K., Bond, M., Hood, L., and Wall, R. (1980). Two mRNAs with different 3' ends encode membrane-bound and secreted forms of immunoglobulin μ chain. Cell *20*, 303-312.

Rogers, K.A., Richardson, J.P., Scinicariello, F., and Attanasio, R. (2006). Molecular characterization of immunoglobulin D in mammals: immunoglobulin heavy constant delta genes in dogs, chimpanzees and four old world monkey species. Immunology *118*, 88-100.

Rowe, D.S., Hug, K., Forni, L., and Pernis, B. (1973). Immunoglobulin D as a lymphocyte receptor. J. Exp. Med. *138*, 965-972.

Rowley, R.B., and Burkhardt, A.L. (1995). Syk protein-tyrosine kinase is regulated by tyrosine-phosphorylated Igα/Igβ immunoreceptor tyrosine activation motif binding and autophosphorylation. J. Biol. Chem. *270*, 11590-11594.

Rust, M.J., Bates, M., and Zhuang, X. (2006). Sub-diffraction-limit imaging by stochastic optical reconstruction microscopy (STORM). Nat. Methods *3*, 793-795.

Sabouri, Z., Perotti, S., Spierings, E., Humburg, P., Yabas, M., Bergmann, H., Horikawa, K., Roots, C., Lambe, S., Young, C.*, et al.* (2016). IgD attenuates the IgM-induced anergy response in transitional and mature B cells. Nat. Commun. *7*, 13381.

Sabouri, Z., Schofield, P., Horikawa, K., Spierings, E., Kipling, D., Randall, K.L., Langley, D., Roome, B., Vazquez-Lombardi, R., Rouet, R.*, et al.* (2014). Redemption of autoantibodies on anergic B cells by variable-region glycosylation and mutation away from self-reactivity. Proc. Natl. Acad. Sci. USA *111*, E2567-2575.

Saijo, K., Schmedt, C., Su, I.H., Karasuyama, H., Lowell, C.A., Reth, M., Adachi, T., Patke, A., Santana, A., and Tarakhovsky, A. (2003). Essential role of Src-family protein tyrosine kinases in NF-κB activation during B cell development. Nat. Immunol. *4*, 274-279.

Samardzic, T., Marinkovic, D., Danzer, C., Gerlach, J., Nitschke, L., and Wirth, T. (2002). Reduction of marginal zone B cells in CD22-deficient mice. Eur. J. Immunol. *32*, 561-567.

Saouaf, S.J., Mahajan, S., Rowley, R.B., Kut, S.A., Fargnoli, J., Burkhardt, A.L., Tsukada, S., Witte, O.N., and Bolen, J.B. (1994). Temporal differences in the activation of three classes of non-transmembrane protein tyrosine kinases following B-cell antigen receptor surface engagement. Proc. Natl. Acad. Sci. USA *91*, 9524-9528.

Sato, M., Adachi, T., and Tsubata, T. (2007). Augmentation of signaling through BCR containing IgE but not that containing IgA due to lack of CD22-mediated signal regulation. J. Immunol. *178*, 2901-2907.

Sato, S., Miller, A.S., Inaoki, M., Bock, C.B., Jansen, P.J., Tang, M.L.K., and Tedder, T.F. (1996). CD22 is both a positive and negative regulator of B lymphocyte antigen receptor signal transduction: altered signaling in CD22-deficient mice. Immunity *5*, 551-562.

Satterthwaite, A.B., Li, Z., and Witte, O.N. (1998a). Btk function in B cell development and response. Semin. Immunol. *10*, 309-316.

Satterthwaite, A.B., Lowell, C.A., Khan, W.N., Sideras, P., Alt, F.W., and Witte, O.N. (1998b). Independent and opposing roles for Btk and Lyn in B and myeloid signaling pathways. J. Exp. Med. *188*, 833-844.

Scapini, P., Pereira, S., Zhang, H., and Lowell, C.A. (2009). Multiple roles of Lyn kinase in myeloid cell signaling and function. Immunol. Rev. *228*, 23-40.

Schamel, W.W.A., and Reth, M. (2000). Stability of the B cell antigen receptor complex. Mol. Immunol. *37*, 253-259.

Scheid, M.P., Huber, M., Damen, J.E., Hughes, M., Kang, V., Neilsen, P., Prestwich, G.D., Krystal, G., and Duronio, V. (2002). Phosphatidylinositol (3,4,5)P3 is essential but not sufficient for protein kinase B (PKB) activation; phosphatidylinositol (3,4)P2 is required for PKB phosphorylation at Ser-473: studies using cells from SH2-containing inositol-5-phosphatase knockout mice. J. Biol. Chem. *277*, 9027-9035.

Schiemann, B., Gommerman, J.L., Vora, K., Cachero, T.G., Shulga-Morskaya, S., Dobles, M., Frew, E., and Scott, M.L. (2001). An essential role for BAFF in the normal development of B cells through a BCMA-independent pathway. Science *293*, 2111-2114.

Schweighoffer, E., Vanes, L., Nys, J., Cantrell, D., McCleary, S., Smithers, N., and Tybulewicz, V.L. (2013). The BAFF receptor transduces survival signals by co-opting the B cell receptor signaling pathway. Immunity *38*, 475-488.

Scribner, C.L., Hansen, C.T., Klinmann, D.M., and Steinberg, A.D. (1987). The interaction of the xid and me genes. J. Immunol. *138*, 3611-3617.

Shaheen, S., Wan, Z., Li, Z., Chau, A., Li, X., Zhang, S., Liu, Y., Yi, J., Zeng, Y., Wang, J.*, et al.* (2017). Substrate stiffness governs the initiation of B cell activation by the concerted signaling of PKCβ and focal adhesion kinase. Elife *6*, e23060.

Sharon, J. (1990). Structural correlates of high antibody affinity: Three engineered amino acid substitutions can increase the affinity of an anti-p-azophenylarsonate antibody 200-fold. Proc. Natl. Acad. Sci. USA *87*, 4814-4817.

Shimizu, A., and Honjo, T. (1984). Immunoglobulin class switching. Cell *36*, 801-803.

Shimizu, A., Takahashi, N., Yaoita, Y., and Honjo, T. (1982). Organization of the constant-region gene family of the mouse immunoglobulin heavy chain. Cell *28*, 499-506.

Shinkai, Y., Rathbun, G., Lam, K.P., Oltz, E.M., Stewart, V., Mendelsohn, M., Charron, J., Datta, M., Young, F., Stall, A.M., and Alt, F.W. (1992). RAG-2-deficient mice lack mature lymphocytes owing to inabilitiy to initiate V(D)J rearrangement. Cell *68*, 855-867.

Shlomchik, M.J. (2008). Sites and stages of autoreactive B cell activation and regulation. Immunity *28*, 18-28.

Shultz, L.D., Schweitzer, P.A., Rajan, T.V., Li, T., Ihle, J.N., Matthews, R.J., Thomas, M.L., and Beier, D.R. (1993). Mutations at the murine motheaten locus are within the hematopoietic cell protein-tyrosine phosphatase (Hcph) gene. Cell *73*, 1445-1454.

Skrzypczynska, K.M., Zhu, J.W., and Weiss, A. (2016). Positive regulation of Lyn kinase by CD148 is required for B cell receptor signaling in B1 but not B2 B cells. Immunity *45*, 1232-1244.

Smalls-Mantey, A., Connors, M., and Sattentau, Q.J. (2013). Comparative efficiency of HIV-1-infected T cell killing by NK cells, monocytes and neutrophils. PLoS One *8*, e74858.

Smith, C.I.E., Satterthwaite, A.B., and Witte, O.N. (2007). X-Linked agammaglobulinemia: a disease of Btk tyrosine kinase. In primary immunodeficiency diseases: a molecular and genetic approach, H.D. Ochs, C.I.E. Smith, and J. Puck, eds. (Oxford University Press), pp. 279-303.

Smith, K.G., and Clatworthy, M.R. (2010). FcγRIIB in autoimmunity and infection: evolutionary and therapeutic implications. Nat. Rev. Immunol. *10*, 328-343.

Smith, K.G.C., Tarlinton, D.M., Doody, G.M., Hibbs, M.L., and Fearon, D.T. (1998). Inhibition of the B cell by CD22: a requirement for Lyn. J. Exp. Med. *187*, 807-811.

Song, H., and Cerny, J. (2003). Functional heterogeneity of marginal zone B cells revealed by their ability to generate both early antibody-forming cells and germinal centers with hypermutation and memory in response to a T-dependent antigen. J. Exp. Med. *198*, 1923-1935.

Srinivasan, L., Sasaki, Y., Calado, D.P., Zhang, B., Paik, J.H., DePinho, R.A., Kutok, J.L., Kearney, J.F., Otipoby, K.L., and Rajewsky, K. (2009). PI3 kinase signals BCR-dependent mature B cell survival. Cell *139*, 573-586.

Stadanlick, J.E., and Cancro, M.P. (2008). BAFF and the plasticity of peripheral B cell tolerance. Curr. Opin. Immunol. *20*, 158-161.

Stadanlick, J.E., Kaileh, M., Karnell, F.G., Scholz, J.L., Miller, J.P., Quinn, W.J., 3rd, Brezski, R.J., Treml, L.S., Jordan, K.A., Monroe, J.G.*, et al.* (2008). Tonic B cell antigen receptor signals supply an NF-κB substrate for prosurvival BLyS signaling. Nat. Immunol. *9*, 1379-1387.

Su, T.T., and Rawlings, D.J. (2002). Transitional B lymphocyte subsets operate as distinct checkpoints in murine splenic B cell development. J. Immunol. *168*, 2101-2110.

Sun, Y., Wei, Z., Hammarstrom, L., and Zhao, Y. (2011). The immunoglobulin δ gene in jawed vertebrates: a comparative overview. Dev. Comp. Immunol. *35*, 975-981.

Sun, Z., Almogren, A., Furtado, P.B., Chowdhury, B., Kerr, M.A., and Perkins, S.J. (2005). Semi-extended solution structure of human myeloma immunoglobulin D determined by constrained X-ray scattering. J. Mol. Biol. *353*, 155-173.

Tabeta, K., Hoebe, K., Janssen, E.M., Du, X., Georgel, P., Crozat, K., Mudd, S., Mann, N., Sovath, S., Goode, J.*, et al.* (2006). The Unc93b1 mutation 3d disrupts exogenous antigen presentation and signaling via Toll-like receptors 3, 7 and 9. Nat. Immunol. *7*, 156-164.

Thien, M., Phan, T.G., Gardam, S., Amesbury, M., Basten, A., Mackay, F., and Brink, R. (2004). Excess BAFF rescues self-reactive B cells from peripheral deletion and allows them to enter forbidden follicular and marginal zone niches. Immunity *20*, 785-798.

Thompson, J.S., Bixler, S.A., Qian, F., Vora, K., Scott, M.L., Cachero, T.G., Hession, C., Schneider, P., Sizing, I.D., Mullen, C.*, et al.* (2001). BAFFR, a newly identified TNF receptor that specifically interacts with BAFF. Science *293*, 2108-2111.

Tiegs, S.L., Russell, D.M., and Nemazee, D. (1993). Receptor editing in self-reactive bone marrow B cells. J. Exp. Med. *177*, 1009-1020.

Tipton, C.M., Fucile, C.F., Darce, J., Chida, A., Ichikawa, T., Gregoretti, I., Schieferl, S., Hom, J., Jenks, S., Feldman, R.J.*, et al.* (2015). Diversity, cellular origin and autoreactivity of antibody-secreting cell population expansions in acute systemic lupus erythematosus. Nat. Immunol. *16*, 755-765.

Toellner, K.M., Jenkinson, W.E., Taylor, D.R., Khan, M., Sze, D.M.Y., Sansom, D.M., Vinuesa, C.G., and MacLennan, I.C.M. (2002). Low-level hypermutation in T cell–independent germinal centers compared with high mutation rates associated with T cell–dependent germinal centers. J. Exp. Med. *195*, 383-389.

Tonegawa, S. (1983). Somatic generation of antibody diversity. Nature *302*, 575-581.

Tucker, P.W., Slightom, J.L., and Blattner, F.R. (1981). Mouse IgA heavy chain gene sequence: implications for evolution of immunoglobulin hinge exons. Proc. Natl. Acad. Sci. USA *78*, 7684-7688.

Turner, M., Gulbranson-Judge, A., Quinn, M.E., Walters, A.E., MacLennan, I.C.M., and Tybulewicz, V.L. (1997). Syk tyrosine kinase is required for the positive selection of immature B cells into the recirculating B cell pool. J. Exp. Med. *186*, 2013-2021.

Turner, M., Mee, P.J., Costello, P.S., Williams, O., Price, A.A., Duddy, L.P., Furlong, M.T., Geahlen, R.L., and Tybulewicz, V.L. (1995). Perinatal lethality and blocked B-cell development in mice lacking the tyrosine kinase Syk. Nature *378*, 298-302.

Ubelhart, R., Hug, E., Bach, M.P., Wossning, T., Duhren-von Minden, M., Horn, A.H., Tsiantoulas, D., Kometani, K., Kurosaki, T., Binder, C.J.*, et al.* (2015). Responsiveness of B cells is regulated by the hinge region of IgD. Nat. Immunol. *16*, 534-543.

Ubelhart, R., and Jumaa, H. (2015). Autoreactivity and the positive selection of B cells. Eur. J. Immunol. *45*, 2971-2977.

Venkitaraman, A.R., Williams, G.T., Dariavach, P., and Neuberger, M.S. (1991). The B-cell antigen receptor of the five immunoglobulin classes. Nature *352*, 777-781.

Verkoczy, L., and Diaz, M. (2014). Autoreactivity in HIV-1 broadly neutralizing antibodies: implications for their function & induction by vaccination. Curr. Opin. HIV AIDS *9*, 224-234.

Verkoczy, L., Diaz, M., Holl, T.M., Ouyang, Y.B., Bouton-Verville, H., Alam, S.M., Liao, H.X., Kelsoe, G., and Haynes, B.F. (2010). Autoreactivity in an HIV-1 broadly reactive neutralizing antibody variable region heavy chain induces immunologic tolerance. Proc. Natl. Acad. Sci. USA *107*, 181-186.

Vidarsson, G., Dekkers, G., and Rispens, T. (2014). IgG subclasses and allotypes: from structure to effector functions. Front. Immunol. *5*, 520.

Wan, T., Beavil, R.L., Fabiane, S.M., Beavil, A.J., Sohi, M.K., Keown, M., Young, R.J., Henry, A.J., Owens, R.J., Gould, H.J., and Sutton, B.J. (2002). The crystal structure of IgE Fc reveals an asymmetrically bent conformation. Nat. Immunol. *3*, 681-686.

Wan, Z., Chen, X., Chen, H., Ji, Q., Chen, Y., Wang, J., Cao, Y., Wang, F., Lou, J., Tang, Z., and Liu, W. (2015). The activation of IgM- or isotype-switched IgG- and IgE-BCR exhibits distinct mechanical force sensitivity and threshold. Elife *4*, e06925.

Wang, D., Feng, J., Wen, R., Marine, J.C., Sangster, M.Y., Parganas, E., Hoffmeyer, A., Jackson, C.W., Cleveland, J.L., Murray, P.J., and Ihle, J.N. (2000). Phospholipase Cγ2 is essential in the functions of B cell and several Fc receptors. Immunity *13*, 25-35.

Wardemann, H., Yurasov, S., Schaefer, A., Young, J.W., Meffre, E., and Nussenzweig, M.C. (2003). Predominant autoantibody production by early human B cell precursors. Science *301*, 1374-1377.

Wei, C.J., Boyington, J.C., McTamney, P.M., Kong, W.P., Pearce, M.B., Xu, L., Andersen, H., Rao, S., Tumpey, T.M., Yang, Z.Y., and Nabel, G.J. (2010). Induction of broadly neutralizing H1N1 influenza antibodies by vaccination. Science *329*, 1060-1064.

Weiss, A., and Littman, D.R. (1994). Signal transduction by lymphocyte antigen receptors. Cell *76*, 263-274.

Whyburn, L.R., Halcomb, K.E., Contreras, C.M., Lowell, C.A., Witte, O.N., and Satterthwaite, A.B. (2003). Reduced dosage of Bruton's tyrosine kinase uncouples B cell hyperresponsiveness from autoimmunity in $Lyn^{-/-}$ mice. J. Immunol. *171*, 1850-1858.

Winoto, A., and Littman, D.R. (2002). Nuclear hormone receptors in T lymphocytes. Cell *109*, S57-S66.

Woof, J.M., and Russell, M.W. (2011). Structure and function relationships in IgA. Mucosal Immunol. *4*, 590-597.

Wu, L.C., and Scheerens, H. (2014). Targeting IgE production in mice and humans. Curr. Opin. Immunol. *31*, 8-15.

Wu, L.C., and Zarrin, A.A. (2014). The production and regulation of IgE by the immune system. Nat. Rev. Immunol. *14*, 247-259.

Xu, Y., Harder, K.W., Huntington, N.D., Hibbs, M.L., and Tarlinton, D.M. (2005). Lyn tyrosine kinase: accentuating the positive and the negative. Immunity *22*, 9-18.

Yang, G., Holl, T.M., Liu, Y., Li, Y., Lu, X., Nicely, N.I., Kepler, T.B., Alam, S.M., Liao, H.X., Cain, D.W.*, et al.* (2013). Identification of autoantigens recognized by the 2F5 and 4E10 broadly neutralizing HIV-1 antibodies. J. Exp. Med. *210*, 241-256.

Yang, J., and Reth, M. (2010a). The dissociation activation model of B cell antigen receptor triggering. FEBS Lett. *584*, 4872-4877.

Yang, J., and Reth, M. (2010b). Oligomeric organization of the B-cell antigen receptor on resting cells. Nature *467*, 465-469.

Yang, Y., Wang, C., Yang, Q., Kantor, A.B., Chu, H., Ghosn, E.E., Qin, G., Mazmanian, S.K., Han, J., and Herzenberg, L.A. (2015). Distinct mechanisms define murine B cell lineage immunoglobulin heavy chain (IgH) repertoires. Elife *4*, e09083.

Yang, Z., Robinson, M.J., Chen, X., Smith, G.A., Taunton, J., Liu, W., and Allen, C.D. (2016). Regulation of B cell fate by chronic activity of the IgE B cell receptor. Elife *5*, e21238.

Yaniv, G., Twig, G., Shor, D.B.A., Furer, A., Sherer, Y., Mozes, O., Komisar, O., Slonimsky, E., Klang, E., Lotan, E.*, et al.* (2015). A volcanic explosion of autoantibodies in systemic lupus erythematosus: A diversity of 180 different antibodies found in SLE patients. Autoimmun. Rev. *14*, 75-79.

Young, M.A., Gonfloni, S., Superti-Furga, G., Roux, B., and Kuriyan, J. (2001). Dynamic coupling between the SH2 and SH3 domains of c-Src and Hck underlies their inactivation by C-terminal tyrosine phosphorylation. Cell *105*, 115-126.

Zhang, S.L., Yu, Y., Roos, J., Kozak, J.A., Deerinck, T.J., Ellisman, M.H., Stauderman, K.A., and Cahalan, M.D. (2005). STIM1 is a Ca^{2+} sensor that activates CRAC channels and migrates from the Ca^{2+} store to the plasma membrane. Nature *437*, 902-905.

Zhang, Z., Goldschmidt, T., and Salter, H. (2012). Possible allelic structure of IgG2a and IgG2c in mice. Mol. Immunol. *50*, 169-171.

Zhu, J.W., Brdicka, T., Katsumoto, T.R., Lin, J., and Weiss, A. (2008). Structurally distinct phosphatases CD45 and CD148 both regulate B cell and macrophage immunoreceptor signaling. Immunity *28*, 183-196.

Zikherman, J., Doan, K., Parameswaran, R., Raschke, W., and Weiss, A. (2012a). Quantitative differences in CD45 expression unmask functions for CD45 in B-cell development, tolerance, and survival. Proc. Natl. Acad. Sci. USA *109*, E3-E12.

Zikherman, J., and Lowell, C.A. (2017). B cell autoimmunity at the extremes. Nat. Immunol. *18*, 1065-1066.

Zikherman, J., Parameswaran, R., Hermiston, M., and Weiss, A. (2013). The structural wedge domain of the receptor-like tyrosine phosphatase CD45 enforces B cell tolerance by regulating substrate specificity. J. Immunol. *190*, 2527-2535.

Zikherman, J., Parameswaran, R., and Weiss, A. (2012b). Endogenous antigen tunes the responsiveness of naive B cells but not T cells. Nature *489*, 160-164.

Publishing Agreement

It is the policy of the University to encourage the distribution of all theses, dissertations, and manuscripts. Copies of all UCSF theses, dissertations, and manuscripts will be routed to the library via the Graduate Division. The library will make all theses, dissertations, and manuscripts accessible to the public and will preserve these to the best of their abilities, in perpetuity.

Please sign the following statement:

I hereby grant permission to the Graduate Division of the University of California, San Francisco to release copies of my thesis, dissertation, or manuscript to the Campus Library to provide access and preservation, in whole or in part, in perpetuity.

Mark A. Nowicki
Author Signature

3/19/18
Date